CONTRACTOR REPORT

SAND81-7128
Unlimited Release
UC-66c

Temperature Histories in Geothermal Wells: Survey of Rock Thermomechanical Properties and Drilling, Production, and Injection Case Studies

Malcolm A. Goodman
Enertech Engineering and Research Co.
Houston, Texas 77098

Prepared by Sandia National Laboratories, Albuquerque, New Mexico 87185 and Livermore, California 94550 for the United States Department of Energy under Contract DE-AC04-76DP00789

Printed July 1981

Prepared for Sandia National Laboratories
under Contract No. 13-8769

Sandia National Laboratories

SF 2900-Q(3-80)

DISCLAIMER

Issued by Sandia National Laboratories, operated for the United States Department of Energy by Sandia Corporation.

Printed in the United States of America
Available from:
National Technical Information Service
U. S. Department of Commerce
5285 Port Royal Road
Springfield, VA 22161
Price: Printed Copy $5.00; Microfiche $3.00

SAND81-7128
Unlimited Release
Printed July 1981

Category
UC-66c

TEMPERATURE HISTORIES IN GEOTHERMAL WELLS
SURVEY OF ROCK THERMOMECHANICAL PROPERTIES
AND
DRILLING, PRODUCTION, AND INJECTION CASE STUDIES*

Malcolm A. Goodman
Enertech Engineering and Research Co.
Houston, TX 77098

*This report was prepared for Sandia National Laboratories under Contract No. 13-8769.

ABSTRACT

Thermal and mechanical properties for geothermal formations are tabulated for a range of temperatures and stress conditions. Data was obtained from the technical literature and direct contacts with industry. Thermal properties include heat capacity, conductivity, and diffusivity. Undisturbed geothermal profiles are also presented. Mechanical properties include Youngs modulus and Poisson ratio.

GEOTEMP thermal simulations of drilling, production and injection are reported for two geothermal regions, the hot dry rock area near Los Alamos and the East Mesa field in the Imperial Valley. Actual drilling, production, and injection histories are simulated. Results are documented in the form of printed GEOTEMP output and plots of temperatures versus depth, radius, and time. Discussion and interpretation of the results are presented for drilling and well completion design to determine:

1. Wellbore temperatures during drilling as a function of depth,

2. Bit temperatures over the drilling history,

3. Cement temperatures from setting to the end of drilling, and

4. Casing and formation temperatures during drilling, production, and injection.

CONTENTS

CONTENTS (Continued)

SUMMARY AND CONCLUSIONS

A. Geothermal Rock Properties

A-1. Thermal and mechanical properties of hard formations (granite and granodiorite) and soft formations (sandstones) are presented for temperatures of 25-250°C and confining pressures ranging from 0-2000 psi. This property data base for geothermal rocks is sufficient for thermal simulation and stress analysis purposes.

A-2. For both hard and soft formations, a representative average value for heat capacity is 1.0 J/gC.

A-3. Thermal conductivity of rocks at geothermal temperatures decreases with increasing temperature. Average value for East Mesa sandstone is 3.50 W/mC. Granite has an average value of 2.1 W/mC.

A-4. For hard formations, an average value for thermal diffusivity at geothermal temperatures is 10.5 (10^{-3} cm^2/sec). East Mesa sandstone ranges from 13.7 - 16.5 (10^{-3} cm^2/sec).

A-5. Values of Youngs modulus range from 6.33-9.61 (10^6 psi) for hard formations and 1.84-3.44 (10^6 psi) for soft formations.

A-6. Representative values of Poisson ratio are 0.15 for hard formations and 0.25 for soft formations.

B. Well Temperature Histories

B-1. With drilling simulation, the GEOTEMP code can provide temperature predictions to assist in selection of drilling fluids, drilling bits, cements, casing, and other well components. Also, operational procedures such as cementing can be improved with good estimates of wellbore and formation temperatures.

B-2. During drilling, temperatures in the circulating fluid are governed mainly by the inlet temperature, flow rate, and thermal characteristics of the wellbore materials. When circulation stops, the fluid and wellbore tend to quickly reach equilibrium with the thermally disturbed formation in the near wellbore region.

B-3. Bit temperatures range between geothermal and inlet temperatures and depend strongly on fluid type and flow rate. Air and foam drilling are not as effective as water and mud drilling for cooling the bit.

B-4. Cement slurry temperatures during circulation of cement, are not strongly affected by the formation temperature which has been reduced by previous drilling operations. During setting, however, the formation temperature governs the cement temperature.

B-5. Casing temperatures during drilling, production and injection may be either above or below undisturbed geothermal temperatures depending on depth, inlet temperature, and flow rate. Casing can experience both compressive and tensile thermal stresses. For the two geothermal regions considered in this study, maximum thermal stresses occur during production and are on the order of 25,000 psi.

B-6. Formation temperature changes due to production and injection are greatest in the near wellbore region and decrease with radial distance from the well. For long term production and injection, most of the thermal disturbance occurs within a radius of 25 feet.

I. GEOTHERMAL ROCK PROPERTIES

I-1 Survey of Available Data

Undisturbed in-situ temperature distribution and thermomechanical properties for typical geothermal formations have been determined from two sources: literature survey and direct contacts with industry. Values of thermal properties are established for heat capacity, thermal conductivity, and thermal diffusivity. Mechanical properties presented are Youngs modulus and Poisson ratio. Although rock thermomechanical property values at low temperatures (<100°C) are available throughout the petroleum industry literature, data at high temperatures and under in-situ stress conditions are very limited. This survey is restricted to property values measured at geothermal temperatures (100° — 250°C).

I-1.1 Literature Search

A literature search for thermal and mechanical properties of geothermal rocks was performed through Petroleum Abstracts. Specific key words identified are:

Geothermal property
Rock property
Thermal property
Rock mechanics.

The search spanned the years 1975 through June 1980.

Table 1 is a summary of the search by year and by key word. From the list of titles under the key words, 55 references were selected from abstract review. Note that the key word "Rock Property" provided more than half of the references. Based on review of the abstracts for these 55 references, 18 papers were retrieved for evaluation. Of these papers, ten provided useful information for geothermal applications and are listed as the first ten papers in the list of References at the end of this report.

I-1.2 Contacts with Industry

Direct requests were made with three geothermal operators (Union, Phillips, and Republic Geothermal) and three geothermal service companies (Dresser, NL Baroid, IMCO) to obtain data on undisturbed geothermal gradients and thermal/mechanical properties. These companies were able to provide information on undisturbed formation temperatures but no data on rock property values.

Measurements of rock property values for geothermal formations were obtained from Terra Tek. In the tests performed at Terra Tek, rock samples were tested not only at elevated temperatures but also under simulated overburden stress and pore pressure.

I-2 Undisturbed Geothermal Gradients

In geothermal regions, undisturbed temperature distributions are generally bilinear consisting of two geothermal gradients. Geothermal temperatures vary considerably depending on location. For selected geothermal regions of New Mexico, Colorado, Utah, and Arizona, Reference [1] provides a listing of representative geothermal gradients.

A range of typical geothermal temperatures is presented in Figures 1 and 2. In Figure 1, the East Mesa of Imperial Valley has a very high initial gradient down to the depth of 2200 feet with a fairly normal gradient below. The top of the production zone in Figure 1 is located at approximately 5300 feet where the temperature is 315°F.

A somewhat different situation exists in Figure 2 for the Los Alamos hot dry rock region. The turnover point is at nearly the same depth as in Figure 1 but the temperature is only 190°F. The gradient below is 2.77°F/100 ft, higher than East Mesa, and the 387°F reservoir is relatively deep at 9600 ft.

I-3 Thermal Properties

Values of thermal properties for selected rock types at geothermal temperatures are presented in Tables 2-5. These data are obtained from References [2-6].

I-3.1 Heat Capacity

For hard formations (granite and granodiorite), heat capacity is approximately 1.0 J/gC. For sandstone, heat capacity is more dependent on depth and temperature, Table 2, with higher values at deeper depths. Range of values in Table 2 is 0.856 - 1.169 J/gC. Average value for East Mesa sandstone is 1.0 J/gC. For thermal modeling purposes, we conclude that a value of 1.0 J/gC is representative for both hard and soft geothermal formations.

I-3.2 Thermal Conductivity

Thermal conductivity values are higher for East Mesa sandstone compared to the harder formations. Conductivity generally decreases with increasing temperature. Average value for the East Mesa sandstone is 3.50 W/mC. The granodiorite in the Los Alamos hot dry rock region, Table 3, has an average value of 2.81 W/mC. Westerly granite, Table 5, is 2.1 W/mC.

I-3.3 Thermal Diffusivity

Thermal diffusivity values decrease with depth and temperature. Table 4 shows a range of values for different rock types. Values in Table 3 for the Los Alamos granodiorite and in Table 5 on the Terra Tek data are in close agreement with the results in Table 4. An average value for these hard formations at geothermal temperatures is 10.5 (10^{-3}) cm^2/sec.

From Tables 2 and 4, the sandstones exhibit a greater dependence on temperature. At 100°C and 250°C the average East Mesa sandstone values are 16.5 (10^{-3}) cm^2/sec and 13.7 (10^{-3}) cm^2/sec, respectively.

I-4 Mechanical Properties

Values for Youngs modulus and Poisson ratio obtained from the literature references are presented in Table 6.

I-4.1 Youngs Modulus

Values for the hard formation in Table 6 range from 6.33 (10^6) psi to 9.61 (10^6) psi. For the sandstones, the range is 1.84 (10^6) psi to 3.44 (10^6) psi.

I-4.2 Poisson Ratio

In general, the Poission ratio for sandstone appears to be slightly greater than granite. Representative values are 0.25 and 0.15 for the soft and hard formations, respectively.

II. WELL TEMPERATURE HISTORIES

GEOTEMP thermal simulations of drilling, production, and injection were conducted for actual wells in two geothermal regions: the hot dry rock area of New Mexico and the East Mesa field of the Imperial Valley in California. Well data for the hot dry rock simulations were provided by Los Alamos Scientific Laboratory. Data for the East Mesa wells were provided by Republic Geothermal Inc. The predictions from these studies are used to determine:

1. Wellbore temperatures during drilling as a function of depth,

2. Bit temperatures over the drilling history,

3. Cement temperatures from setting to the end of drilling,

4. Casing and formation temperatures at selected depths over the drilling history,

5. Casing and formation temperatures during production and injection.

The GEOTEMP simulations for the wells in the two geothermal regions represent a wide range of fluids and flow histories. For the East Mesa wells, drilling is done with conventional muds and production/injection flow rates are high. In the hot dry rock area, drilling fluids include air, foam, water and mud, and the drilling schedule spans almost one year; production/injection histories are related to the circulation loop through the reservoir.

II-1 The GEOTEMP Simulation

The major technical features of GEOTEMP are summarized in the following:

1. The flowing stream energy balance is a fully transient analysis with vertical heat convection, and radial heat conduction. Such a fully transient behavior has not previously been available for public use.

2. A composite of annular materials makes up the wellbore description, including the steel, cement, and fluids present in a well, Figure 3. A fully transient radial heat conduction model accounts for the wellbore region. Material heat capacities and natural convection in annular fluids are both included.

3. Radial and vertical heat conduction are the basis for the transient energy transfer in the soil. A key feature in the thermal simulator is the direct coupling of soil and well temperature calculations.

Particular emphasis has been placed on highly transient short time intervals, complex flow histories such as occur in drilling, and flexibility to allow sequential combinations of all flowing possibilities. With the code described in this paper, the complete life of a well can be modeled with one computer run for drilling and circulation during completion, through production and circulation during workover, additional production or injection through the life of a well, and even shut-in after a well is dead.

The original GEOTEMP was developed with only a single primary flowing fluid. The modified GEOTEMP currently under development allows several sifferent wellbore fluids to be defined, and allows the user to specify the injection, production or circulation of any fluid at any time in the life of the well. Further, more than one fluid may be in the wellbore at any time, and the displacement of one fluid by another is automatically computed. The simulation of a cementing operation is one application of this capability.

The original GEOTEMP was developed to model liquid wellbore systems. The modified GEOTEMP now has the capability of simulating air and nitrogen drilling. The simulation can switch between air drilling and mud drilling at any time desired.

The GEOTEMP simulator has been tested against analytic solutions to several heat transfer problems and been shown to be accurate. Field data was acquired from geothermal and petroleum wells for flowing and shut-in conditions to correlate with GEOTEMP. The performance of the thermal simulator in modeling this field data was adequate compared to the quality of the data [11, 12].

II-2 Imperial Valley Well Descriptions For Drilling, Production, and Injection

Drilling and production simulations were made for Republic Geothermal well #56-30. Injection wells in the Imperial Valley have a different casing program than production wells. Republic Geothermal well #52-29 was used for injection simulation.

II-2.1 Drilling Data for East Mesa Well #56-30

II-2.1.1 Well Completion

The actual well completion is shown in Figure 4. Two liners are used. The 8-5/8 inch liner is completely cemented. The 6-5/8 inch liner is slotted and set opposite the production zone. Total depth is 7520 feet. For application to GEOTEMP,

the liners have been modelled as casings extending back to surface. GEOTEMP requires that all well casings start at the surface as shown in Figure 3. Table 7 gives the casing program used in the simulation.

For drilling simulation, the production liner (6-5/8 casing in Table 7) is not set until the end of drilling and, hence, will have minimal effect on the thermal behavior during drilling. The 8-5/8 inch casing, (instead of liner) will introduce some error in the upper zone above 1332 feet, but the thermal effects are small because of the small radii differences between casings.

II-2.1.2 Drilling History

The actual drilling schedule for the Republic Geothermal Well #56-30 is shown by the circles in Figure 5. Data for the drilling schedule, and for drilling fluids, flow rates, and inlet temperatures, were obtained from the daily drilling reports provided by Republic Geothermal.

For GEOTEMP simulation, the drilling schedule in Figure 5 is divided into seven segments and modelled as shown by the dashed lines between closed circles. Each segment between closed circles represents a distinct time interval for which the drilling parameters are held constant. These parameters include penetration rate, circulation rate, fluid type, inlet temperature, and circulation time per day. Based on data from the daily drilling reports, average values for these parameters are determined for each time segment, Table 8.

II-2.1.3 Drilling Fluid and Formation Properties

Drilling mud with different properties is used to drill different parts of the hole. Table 8 presents the fluid properties for four separate muds used to drill the well.

Formation thermal properties correspond to values given in Table 2. The undisturbed geothermal gradient is described in Figure 1.

II-2.2 Production Data for East Mesa Well #56-30

II-2.2.1 Well Completion

For production the well completion corresponds to Figure 4 with two exceptions:

1. A downhole pump is placed at a depth of 1200 feet inside the 13-3/8 inch casing, with 11-3/4 inch casing from the pump to the surface. The annulus outside the 11-3/4 inch casing contains water from the pump level to 800 feet and steam above.

2. The top of the production zone is 5320 feet. For thermal simulation purposes we assume the production fluid enters the well at this depth and, hence, it represents the bottom of the well.

Since GEOTEMP can model variable cross-sectional area in production tubing, the flow system of liner, casing, and pump are treated as a single "tubing string" as shown in Figure 6. The tubing and casing specifications for GEOTEMP application are listed in Table 9. Note that the tubing consists of four intervals.

II-2.2.2 Production Rates and Fluid Properties

Flow rate is constant at 735 M lb/hr (50,360 bbl/day) for 25 years.

Inlet temperature of the production fluid varies with time, Figure 7. Density and rheological properties of the production fluid correspond to water with 2134 mg/L of dissolved solids.

Special modifications to GEOTEMP were implemented to model the annular steam region above 800 feet. The steam is treated as a low density fluid with the following specific properties [13] for steam at 300°F and 14.7 psi:

Density = 0.00438 ppg
Yield Point = 0.0
Plastic Viscosity = 0.01415 cp
Thermal Conductivity = 0.02508 BTU/hr ft F
Specific Heat Capacity = 0.5 BTU/lb F.

II-2.3 Injection Data for East Mesa Well #52-29

II-2.3.1 Well Completion and Geothermal Gradient

The injection well #52-29 extends to a total depth of 4524 feet with two slotted liners, one from 1138 - 3382 feet and the other from 3276 - 4524 feet. The injection zones are located below the 16 inch casing set at 2470 feet. For GEOTEMP simulation, the well is modelled down to this depth as shown in Figure 8. Tubing with variable cross-section is used to simulate the injection flow area. The tubing and casing specifications are given in Table 10.

Undisturbed geothermal temperatures for the injection well #52-29 are somewhat different than the production well #56-30. Figure 9 presents the bilinear gradient for the injection simulation.

II-2.3.2 Injection Rates and Fluid Properties

Injection flow rates are high; one injection well reinjects fluid from five production wells. The rate used for well #52-29 is 3250 M lb/hr (222,625 bbl/day).

The injection period simulated is 15 years. Flow rate and inlet temperature, 212°F, are constant over the entire period. Injected fluid is water with the same density and rheological properties as the production fluid.

II-3 Hot Dry Rock Well Descriptions For Drilling, Production and Injection

Simulations were performed for the Los Alamos GT-2 well. Well history and completion data were obtained from daily drilling reports and direct contact with Los Alamos personnel.

II-3.1 Well Completion and Formation Properties

Figure 10 shows the GT-2 well completion for drilling, production and injection simulations. Drill pipe is 5-1/2 inches. All casings are cemented back to surface, except the production (and injection) casing which is cemented over the bottom 2400 feet. The bottom of the well for production and injection corresponds to the hot dry rock depth of 8500 feet.

The undisturbed geothermal temperatures for the GT-2 well are plotted in Figure 2. Rock thermal properties are given in Table 3.

II-3.2 Drilling Data

II-3.2.1 Drilling History

The actual drilling schedule, together with the simulated history, is shown in Figure 11. Twenty-two separate time segments spanning 295 days characterize the drilling of the GT-2 well. Table 11 summarizes the drilling history.

II-3.2.2 Drilling Fluid Properties

Six different fluids, including air and foam, are used to drill this well. Properties of the different drilling muds are presented in Table 11. Fluid number 4 is cement slurry.

For the GEOTEMP simulation, the foam drilling fluid is modelled as a compressible fluid (namely, air since the foam consists of more than 95% air by volume). A high viscosity, 100 cp, is used for the foam (see Reference [14]). Heat transfer coefficients and other thermal properties for the foam are computed from the foam viscosity using air correlations internal to GEOTEMP.

II-3.3 Production and Injection Data for the GT-2 Well

Since the hot dry rock energy extraction concept involves a circulation loop through a fractured reservoir, the injection and production histories and fluid properties are related. For

GEOTEMP simulation, the data from a 75 day flow experiment has been modelled and extrapolated to 180 days [15].

The circulation fluid through the injection-production loop is water. Inlet temperature for the injection well is 25°C. As the water flows through the hot dry rock reservoir, the water is heated. The bottom hole inlet temperature for the production well is given in Figure 12.

Flow rates for the injection and production wells vary with time because fluid is lost to the reservoir. The injection and production rates for the 180 day flow period are presented in Figure 13.

II-4 Predicted Results

II-4.1 GEOTEMP Output

The printed output for each of the six cases (drilling, production, and injection for the two wells) has been presented under separate cover. The GEOTEMP output consists of the following:

a. Tabulated input data for the well completion and fluid properties

b. Changing flow parameters data

c. Temperature distribution (with depth and radius) at the end of each change card time increment.

II-4.2 Discussion of Drilling Simulations

II-4.2.1 Wellbore Temperatures

Figures 14-17 show the variation of wellbore temperatures with depth in the Los Alamos well at two selected time periods. Figure 14 shows the temperatures at the end of drilling circulation on day 77. Figure 15 shows the temperatures at the end of the shut-in period of day 77. Recall that each day of drilling in GEOTEMP is divided into a circulation part and a shut-in part. This drilling/shut-in pattern is repeated for the Los Alamos well in Figures 16 and 17 and for the Republic Geothermal well in Figure 18 and 19. In Figures 14 - 19 the lines with circles give the drill pipe temperatures, the lines with squares give the annulus temperatures, and the unmarked lines give the undisturbed geothermal temperature.

The key to the understanding of Figures 14-19 is the concept of the wellbore as a cross-flow heat exchanger. In Figures 14, 16 and 18 the annulus temperature exceeds the drill

pipe temperature. Thus, the drilling fluid is heated as it flows down the drill pipe and its temperature increases continuously. The temperature of the annulus fluid is more difficult to predict because, while the annulus fluid is being cooled by the drill pipe fluid, it may be either heated or cooled by the surrounding soil, depending on depth. The balance between the cooling effect of the drill pipe fluid and the heating effect of the formation determines if the annulus fluid heats up or cools off. Of course, above the depth where the annulus temperature exceeds the geothermal temperature, the annulus temperature always decreases. Figure 14 shows the formation to be dominant in the annulus heat transfer. Note that the annulus temperature continues to increase until it crosses the geothermal line. In Figure 16, the drill pipe fluid has more influence, and the annulus temperature starts to decrease before the geothermal line is crossed. Figure 18 shows a dominant effect by the drill pipe, thus the annulus fluid cools continuously.

Mass flow rate is the governing factor in the differences among Figures 14, 16, and 18. Figure 14 represents an air drilling simulation with a relatively low mass flow rate. The formation temperature governs the annulus heat transfer and there is a relatively large temperature difference between the annulus and drill pipe temperatures. Figure 18 results from the high mass flow rate of a conventional drilling mud. The annulus and drill pipe temperatures are nearly the same and the formation temperature has less relative effect on the fluid heat transfer. Figure 16 represents an intermediate case.

Figures 15, 17, and 19 show the effect of shut-in on the wellbore temperatures. In each case, the temperatures move toward the undisturbed geothermal temperatures. In Figure 15, the drill pipe temperature has lagged 15^{o}-20^{o} behind the annulus temperature, and this indicates the reduced ability of air to transfer heat compared to liquid systems. In Figures 17 and 19, the drill pipe and annulus temperatures in the liquid wellbore fluids are within a couple of degrees of each other. While the temperatures in all cases have not reached the geothermal temperature, it will be shown in Figures 22 and 23 that the wellbore temperatures have reached the temperature of the formation immediately in contact with the well. The conclusion is that a typical shut-in period is long enough for the wellbore fluid to reach equilibrium with the formation, but not long enough for the formation to return to its undisturbed temperature.

II-4.2.2 Bit Temperatures

Figures 20 and 21 give the temperatures at the drill bit over the drilling history of the Los Alamos and Republic Geothermal wells respectively. Also indicated on the figures are the inlet temperatures, marked with circles, and the geothermal temperatures, marked with a solid line. These two curves represent extreme temperatures for the bit, and Figures 20 and 21 show that the bit temperature stays between them over the drilling history.

The Los Alamos well is the most interesting because of the variety of drilling fluids and circulation rates used.

One notable result is that foam and air drilling are not as effective as conventional drilling fluids in cooling the bit. Air and foam drilling are indicated on Figure 20, and in each case the bit temperature shows a significant increase over drilling with liquid systems. A temperature increase late in the drilling history indicates a reduction in daily circulation time from 18 to three hours per day. An increase to five hours of circulation per day reduced the bit temperature by 40-50°.

Figure 21, though not as dramatic as the Los Alamos simulation, clearly shows the effect of time on the bottom hole temperature in the Republic Geothermal well. At the eighth day and the twenty-fourth, the daily hours of circulation were reduced because of logging operations, and in each case the bottom hole temperature increased, compared to bottom hole temperatures during drilling.

II-4.2.3 Cementing Temperatures

Figures 22 and 23 show an application of GEOTEMP to cementing operations. Figure 22 shows the radial temperature distribution at the end of cementing (square symbols) and at the end of "waiting on cement" time for the Los Alamos well. The solid line represents the initial undisturbed geothermal temperature. Figure 23 shows a similar plot for the Republic Geothermal well. In each case, the cement is initially at a temperature 70° to 80° below the formation temperature. This formation temperature has been cooled by drilling operations by 20° in the Los Alamos well and 10° in the Republic Geothermal well. At the end of the waiting period, the cement temperature has risen to the formation temperature but it is still cooler than the initial undisturbed temperature.

II-4.2.4 Casing Temperatures

Figures 24-27 relate temperature predictions to casing design. Figures 24 and 25 show the temperature of the 13-3/8" surface casing used in the Los Alamos well at two different depths over the drilling history of the well. Figures 26 and 27 show the same results for the Republic Geothermal well. In each figure, square symbols indicate maximum temperatures, circles indicate minimum temperatures, and the solid line shows the undisturbed temperature as reference. The maximum and minimum temperatures represent the range due to the shut-in and circulating periods of each day.

The temperature variation of about 60°F indicated at the casing seat of the Los Alamos well (Figure 24) corresponds to thermal stress changes of about 10,000 psi. The temperature changes at 400 ft range about 20°F, corresponding to 3,500 psi

stress changes. These stress changes are large enough that they need to be considered in the well completion design. Figures 26 and 27 indicate a temperature range of about 30°F at the surface casing seat. The temperatures at 1400 ft are uniformly below the undisturbed temperature and at 400 ft the temperatures are above the geothermal temperature. Thus, at shut-in, the cemented casing at 1400 ft will experience compressive thermal stress and the casing at 400 ft will feel tensile thermal stresses.

II-4.3 Discussion of Production Simulation

II-4.3.1 Temperature-Depth Profiles

Figures 28 and 29 show the undisturbed geothermal profile together with flow string and annulus temperatures at two selected times for the Los Alamos well. Figure 30 presents the profiles for the Republic Geothermal well. In the Los Alamos well, the inlet temperature at bottomhole is less than the geothermal temperature because of the cooling from the fluid injected for the circulation loop through the reservoir. Since the production inlet temperature continues to decrease with time (see Figure 13), the bottomhole temperature in Figure 29 is less than that in Figure 28.

The early time behavior in the Los Alamos well, Figure 28, shows a typical production distribution with wellbore temperatures greater than geothermal and with the annulus temperature progressively cooler than the flow string temperature as the fluid travels up the hole. In Figure 29, the distribution is quite different because of the influence of two factors. First, the significantly lower inlet temperature causes the annulus temperature to be higher than the flow string temperature up to 3500 feet. And, secondly, the lower heat transfer capability of the cement over the lower 2400 feet generates larger differences between annulus and flow string, compared to the higher heat transfer of convecting fluid above the cement.

In the Republic Geothermal well, Figure 30, the thermal resistance of the annulus materials creates an unusual annulus temperature profile, particularly when compared to the flow string temperature which is nearly constant with depth. The uniform production temperature with depth is due to the high production rates. In the annulus, the cement governs the behavior from 1200 feet to total depth (similar to the response in Figure 28). Water in the annulus between 800-1200 feet is highly convective and, hence, the annulus and flow string temperatures are nearly the same. Above 800 feet, the steam in the annulus, although convective, has relatively low heat capacity and, therefore, creates an insulating effect. At the surface, the predicted temperature difference between the annulus and production fluid is almost 100°F.

II-4.3.2 Production Casing Temperatures

Figures 31 and 32 present production string temperatures with time for a selected depth in each well. The depth in each case is selected to demonstrate the influence of the wellbore assembly. For the Los Alamos well, the 1600 foot depth represents the bottom of the 13-3/8 inch casing (see Figure 10). In Figure 32, the 1200 foot depth corresponds to the downhole pump location.

Both figures show maximum temperatures that are significantly greater than the undisturbed geothermal temperature denoted by the straight line. Also, both plots exhibit trends similar to the inlet temperature histories presented in Figures 7 and 12. In the Los Alamos well, the hump at 15 days is due to the heating transient from the production fluid. The decline after 15 days follows the inlet temperature decline.

For temperature changes from undisturbed conditions, the production casing will experience compressive stresses. The maximum ΔT at the specified depth in Figure 31 is 120°F which generates a stress of about 20,000 psi. In Figure 32, the maximum ΔT at 1200 feet is 140°F which gives nearly 25,000 psi.

II-4.3.3 Formation Temperatures

Radial temperature distributions at the end of production are shown in Figures 33-35. The temperature disturbance due to hot fluid production decreases with increasing radial distance from the well. Most of the disturbance in the formation occurs within a radius of 20 feet.

In Figures 33 and 34, the radial distributions show a uniformly decreasing temperature. At these depths (1600 feet for the Los Alamos well and 1200 feet for the Republic Geothermal well), the production string is in intimate contact with the formation through the cement and well casings.

The profile in Figure 35 for the Republic Geothermal well demonstrates a significantly different behavior due to the steam in the annulus above 800 feet. The low heat transfer capability of the steam contains the heat within the wellbore, causing less disturbance in the surrounding formations. Most of the temperature drop between the production string and formation occurs within the first foot. In Figure 35, the maximum temperature disturbance in the formation is only about 40°F, compared to about 80°F in Figure 34.

II-4.4 Discussion of Injection Simulations

II-4.4.1 Temperature-Depth Profiles

Figures 36 and 37 present injection temperature profiles for the flow string and annulus in the Los Alamos well after 25 days and 180 days, respectively. At the early time, Figure 36, the flow string and annulus temperatures show uniform behavior with depth, similar to early time production as shown in Figure 28. At the end of the injection period, Figure 37, the annulus materials dominate the thermal response, again similar to the production behavior in Figure 29.

For the Republic Geothermal well, Figure 38, the temperature in the flow string and annulus are completely governed by the high flow rate. After 15 years of injection at constant inlet temperature and flow rate, the steady state temperature profile exhibits uniform temperature from top to bottom. Because of the high injection rates, the formation geothermal temperatures have little effect on the wellbore temperatures.

II-4.4.2 Injection Casing Temperature

Flow string temperature at a depth of 1600 feet in the Los Alamos well and 1200 feet in the Republic Geothermal well are plotted versus injection time in Figures 39 and 40, respectively. These depths correspond to the 13-3/8 inch casing shoe in the Los Alamos well and just below the liner hanger in the Republic Geothermal well. Except for the early time response in the Los Alamos well, Figures 39 and 40 show constant temperature with time, indicating that the injection casing quickly reaches steady state temperature which is cooler than geothermal for the Los Alamos well but hotter than geothermal for the Republic well. The annulus temperature is also plotted in Figure 39 and shows a slightly greater transient response to the geothermal then does the injection casing temperature which is governed primarily by the flow rate and inlet temperature.

The cooling of 60°F, Figure 39, between the undisturbed geothermal temperature and the injection casing temperature generates a tensile stress of about 10,000 psi at the 1600 foot depth. For the Republic Geothermal well, Figure 40, the liner at 1200 feet is heated 40°F which causes a compressive stress of about 7,000 psi.

II-4.4.3 Formation Temperatures

The cooling of the formation around the Los Alamos well and the heating around the Republic Geothermal well are demonstrated in Figures 41 and 42. The radial distributions show that the bulk of the thermal effects are contained within a radius of about 30 feet, even after 15 years of injection for the Republic Geothermal well. In both wells, the thermal disturbance in the formation at the specified depths is not great. At a radius of 10 feet, the temperature change in both wells is only about 20°F.

REFERENCES

1. Rieter, M., Mansure, A. J., and Shearer, C., "Geothermal Characteristics of the Colorado Plateau," Tectonophysics, V. 61, 1979.

2. "Rock Properties Source Book," Terra Tek Report TR-80-13 submitted to DOE Division of Geothermal Energy, March 1980.

3. Murphy, H. D. and Lawton, R. G., "Downhole Measurements of Thermal Conductivity in Geothermal Reservoirs," J. Pressure Vessel Technology, ASME Petroleum Division, November 1977.

4. Sibbitt, W. L., Dodson, J. G., and Tester, J. W., "Thermal Conductivity of Crystalline Rocks Associated with Energy Extraction from Hot Dry Rock Geothermal Systems," J. Geophysical Research, V. 84, March 1979.

5. Hanley, E. J., Dewitt, D. P., and Roy R. F., "The Thermal Diffusivity of Eight Well-Characterized Rocks for the Temperature Range 300-1000 K," Engineering Geology, V. 12, 1978.

6. Ennis, D. O., Butters, S. W., McFarland, C. B., and Jones, A. H., "Capabilities to Determine Rock Properties at Simulated Geothermal Conditions," J. Energy Resources Technology, ASME Petroleum Division, V. 101, June 1979.

7. Aktan, T. and Faroug Ali, S. M., "Effect of Cyclic and In Situ Heating on the Absolute Permeabilities, Elastic Constants, and Electrical Resistivities of Rocks," Paper SPE 5633 presented at the 50th Annual Fall Meeting of SPE-AIME, Dallas, 1975.

8. Kumar, J., "The Effect of Poisson's Ratio on Rock Properties," Paper SPE 6094 presented at the 51st Annual Fall Technical Conference of SPE-AIME, New Orleans, 1976.

9. Kulhawy, F. H., "Stress Deformation Properties of Rock and Rock Discontinuities," Engineering Geology, V. 9, 1975.

10. Roegiers, J. C. and Thill, R. E., "Rock Characterization at a Geothermal Site," Proceedings of the 17th Rock Mechanics U. S. Symposium, Utah University, 1976.

11. Wooley, G. R.," Wellbore and Soil Thermal Simulation for Geothermal Wells," Sandia Laboratories Report, 1978.

12. Wooley, G. R., "Computing Downhole Temperatures in Circulation, Injection, and Production Wells," JPT, September, 1980.

13. Keenan, J. H., Keyes, F. G., Hill, P. G., and Moore, J. G., Steam Tables: Thermodynamic Properties of Water Including Vapor, Liquid, and Solid Phases,, John Wiley & Sons, 1969.

14. Beyer, A. H., Millhone, R. S. and Foote, R. W., "Flow Behavior of Foam as a Well Circulating Fluid," Paper SPE 3986 presented at the 47th Annual Fall Meeting of SPE-AIME San Antonio, 1972.

15. Tester, J. W. and Albright, J. N., "Hot Dry Rock Energy Extraction Field Test," LASL Report LA-7771-MS, April 1979.

TABLES

TABLE 1

Literature Search for Thermomechanical Rock Properties

Tabulated Numbers Indicate
Abstracts Reviewed

Bracketed Numbers Indicate
Papers Selected

Key Word	1975	1976	1977	1978	1979	Thru June 1980	Total
Geothermal Property					3(0)	2(1)	5(1)
Rock Property	7(3)	3(2)	7(3)	2(2)	8(2)	5(0)	32(12)
Thermal Property			1(1)	1(0)			2(1)
Rock Mechanics		2(2)		2(0)	2(1)	1(0)	7(3)
Other			1(0)	1(0)	7(1)		9(1)
TOTAL	7(3)	5(4)	9(4)	6(2)	20(4)	8(1)	55(18)

TABLE 2

Thermal Properties for East Mesa Sandstone (Ref. 2)

Sample Depth, Ft	5505				7150				AVERAGE
Confining Pressure, MPa	37.8				49.0				
Pore Pressure, MPa	16.6				21.4				
Temperature, °C	23	100	175	250	23	100	175	250	
Thermal Conductivity, W/m°C	4.08	3.47	3.30	2.89	4.26	3.64	3.42	2.91	3.50
Heat* Capacity, J/g°C	.932	.875	.856	.898	1.169	1.079	1.086	1.019	1.00
Thermal Diffusivity, cm^2/S	.020	.0181	.0176	.0147	.0162	.0150	.0140	.0127	.016
Density, g/cm^3	2.19	2.19	2.19	2.19	2.25	2.25	2.25	2.25	2.20

*Calculated from $\kappa = k/\rho c$

TABLE 3

Thermal Properties for LASL Hot Dry Rock (Ref. 3, 4)

Depth, Ft	6153				9608				AVERAGE
Rock Type	Gneiss Granodiorite				Biotite Granodiorite				
Temp., °C	25	100	150	250	25	100	150	250	
Thermal Conductivity, W/mC	3.343	2.992	2.836	2.608	3.005	2.728	2.587	2.376	2.81
Density g/m^3	2.7	2.7	2.7	2.7	2.7	2.7	2.7	2.7	2.7
Heat Capacity, J/gC	1.0	1.0	1.0	1.0	1.0	1.0	1.0	1.0	1.0
Thermal Diffusivity cm^2/S	.0124	0.110	.0105	.0097	.0111	.0101	.0096	.0088	.0104

TABLE 4

Thermal Diffusivity of Hard and Soft Rocks

at Geothermal Temperatures (Ref. 5)

Rock Type	Westerly Granite		Barre Granite		St. Cloud Granodiorite		Berea Sandstone	
Density, g/cm^3	2.63		2.63		2.72		2.15	
Temperature, °C	100	200	100	200	100	200	100	200
Thermal Diffusivity $(10^{-3})cm^2/S$	11.5	9.5	12.0	10.0	11.0	9.0	14.0	10.5

TABLE 5

Thermal Properties of Granite at

Geothermal Temperatures and Pressures (Ref. 2)

Temperature, °C	100	200
Confining Pressure, psi	1000	1000
Thermal Conductivity, W/mC	2.3	1.9
Heat Capacity, J/gC	0.900	1.050
Thermal Diffusivity, cm^2/S	0.011	0.008
Density, g/m^3	2.32	2.26

TABLE 6

Mechanical Properties of Rocks

Rock Type	Youngs Modulus (10^6)psi	Poisson Ratio	Test Conditions	Source (See Ref.)
East Mesa Sandstone	1.84	0.21	2000 psi 175°C	2
Berea Sandstone	3.44	0.23	5000 psi 300°F	7
Berea Sandstone	2.80	0.38	Uniaxial Ambient Temp.	9
Boise Sandstone	2.91	0.12	5000 psi 300°F	7
Westerly Granite	6.33	0.15	2000 psi 200°C	6
Biotite Granodiorite	9.61	-	Uniaxial Ambient Temp.	10
Granite	7.55	0.16	Uniaxial Ambient Temp.	9

TABLE 7

Republic Geothermal 56-30

Well Completion

	Size	Weight/Ft.	Setting Depth
Conductor Pipe	20"	94.0	90
Surface Casing	13-3/8"	54.5	1503
Protective Casing	8-5/8"	32.0	5320
Production Casing	6-5/8"	28.0	7520
Drill Pipe	3-1/2"	9.5	N.A.

TABLE 8

Republic Geothermal 56-30

Drilling History

Time (Days)	Depth (Ft.)	Circ. Rate	Hrs. Circ. Per Day	Fluid*
0	0	480 gal/min	17.0	1
1	1513	480 gal/min	5.0	1
2	1513	500 gal/min	20.0	2
10	5330	360 gal/min	2.0	3
17	5330	360 gal/min	17.0	4
24	7520	400 gal/min	2.0	4

*Fluid	Density (Lb/Gal)	Plastic Visc. (Centipoise)	Yield Point (Lb/100 Ft^2)
1	8.8	4.0	4.0
2	9.0	7.0	4.0
3	8.9	22.0	17.0
4	8.9	9.0	5.0

TABLE 9

Production Tubing and Casing Geometry

For Republic Geothermal Simulation

Tubing Interval	I.D. Inches	O.D. Inches	Top Ft	Bottom Ft	Cement Ft
1	11.100	11.750	0	1200	0
2	12.500	12.580	1200	1332	132
3	7.921	8.625	1332	5132	3800
4	5.791	6.625	5132	5320	188

Casing	I.D. Inched	O.D. Inched	Setting Depth, Ft	Cement Ft
1	12.615	13.375	5320	5320
2	13.500	14.000	1530	1530
3	19.124	20.000	90	90

TABLE 10

Injection Tubing and Casing Geometry

For Republic Geothermal Simulation

Tubing Interval	I.D. Inches	O.D. Inches	Top Ft	Bottom Ft	Cement Ft
1	15.124	16.00	0	1138	1138
2	11.000	11.75	1138	2470	0

Casing	I.D. Inches	O.D. Inches	Setting Depth, Ft	Cement Ft
1	16.500	16.75	2470	2470
2	19.124	20.00	90	90

TABLE 11

Los Alamos Hot Dry Rock GT-2 Well

Drilling History

Time (Days)	Depth (Ft)	Circ. Rate	Hrs. Circ Per Day	Fluid*
0	0	125 gal/min	8.0	2
11.0	1595	125 gal/min	8.0	1
25.0	1595	125 gal/min	3.0	4
27.0	1595	300 SCF/min	8.0	Foam
48.0	2514	125 gal/min	3.0	4
50 0	2514	1245 SCF/min	11.0	Air
65.0	3556	1270 SCF/min	6.0	Air
78.0	3556	125 gal/min	5.0	1
87.0	3727	1275 SCF/min	3.0	Air
91.0	3727	125 gal/min	3.0	1
101.0	3727	1290 SCF/min	14.0	Air
105.0	3963	125 gal/min	15.0	1
114.0	4556	125 gal/min	11.0	3
148.0	6356	125 gal/min	0.0	1
194.0	6356	125 gal/min	13.0	1
199.0	6700	125 gal/min	5.0	1
236.0	6700	125 gal/min	15.0	1
258.0	8577	125 gal/min	1.0	1
263.0	8577	125 gal/min	18.0	1
269.0	9436	125 gal/min	3.0	1
276.0	9549	125 gal/min	5.0	1
292.0	9549	125 gal/min	5.0	1
295.0	9610	125 gal/min	5.0	1

*Fluid	Density (Lb/Gal)	Plastic Visc. (Centipoise)	Yield Point (Lb/100 Ft^2)
1	8.3	1.0	0.0
2	9.3	10.0	3.0
3	8.6	5.0	2.0
4	15.1	30.0	50.0

ILLUSTRATIONS

FIGURE 1: Geothermal Temperature Profile
From East Mesa Well #56-30

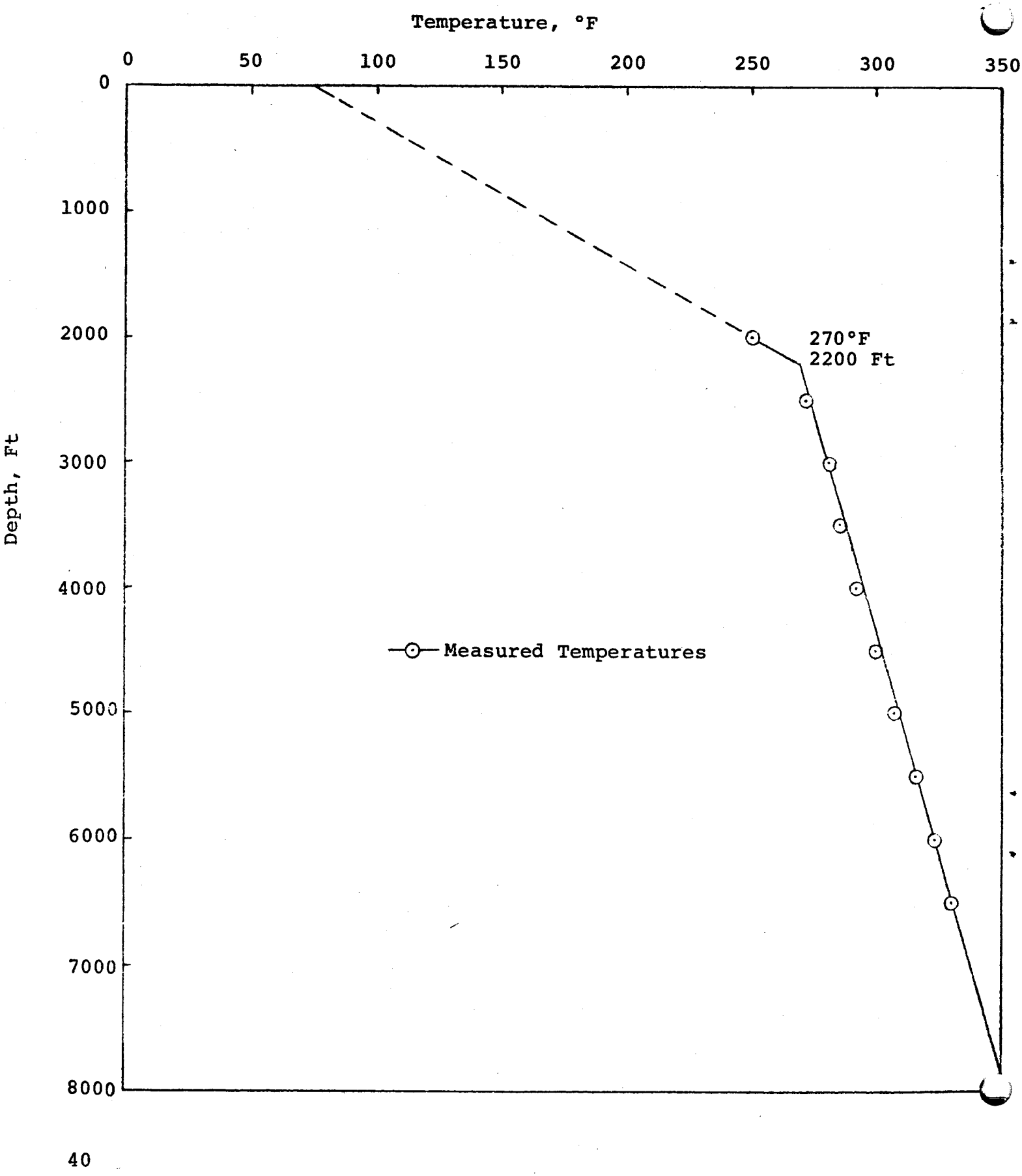

FIGURE 2: Geothermal Temperature Profile in the Los Alamos Hot Dry Rock Region

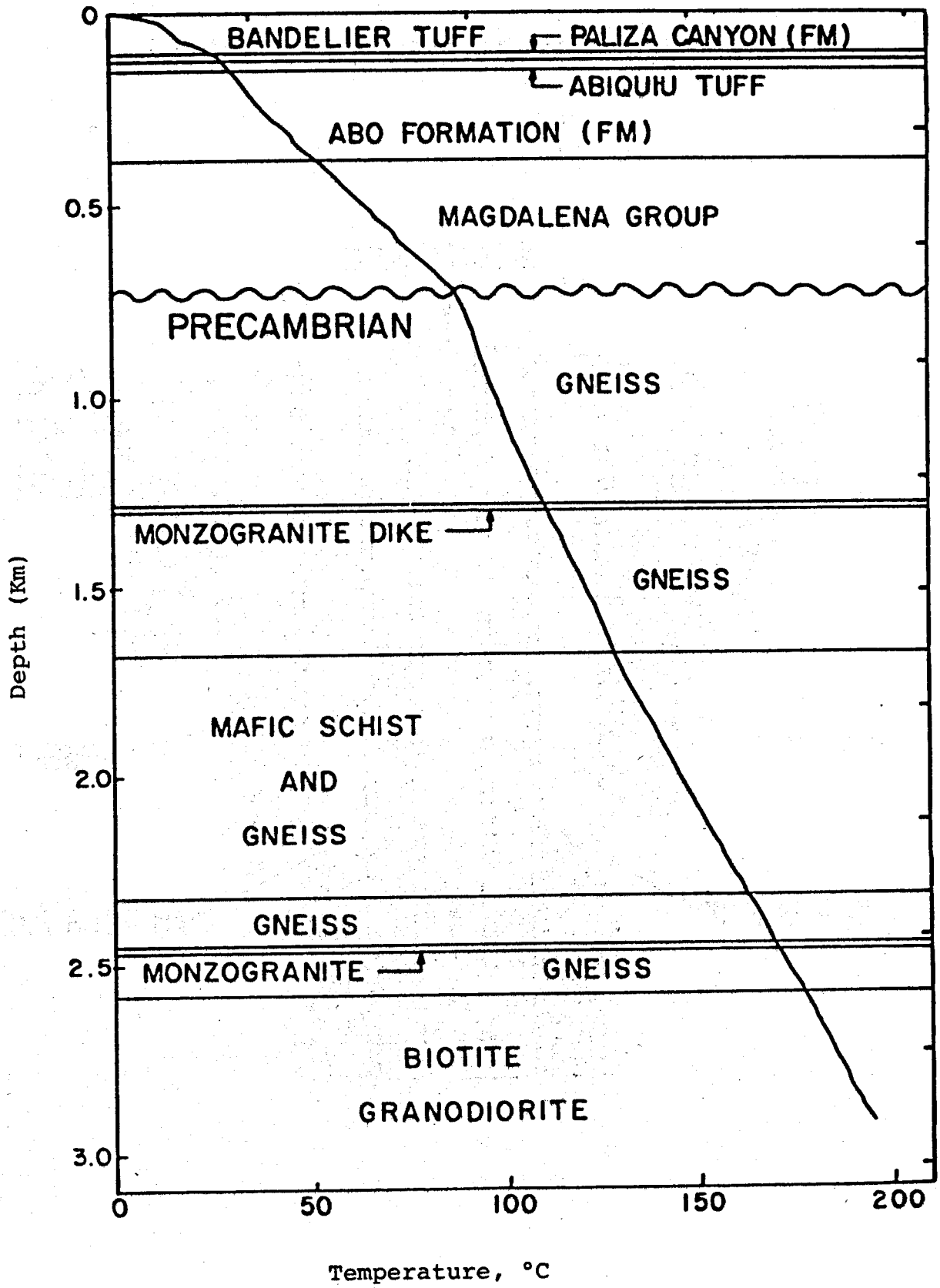

FIGURE 3: GEOTEMP Wellbore Completion Model

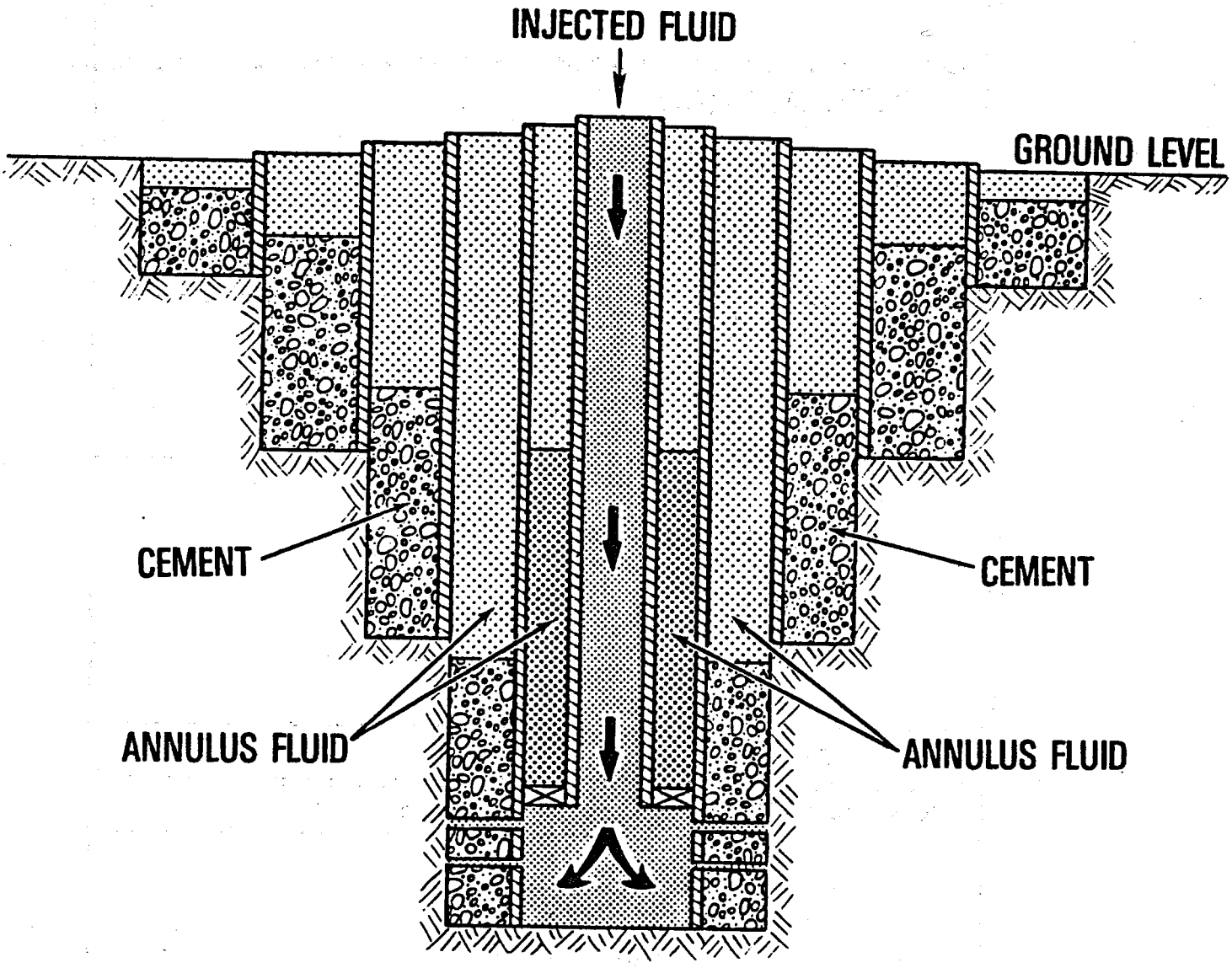

FIGURE 4: Well Completion for Republic Geothermal Well #56-30

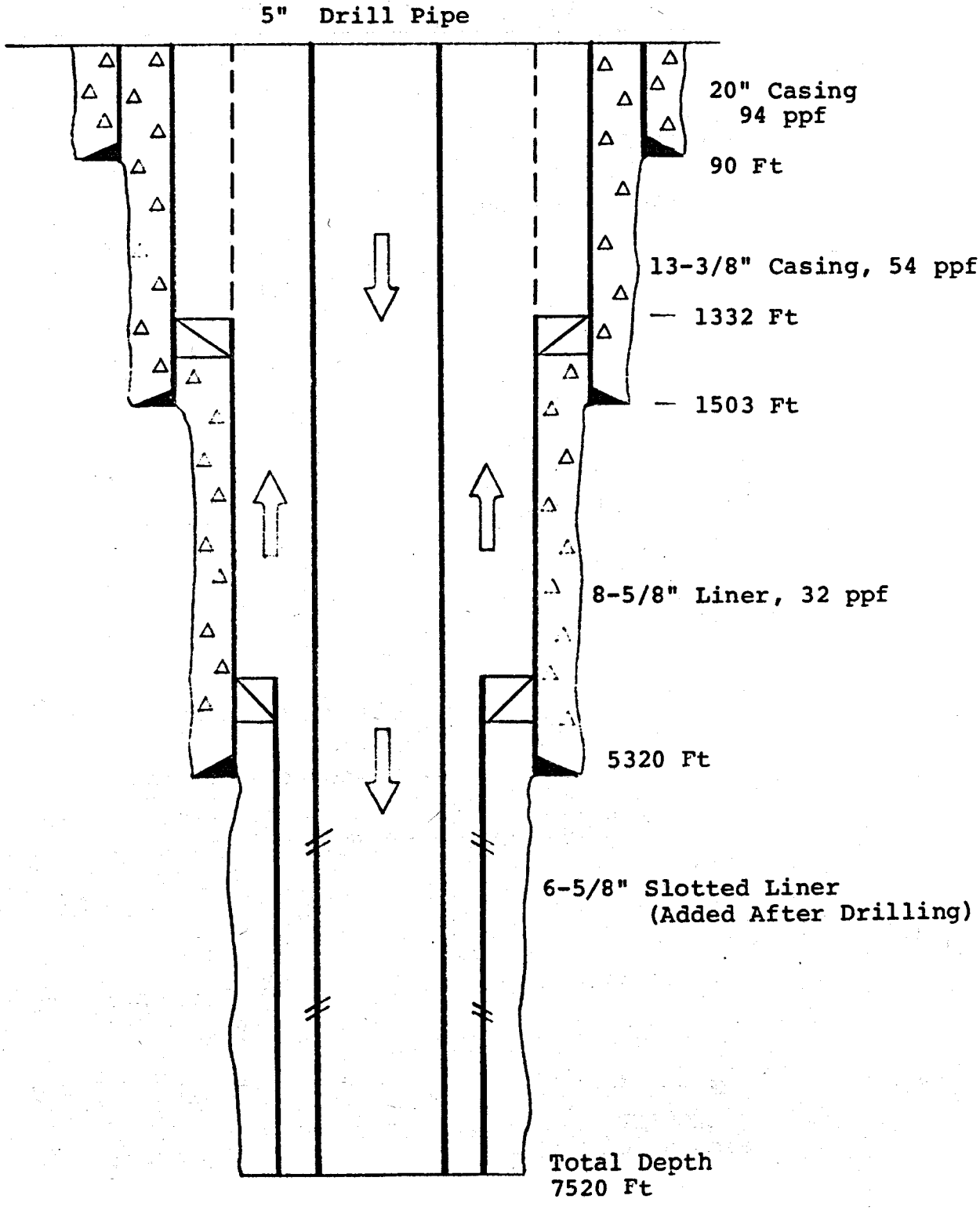

FIGURE 5: Drilling Schedule For
Republic Geothermal Well #56-30

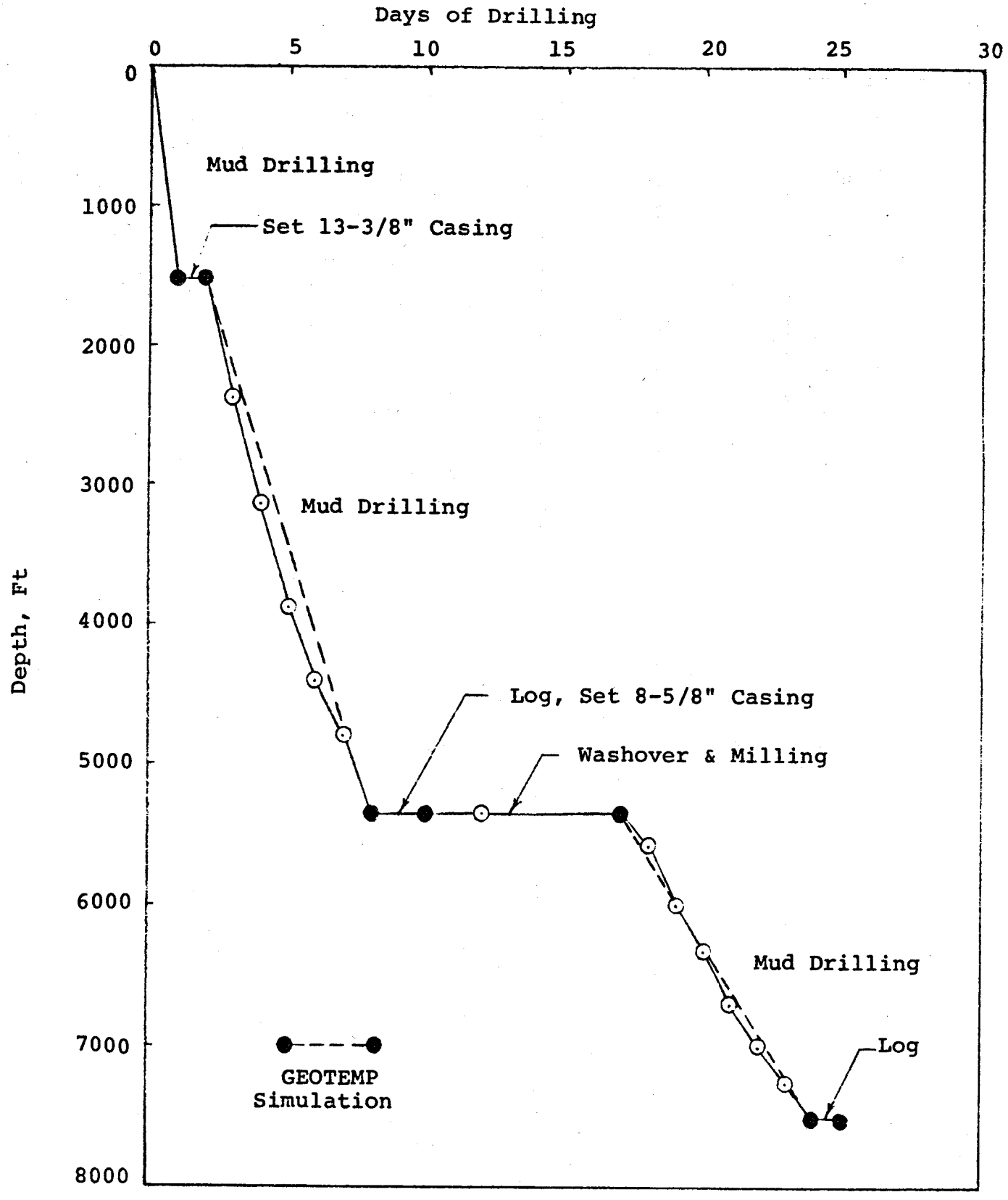

FIGURE 6: Production Well #56-30 for GEOTEMP Simulation

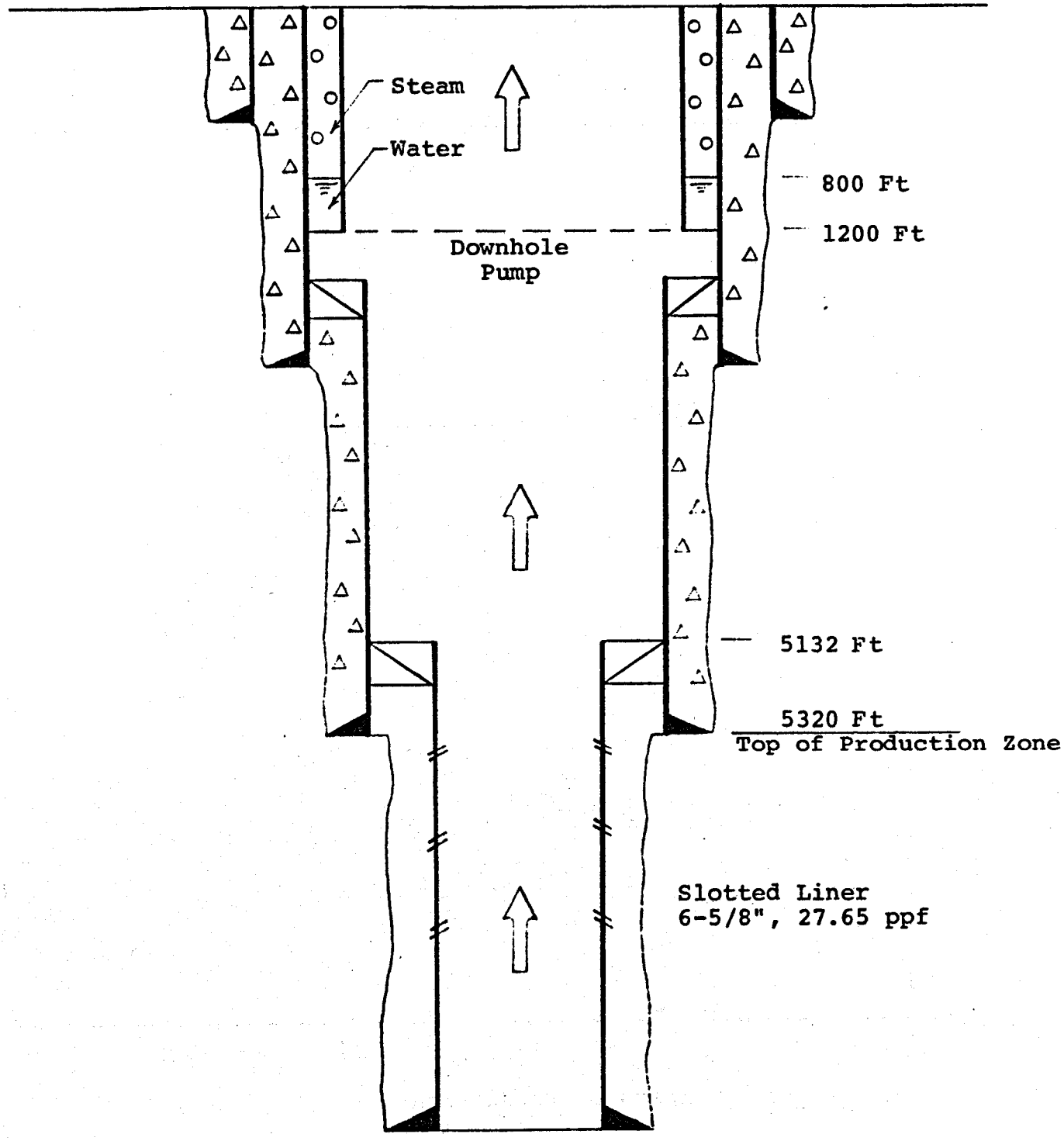

FIGURE 7: Inlet Production Temperature History
For Republic Geothermal Well #56-30

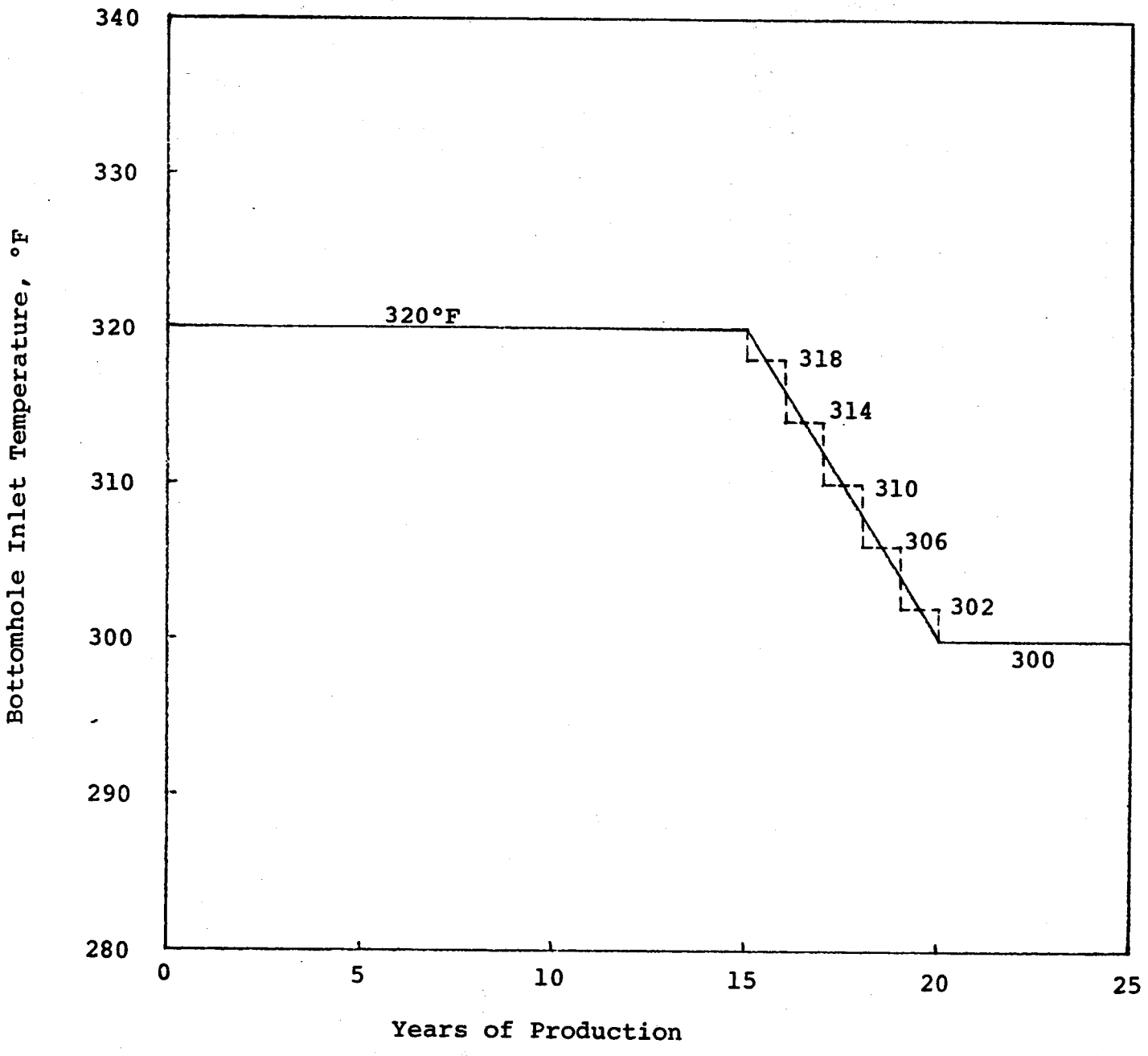

FIGURE 8: Republic Geothermal Injection
Well #52-29 for GEOTEMP Simulation

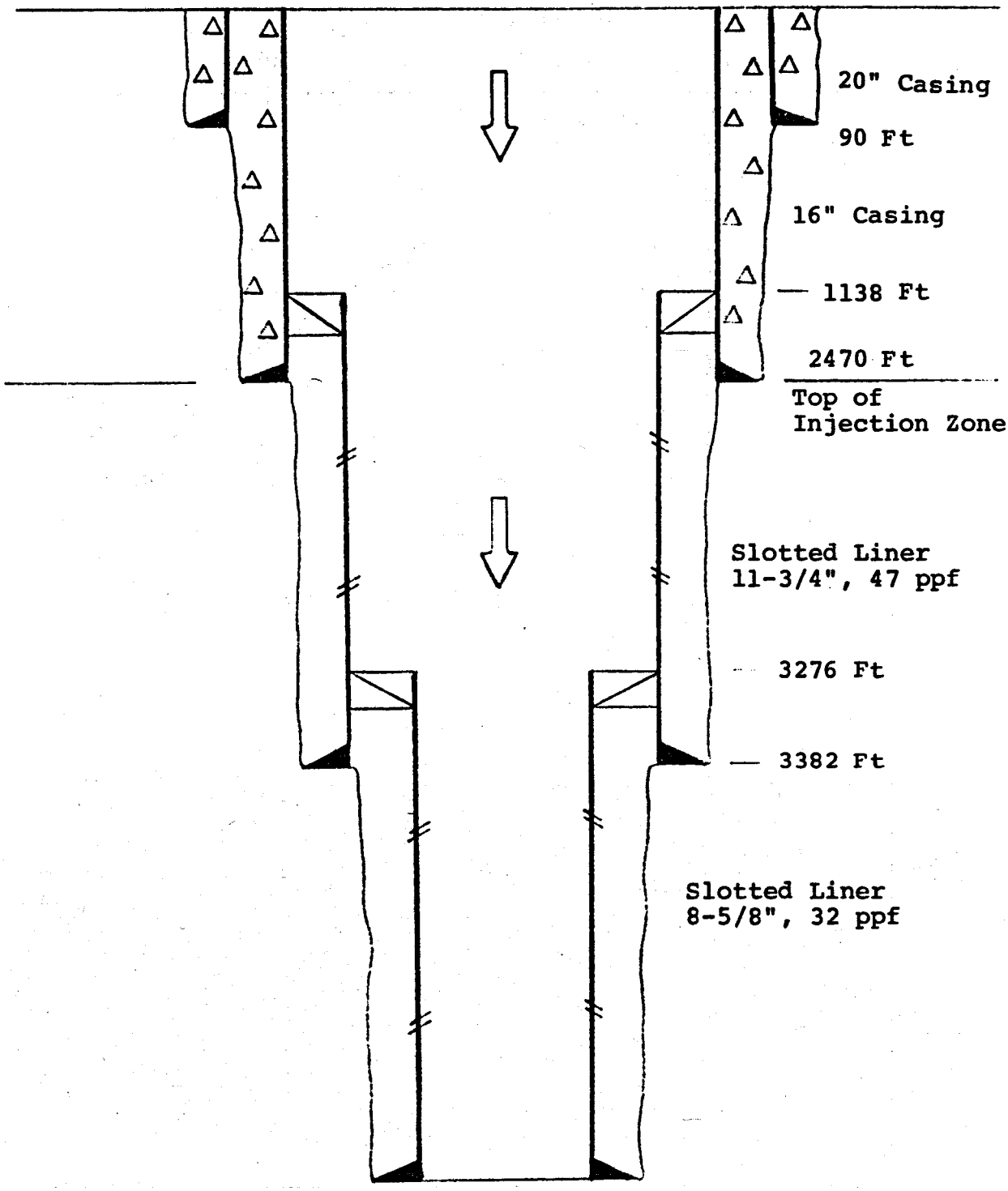

FIGURE 9: Undisturbed Geothermal Profile
for Republic Geothermal Well #52-29

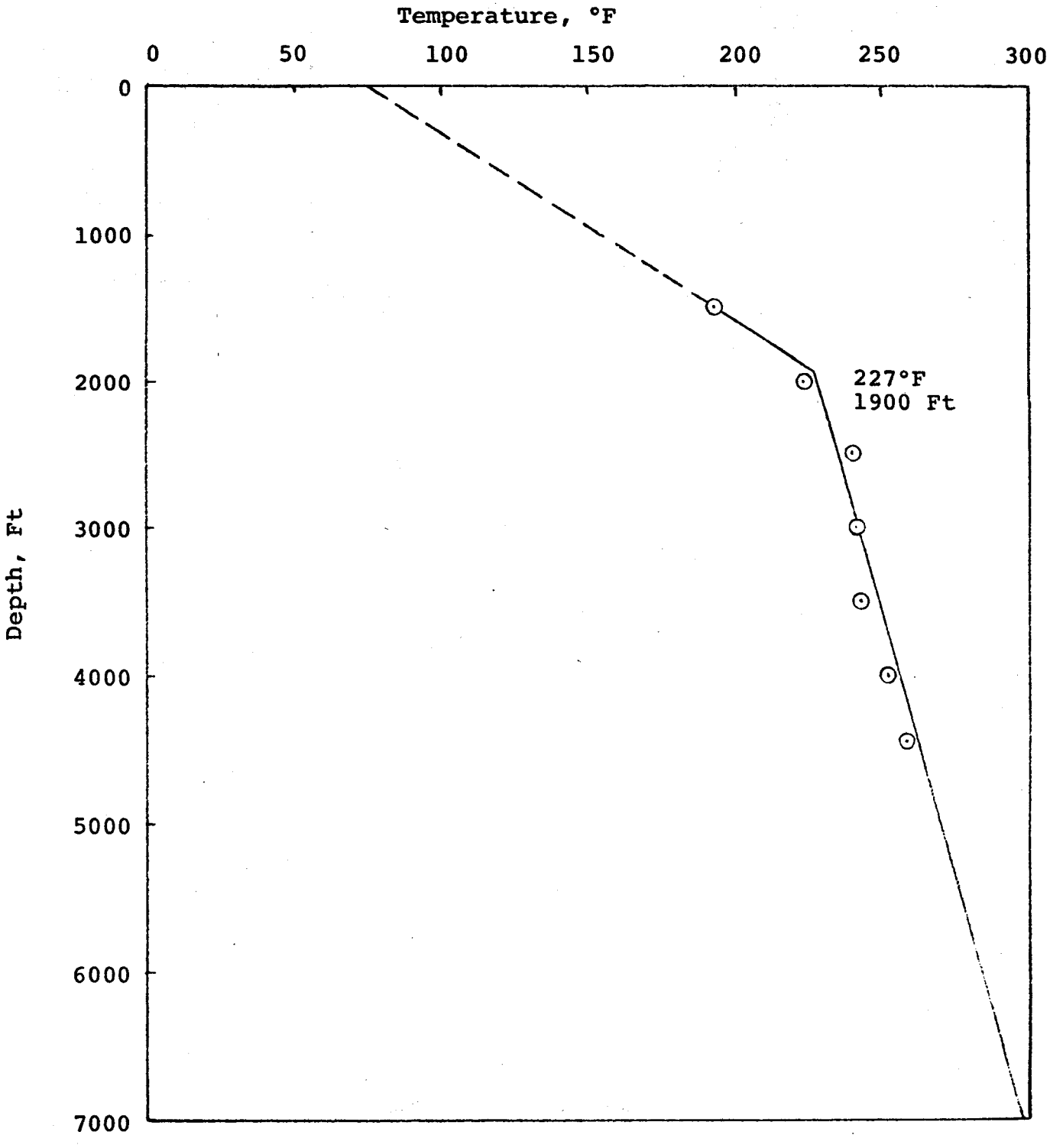

FIGURE 10

GT-2 WELL COMPLETION
FOR GEOTEMP SIMULATION

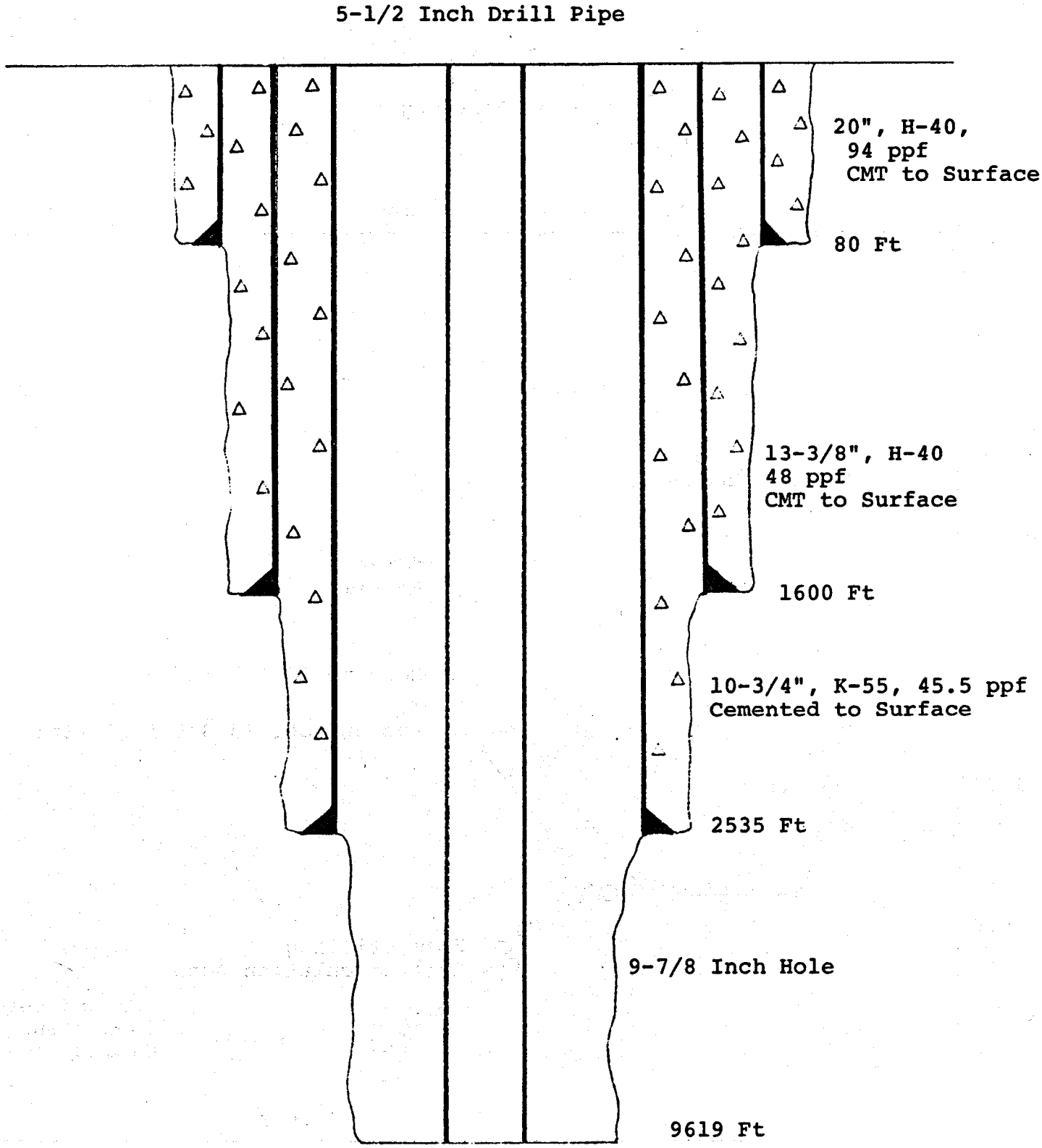

FIGURE 11: Drilling Schedule for Los Alamos GT-2 Well (Dashed straight lines between closed circles represent GEOTEMP simulation)

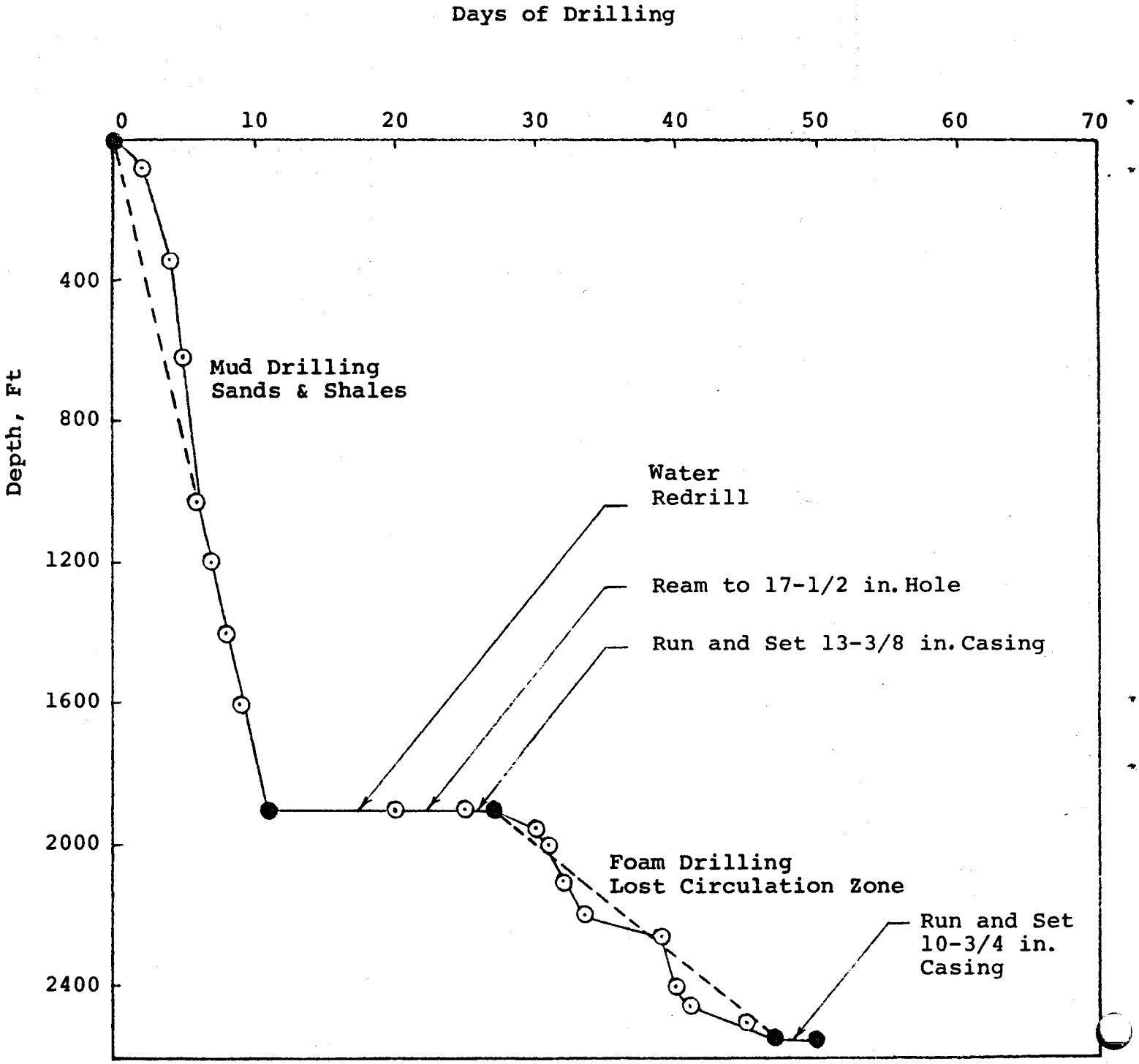

FIGURE 11 (Continued): GT-2 Drilling Schedule

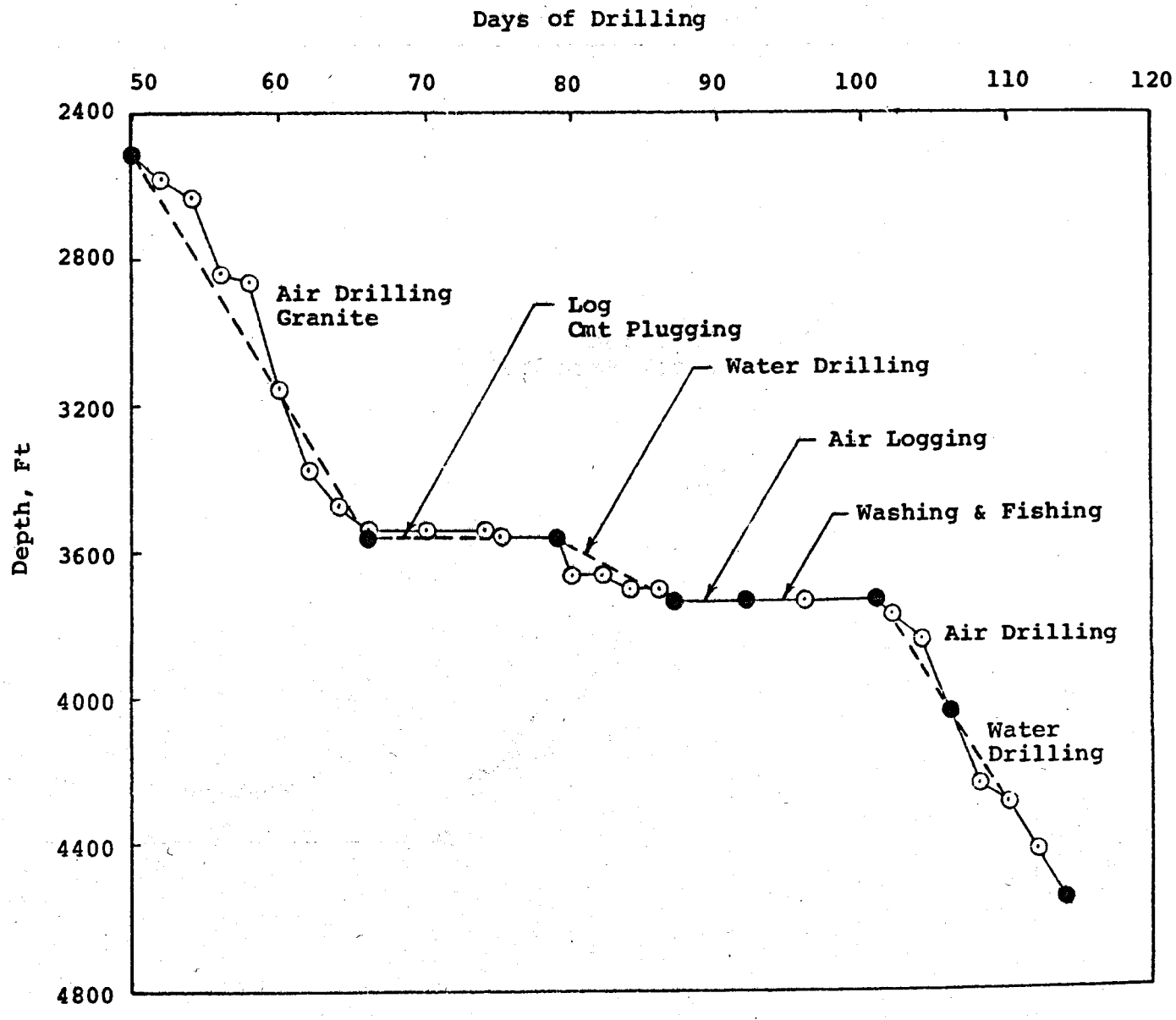

FIGURE 11 (Continued): GT-2 Drilling Schedule

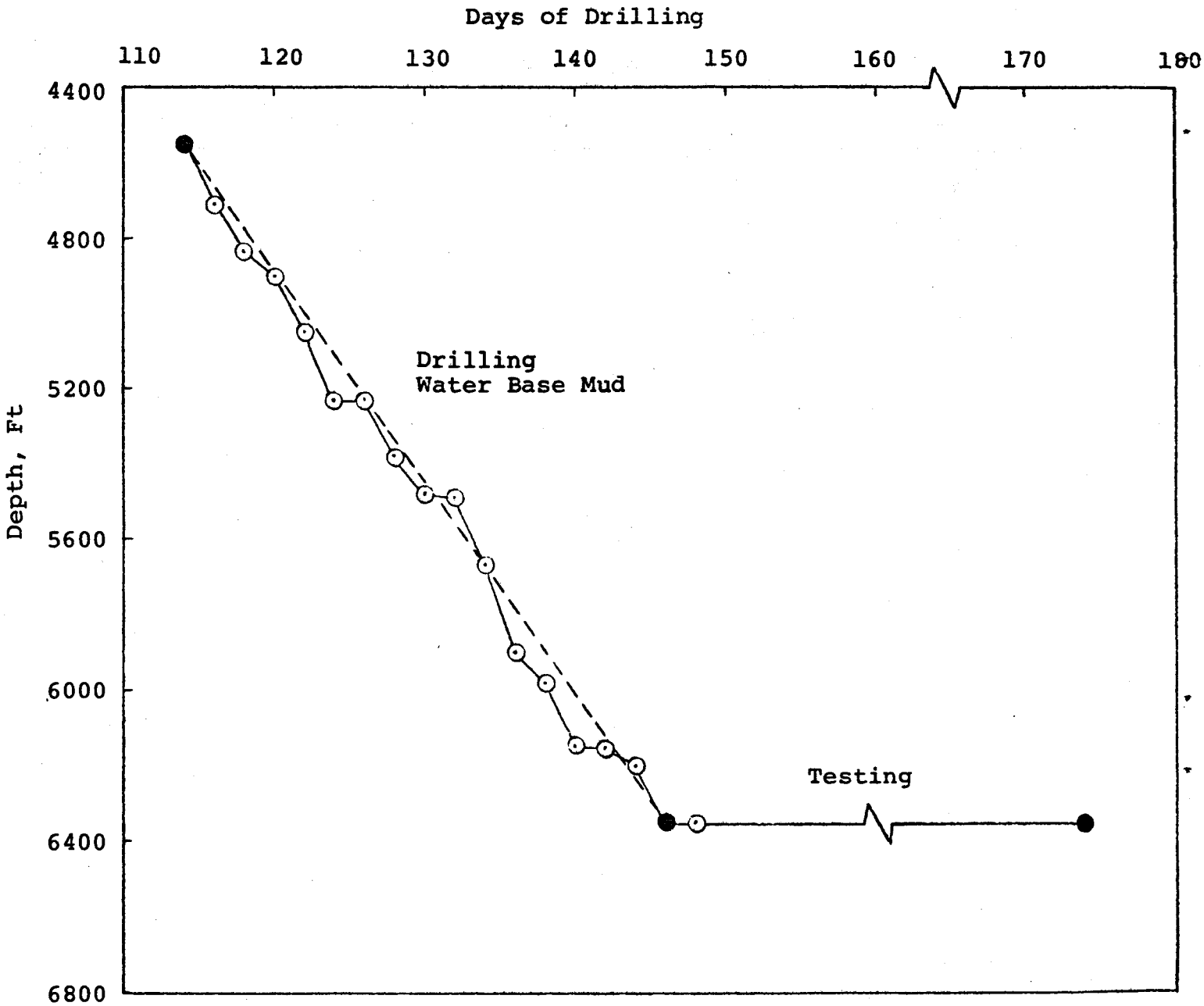

FIGURE 11 (Continued): GT-2 Drilling Schedule

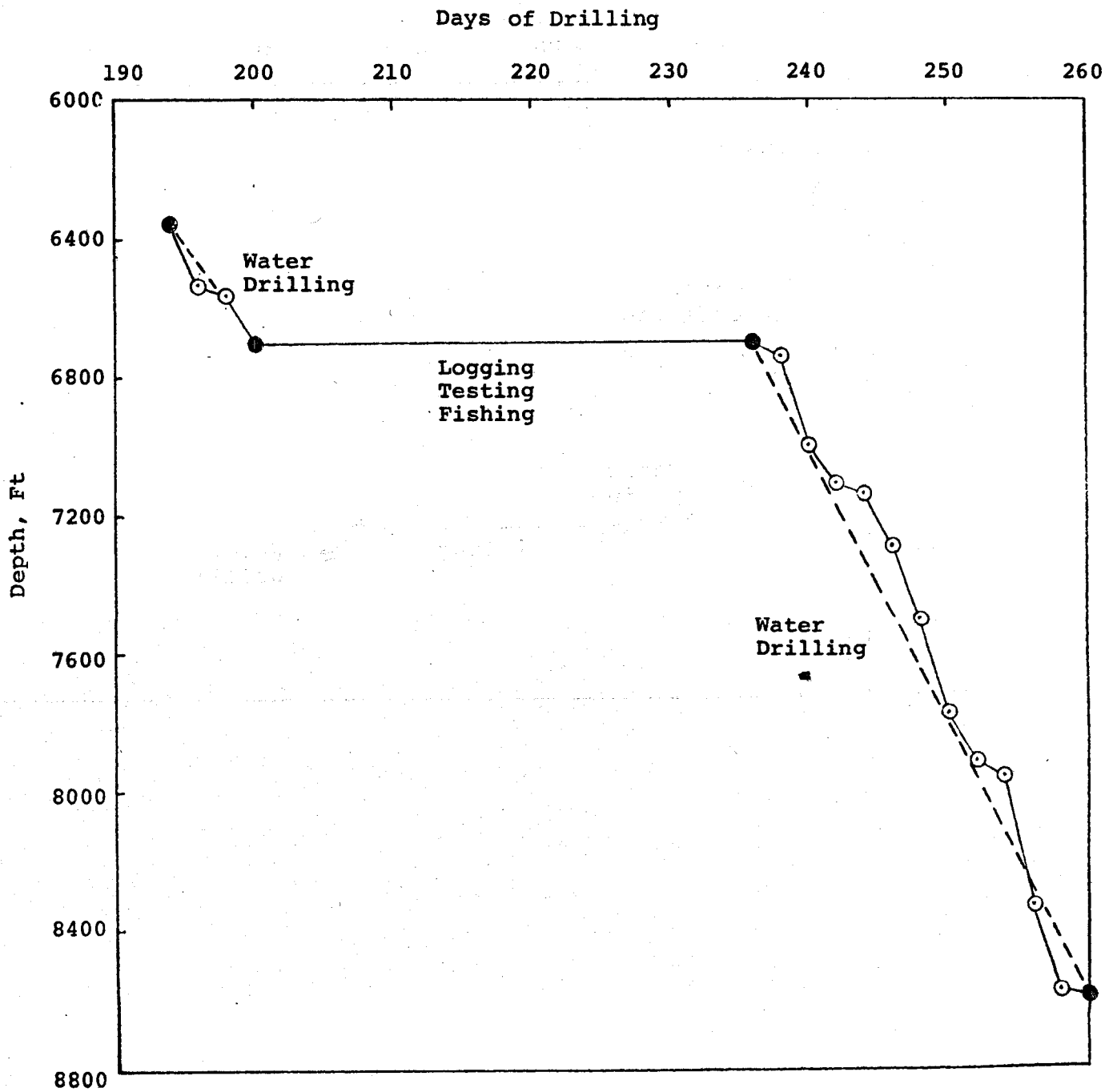

FIGURE 11 (Continued): GT-2 Drilling Schedule

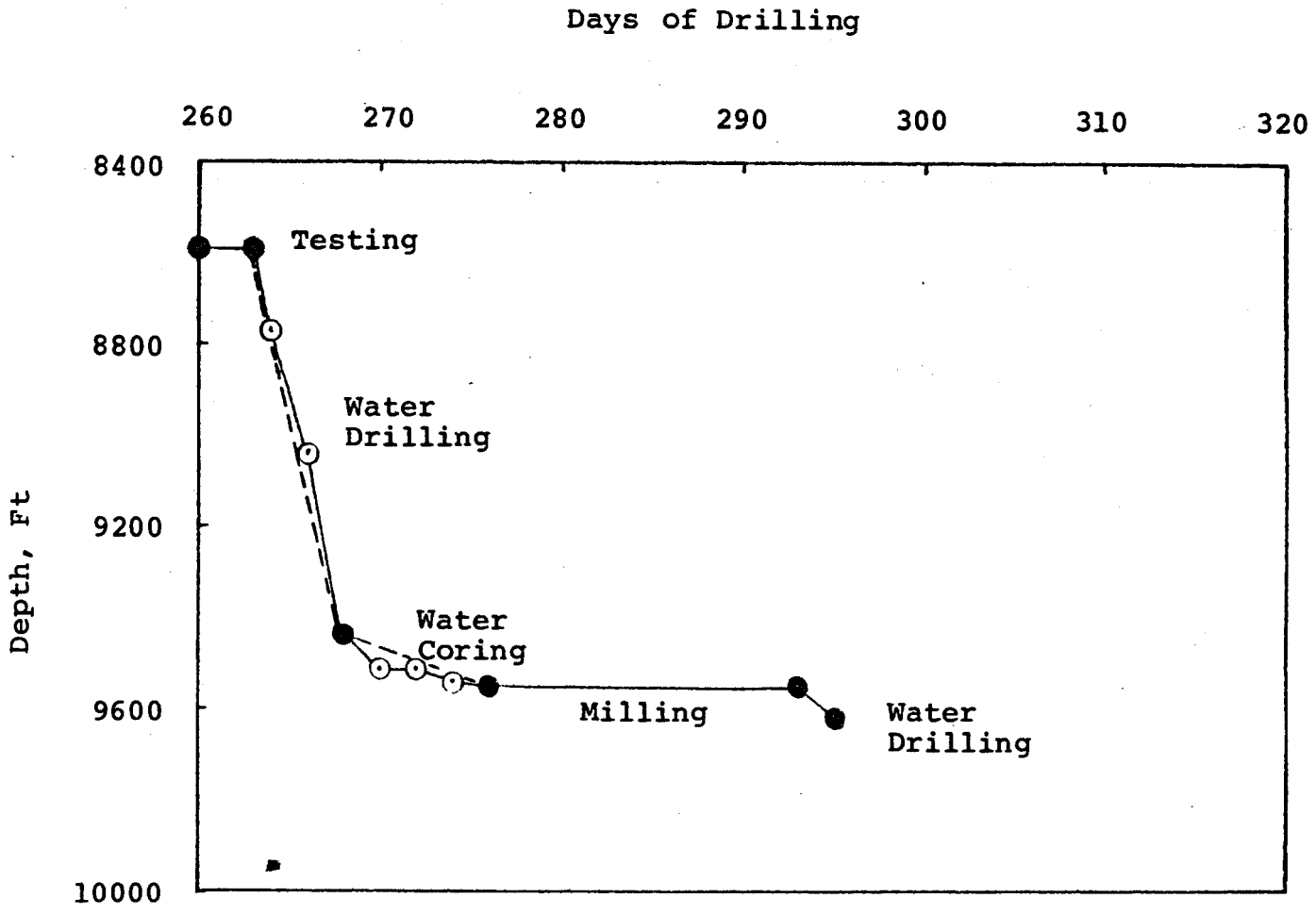

FIGURE 12: Production Inlet Temperature Variation With Time for Hot Dry Rock Circulation Loop

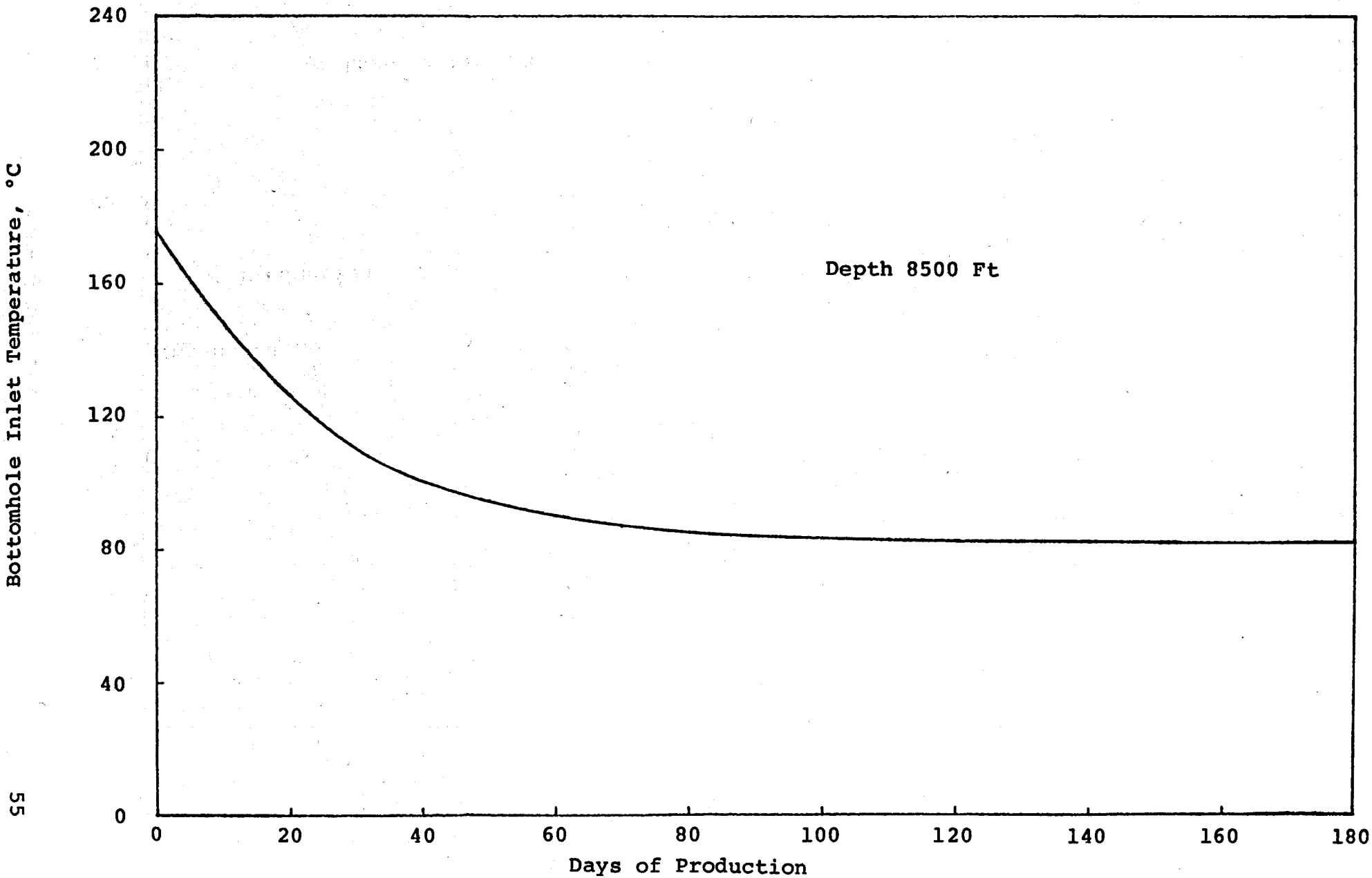

FIGURE 13: Injection and Production Rates for Hot Dry Rock Circulation Loop

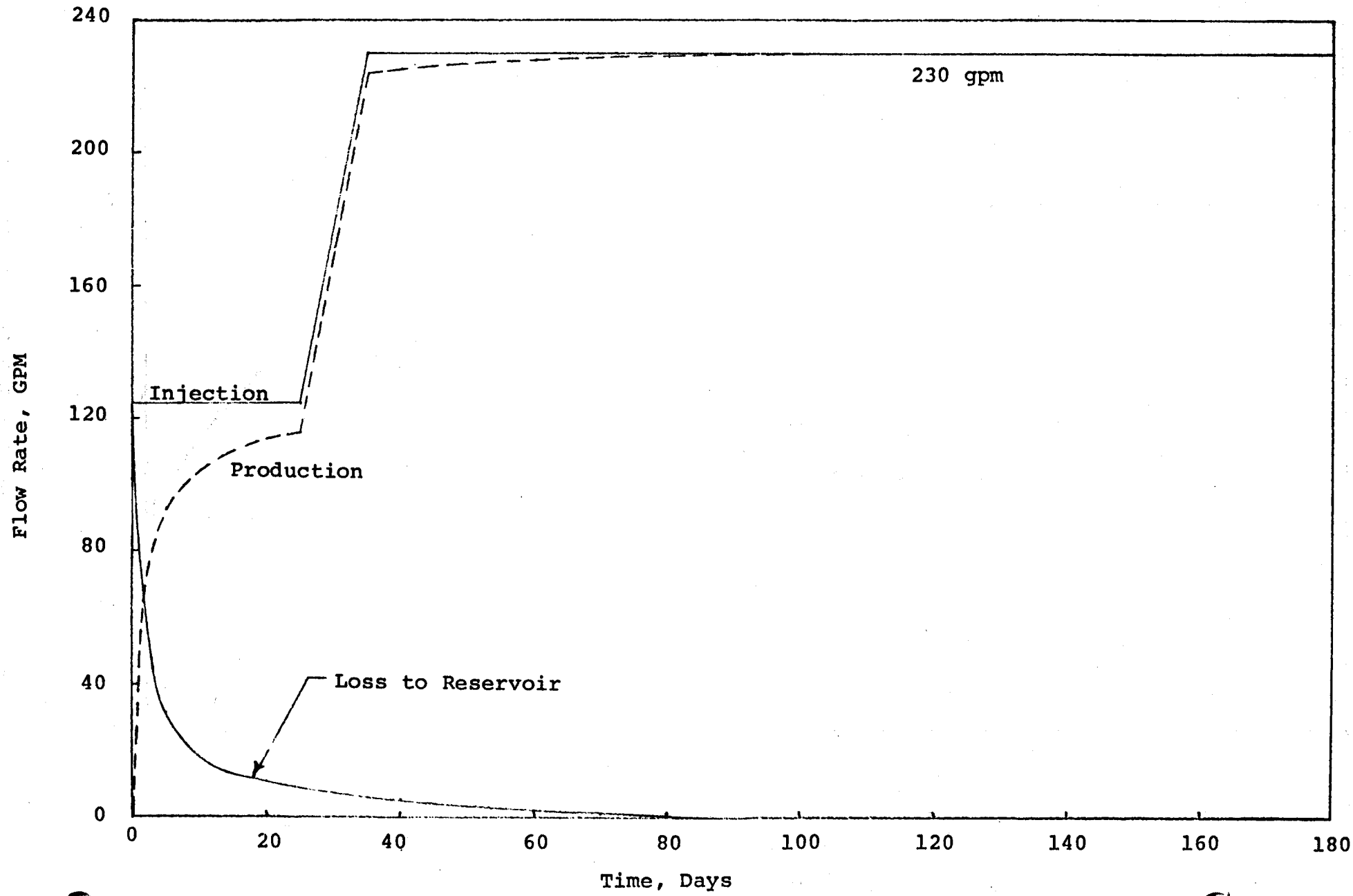

FIGURE 14: Los Alamos GT-2 Drilling
Temperature Profiles

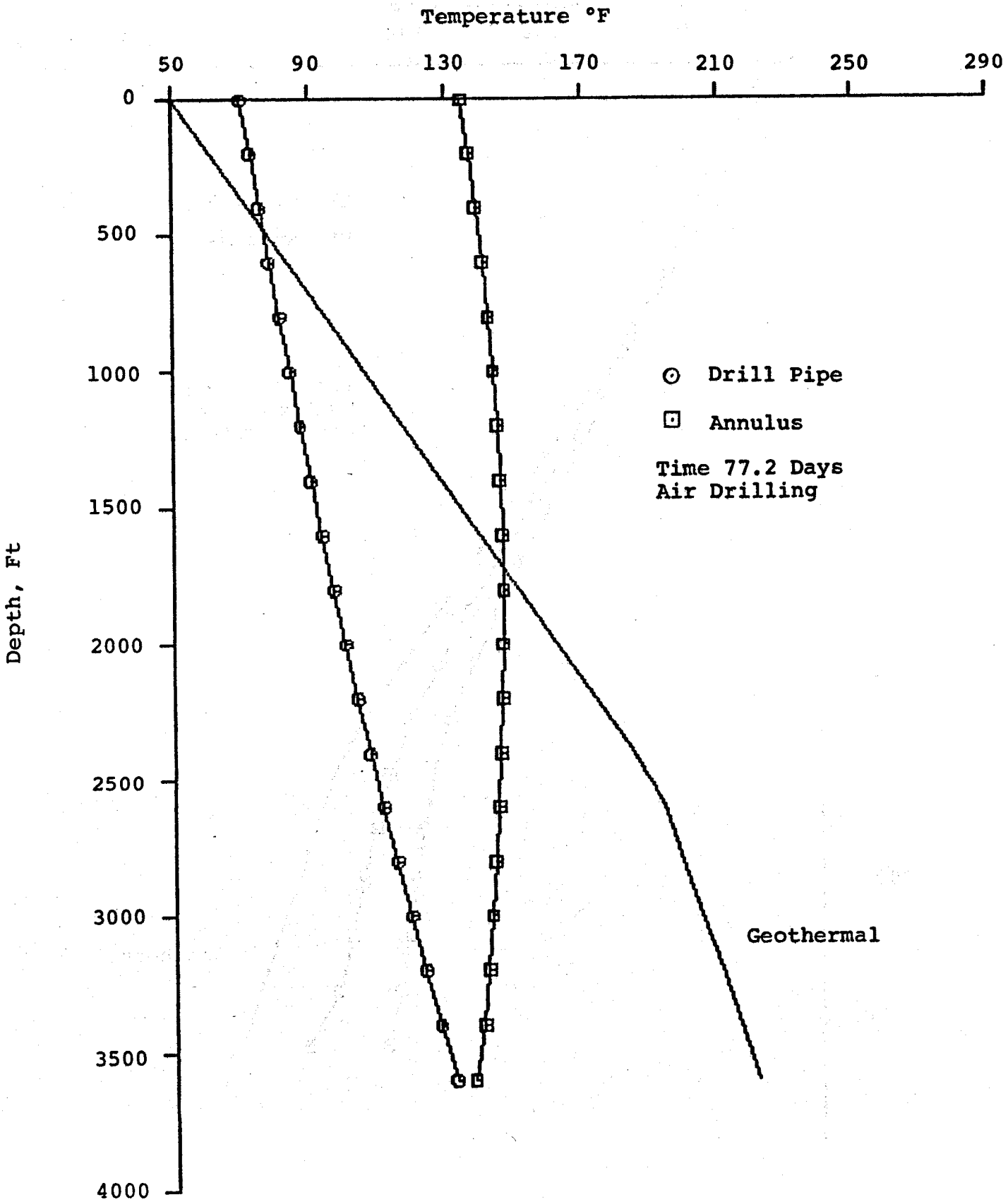

FIGURE 15: Los Alamos GT-2 Drilling Temperature Profiles

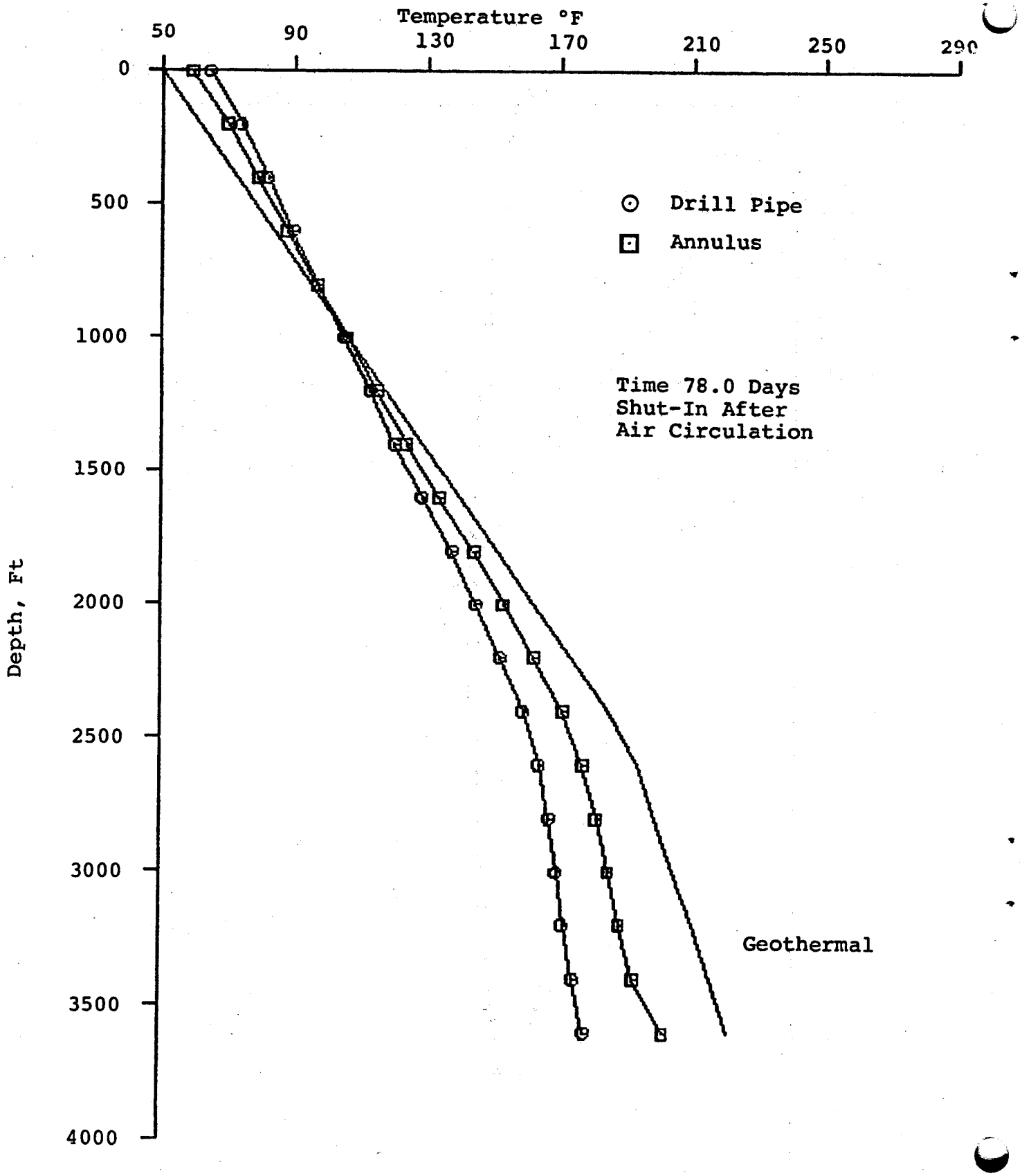

FIGURE 16: Los Alamos GT-2 Drilling
Temperature Profiles

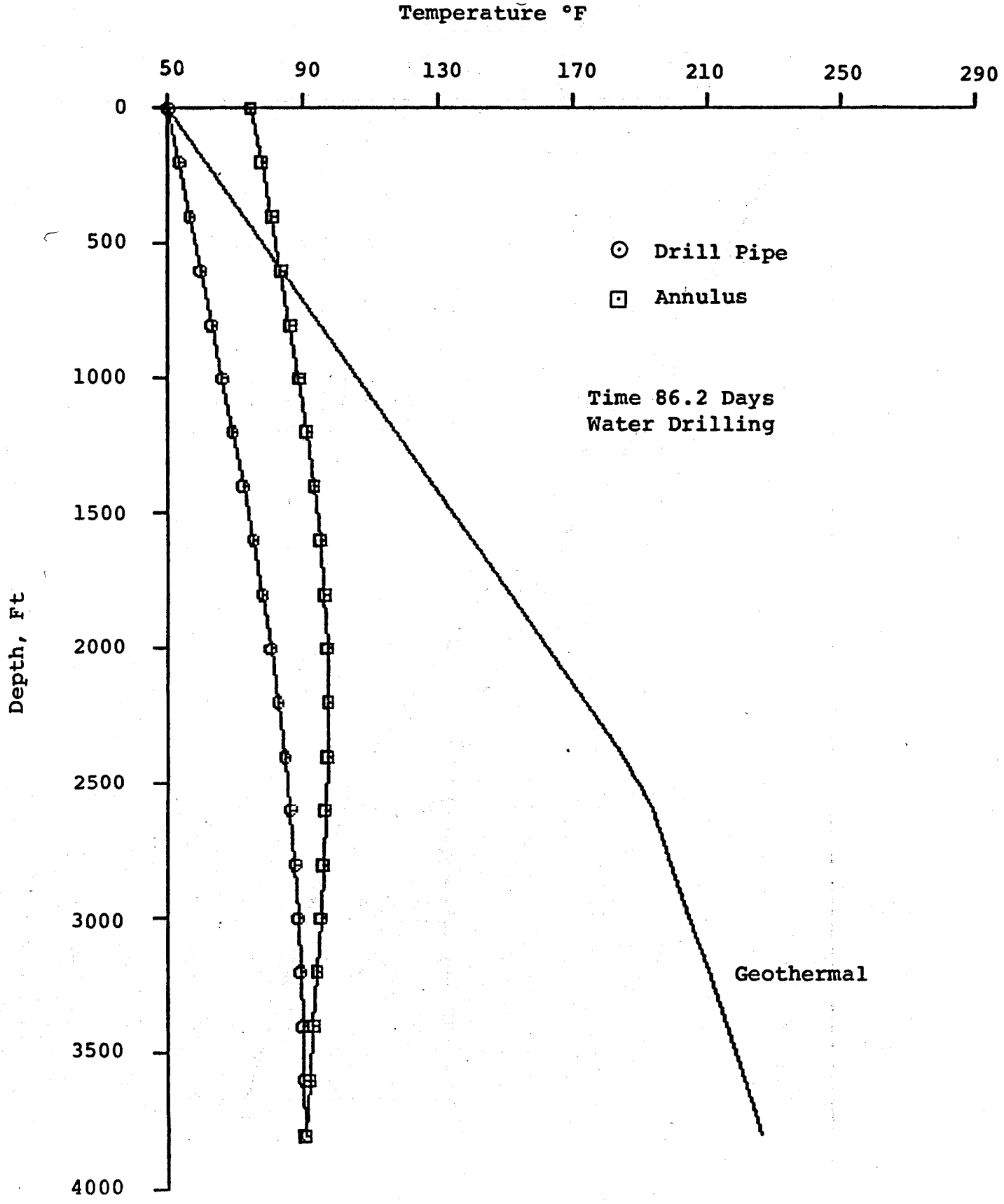

FIGURE 17: Los Alamos GT-2 Well Drilling Temperature Profiles

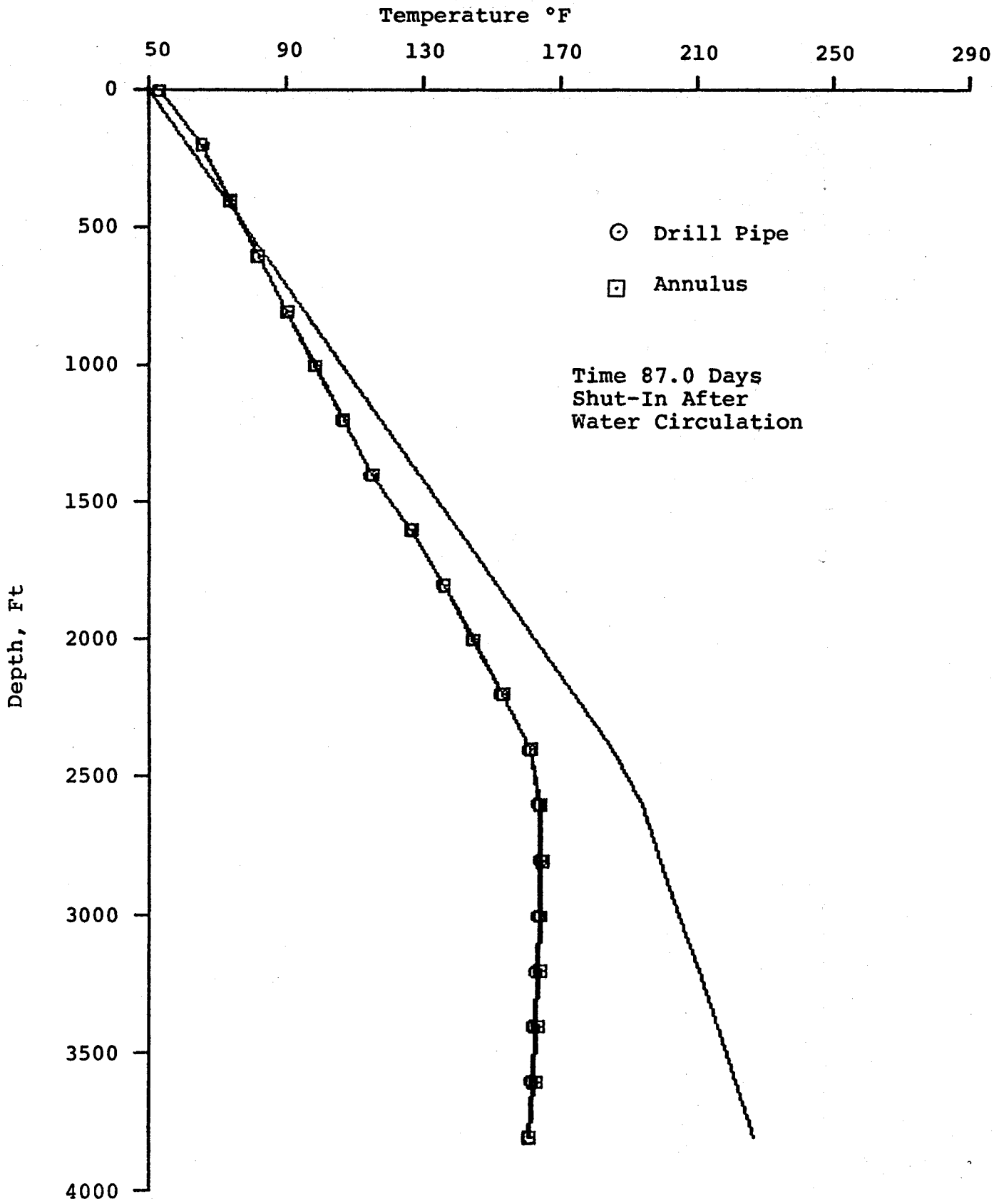

FIGURE 18: Republic Geothermal Well 56-30
Drilling Temperature Profile

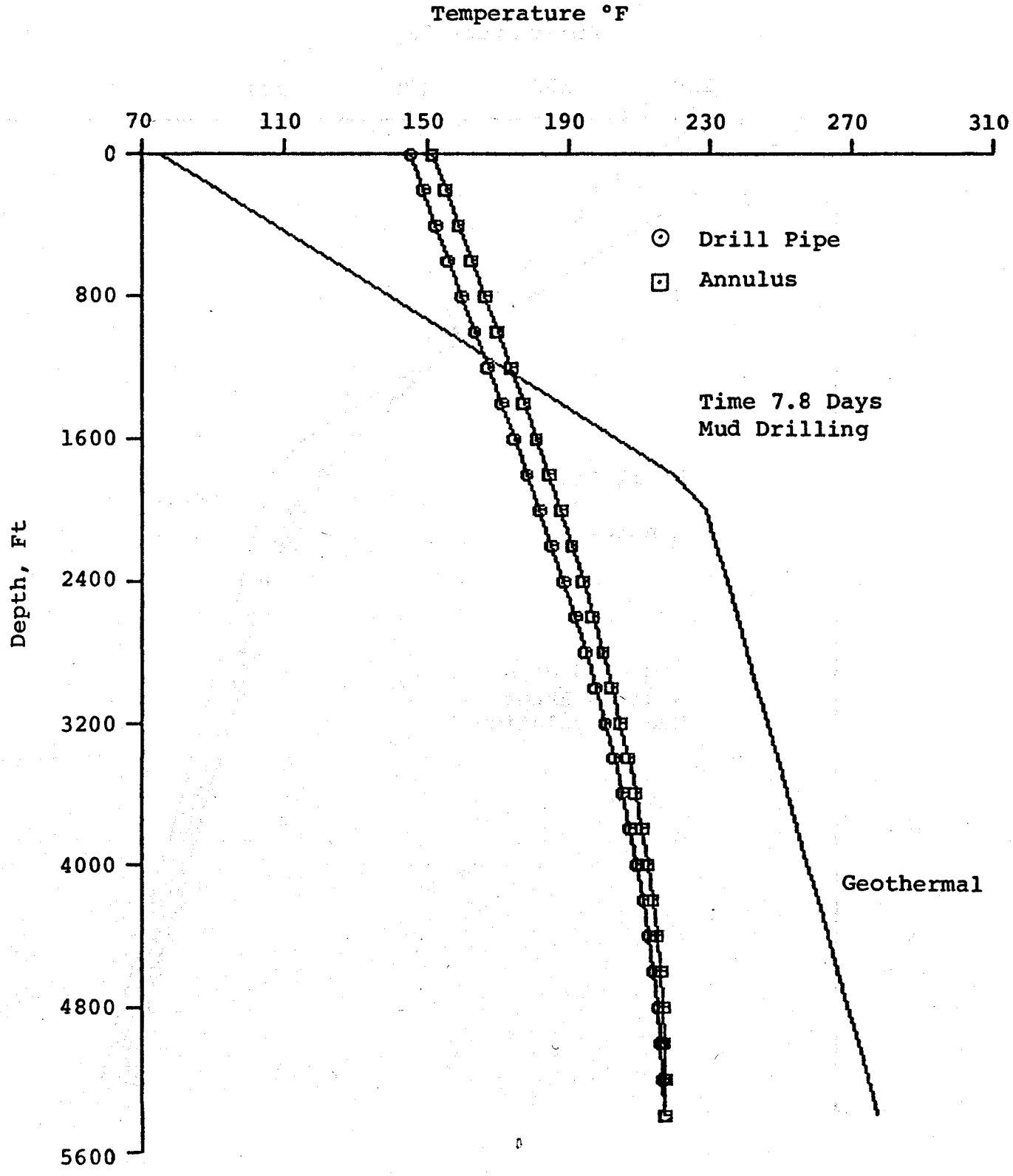

FIGURE 19: Republic Geothermal Well 56-30
Drilling Temperature Profiles

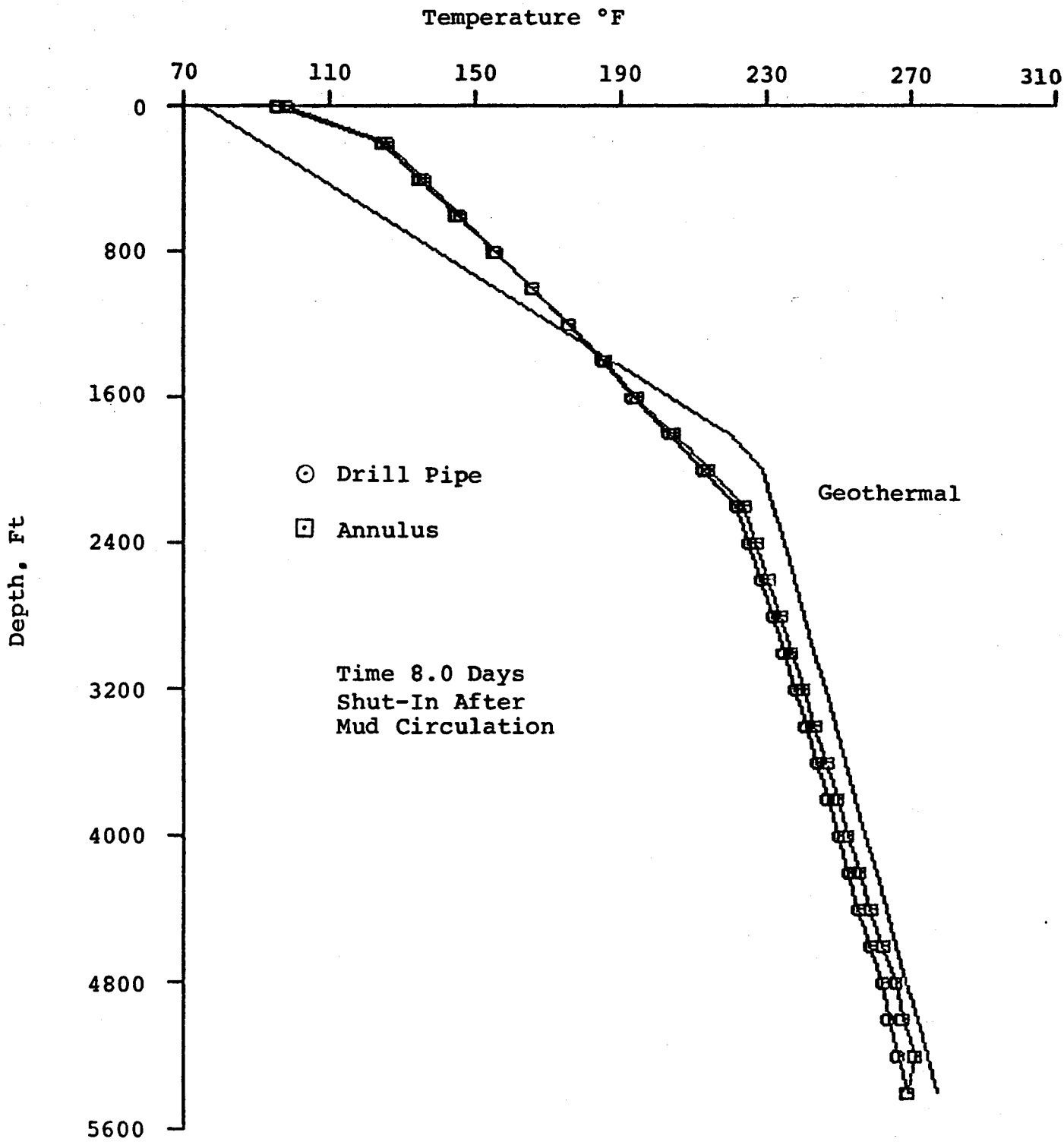

FIGURE 20: Los Alamos GT-2 Drill Bit Temperatures

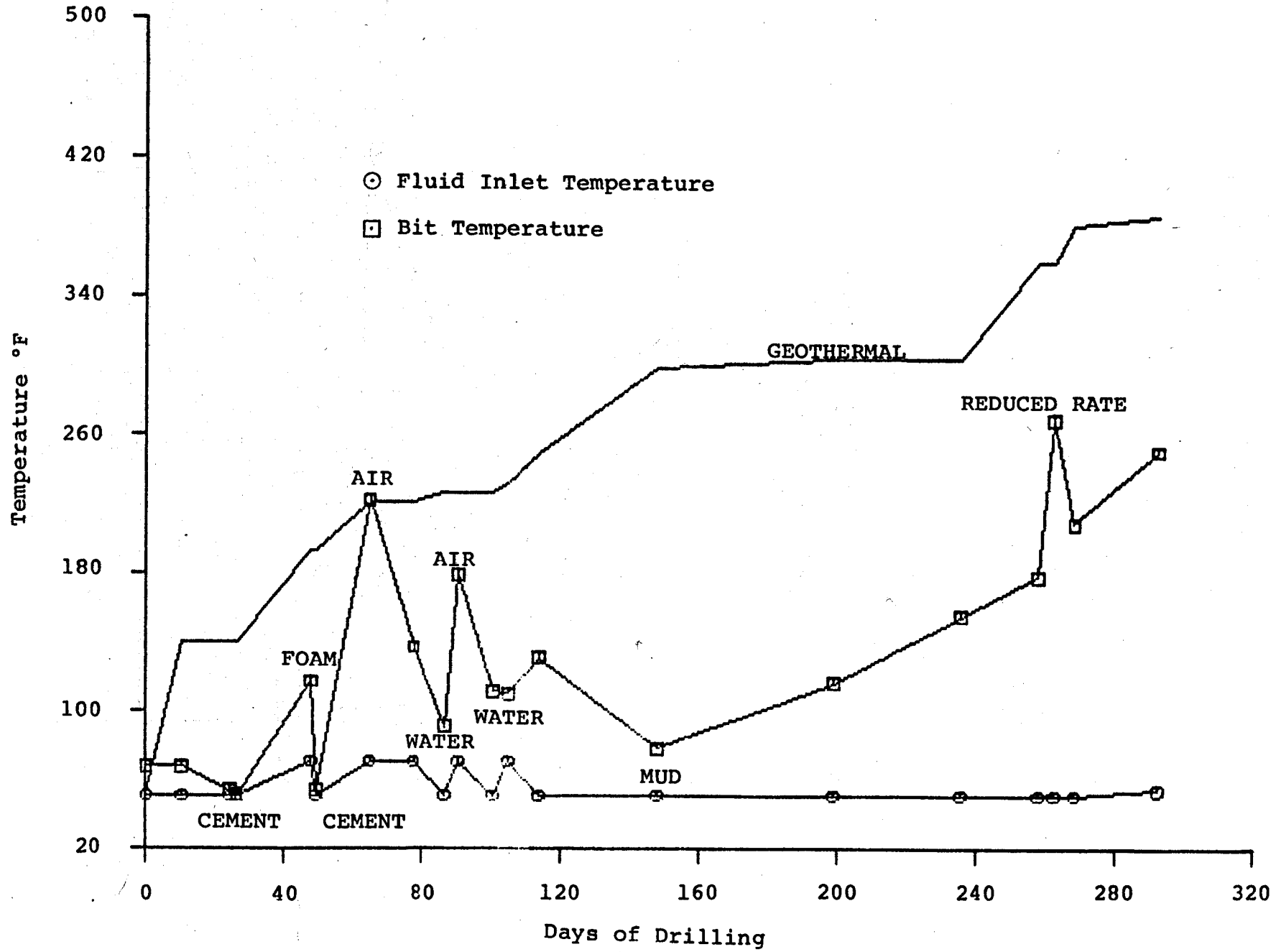

FIGURE 21: Republic Geothermal 56-30
Drill Bit Temperatures

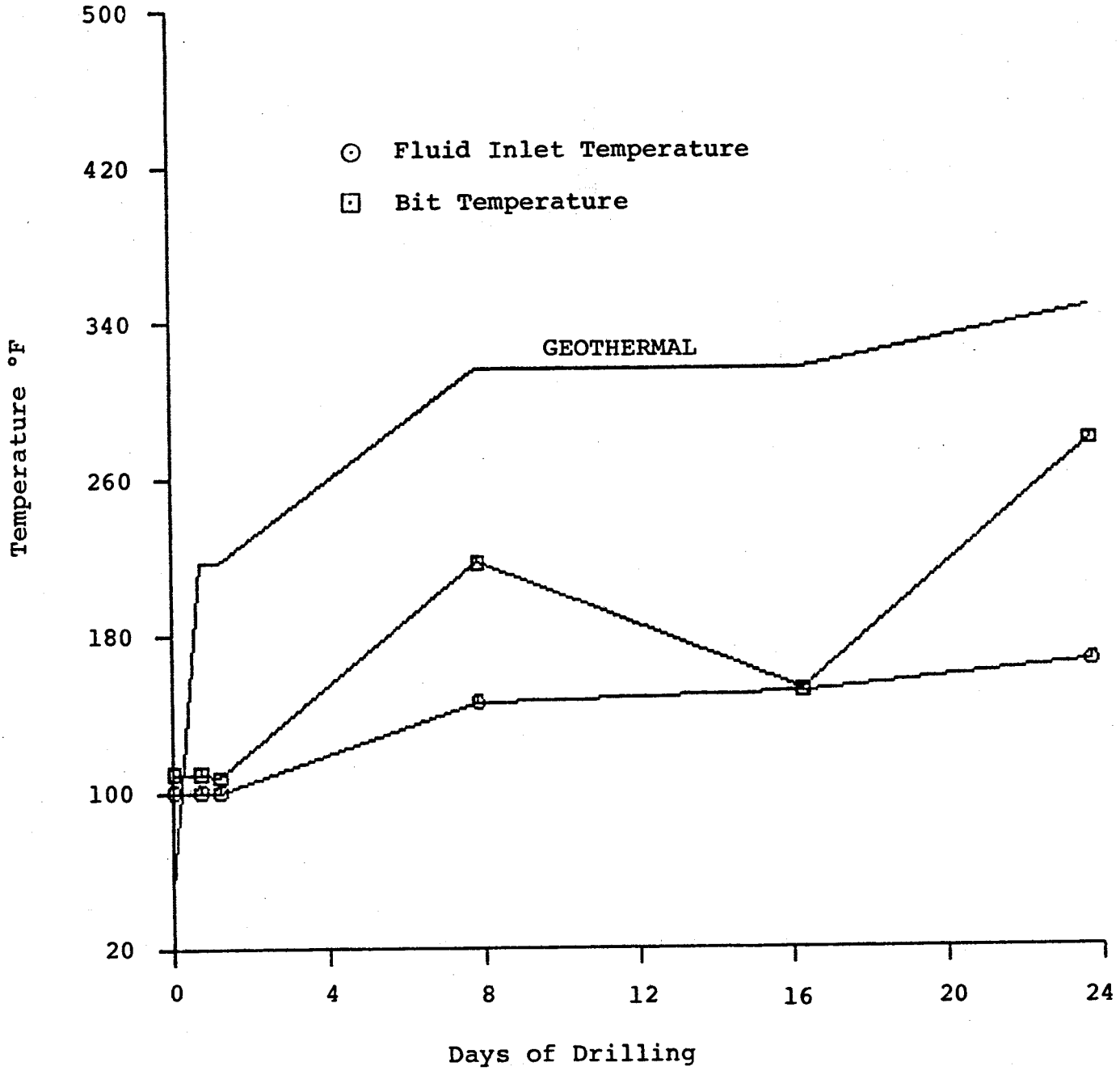

FIGURE 22: Los Alamos GT-2 Cement and Formation Temperatures

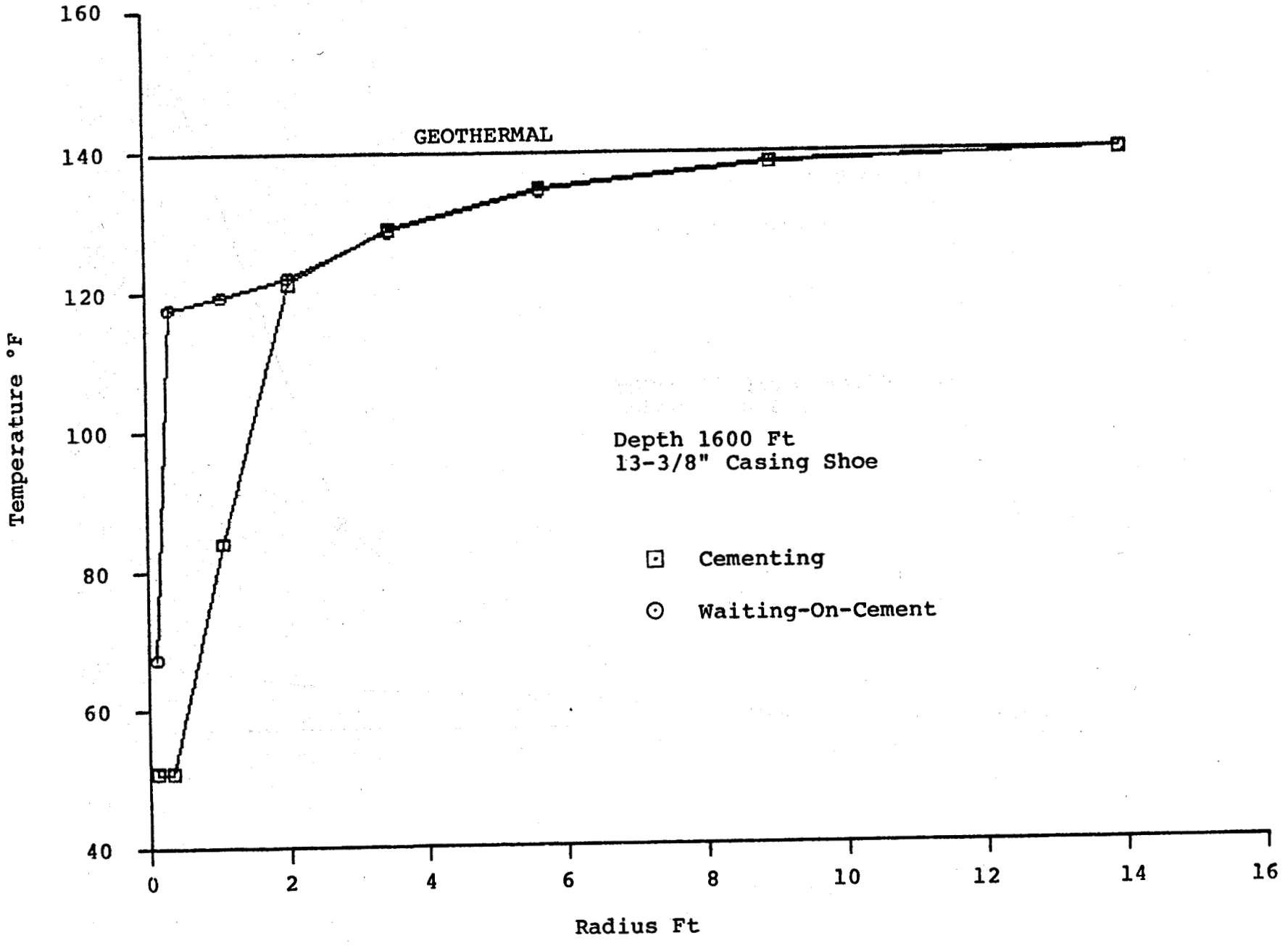

FIGURE 23: Republic Geothermal 56-30 Cement and Formation Temperatures

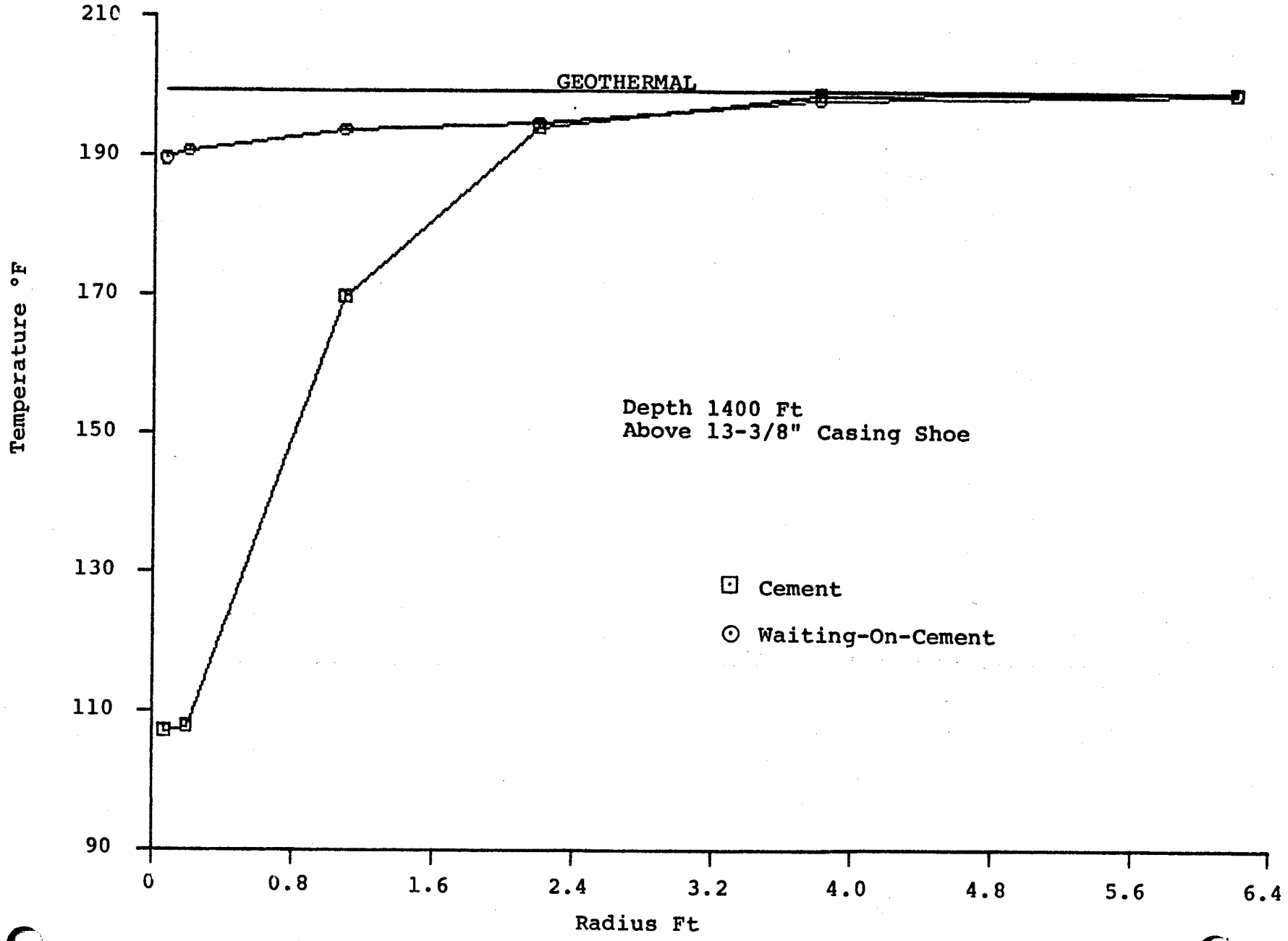

FIGURE 24: Los Alamos GT-2 Casing Temperature History During Drilling

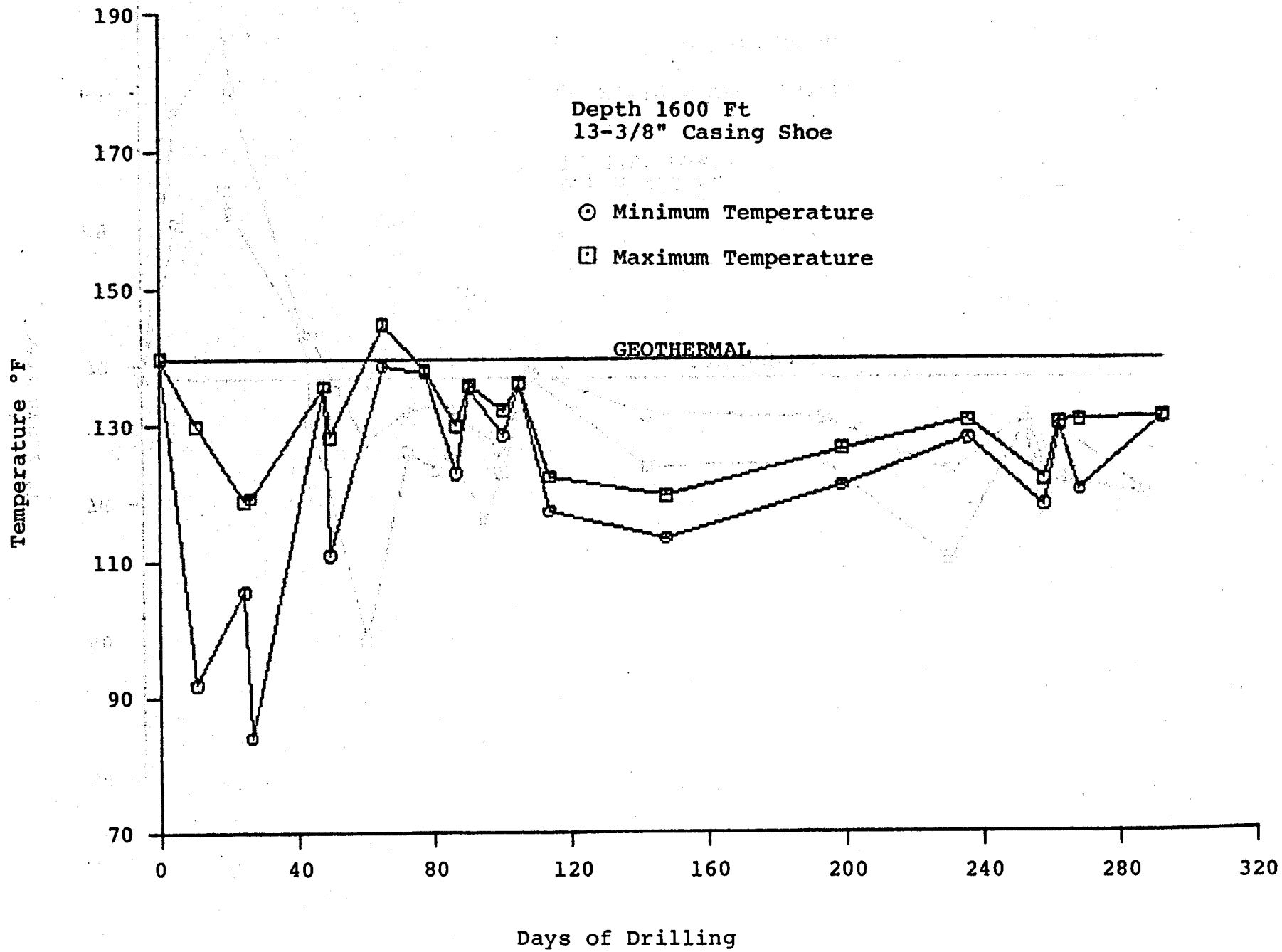

FIGURE 25: Los Alamos GT-2 Casing Temperature History During Drilling

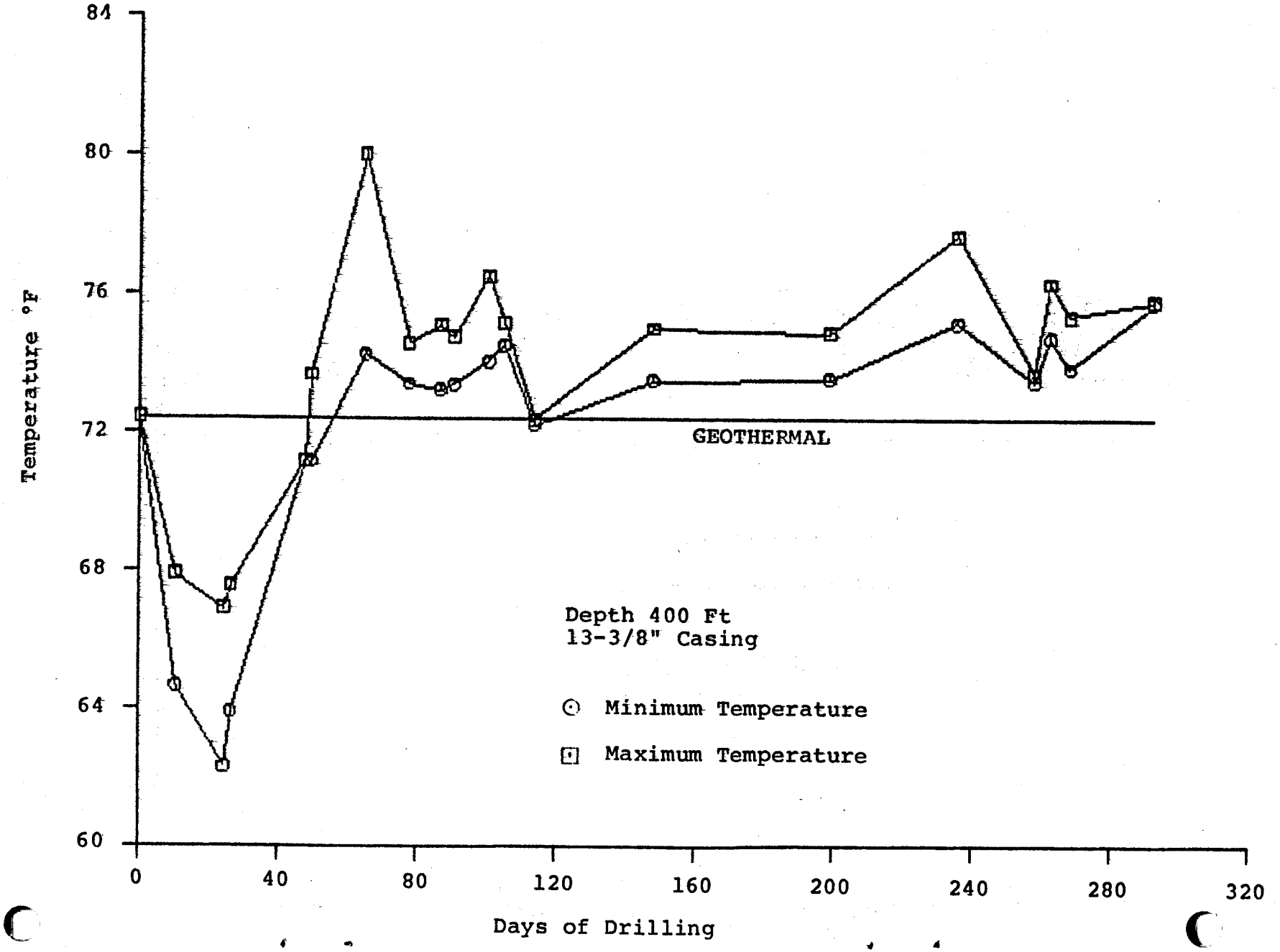

FIGURE 26: Republic Geothermal 56-30 Casing
Temperature History During Drilling

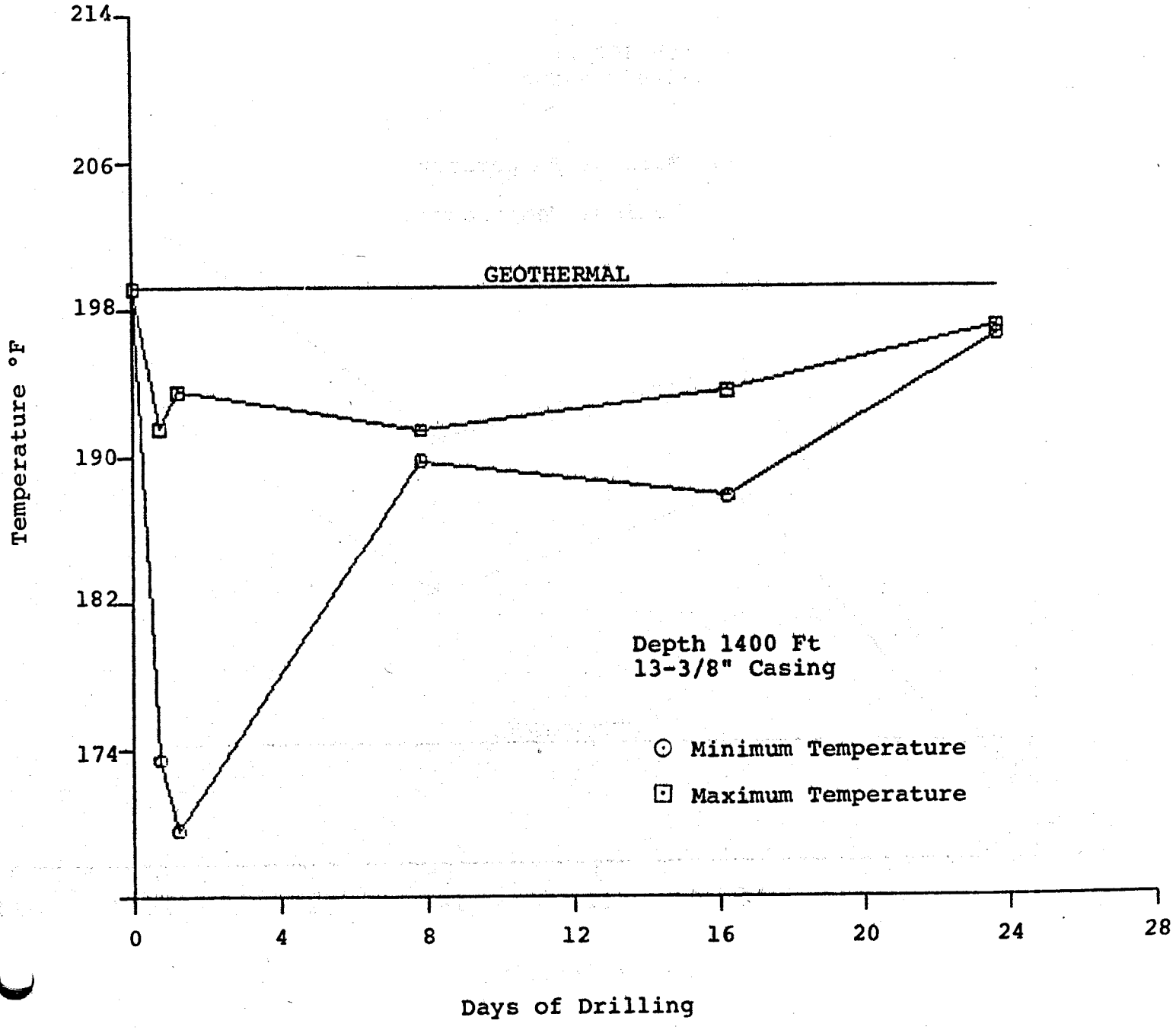

FIGURE 27: Republic Geothermal 56-30
Casing Temperature History
During Drilling

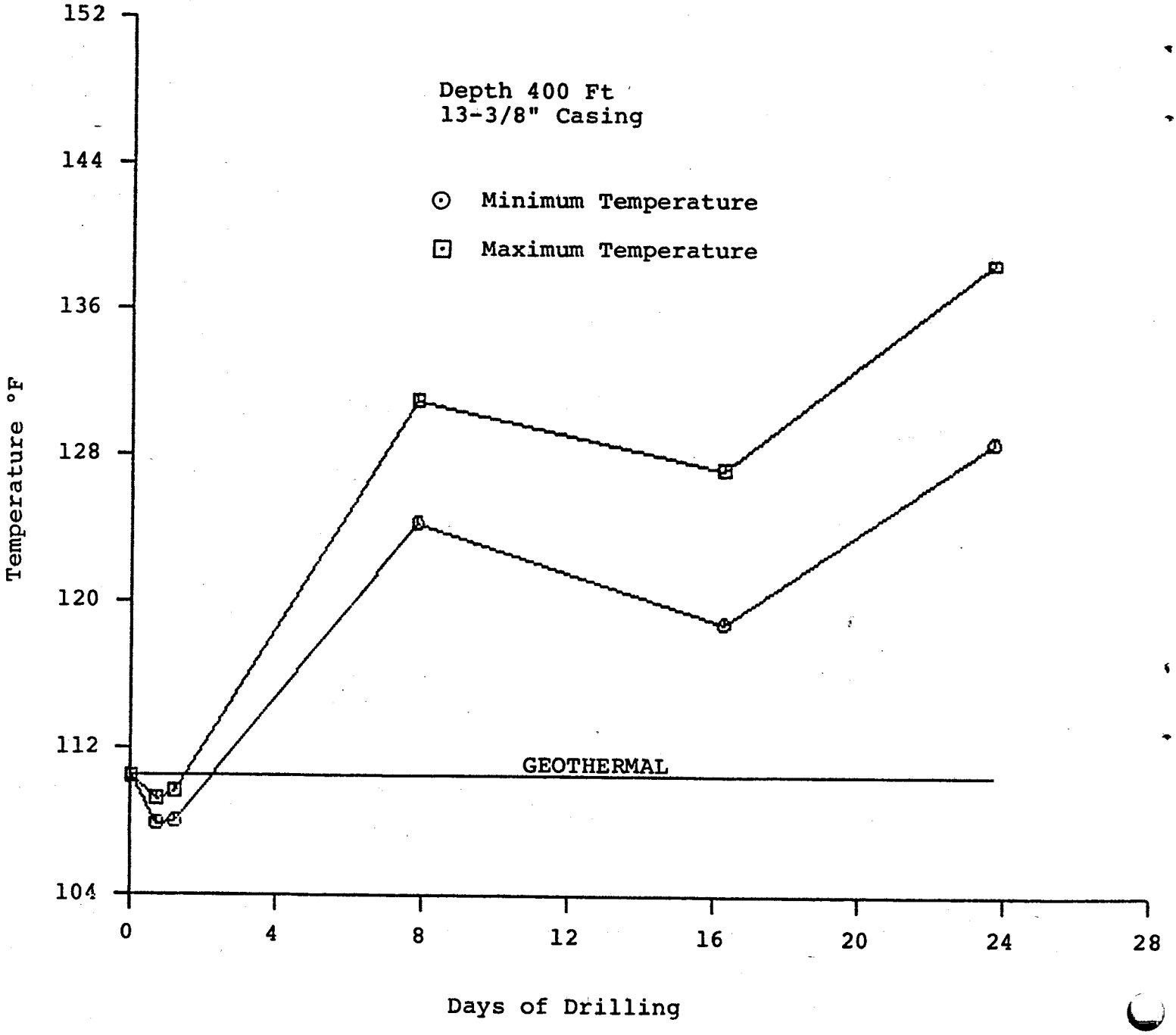

FIGURE 28: Los Alamos GT-2 Production Temperature Profiles at Early Time

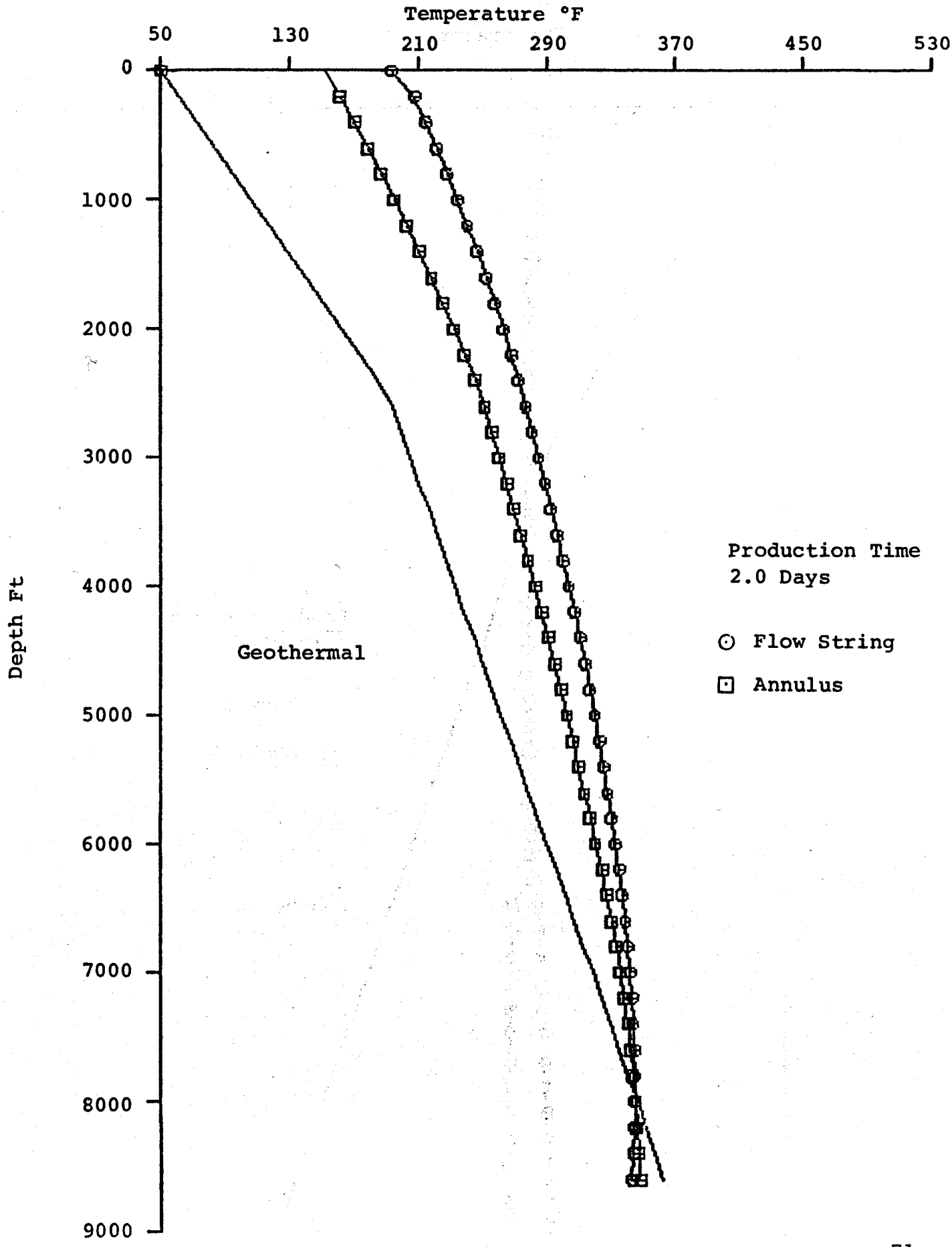

FIGURE 29: Los Alamos GT-2 Production Temperature Profiles

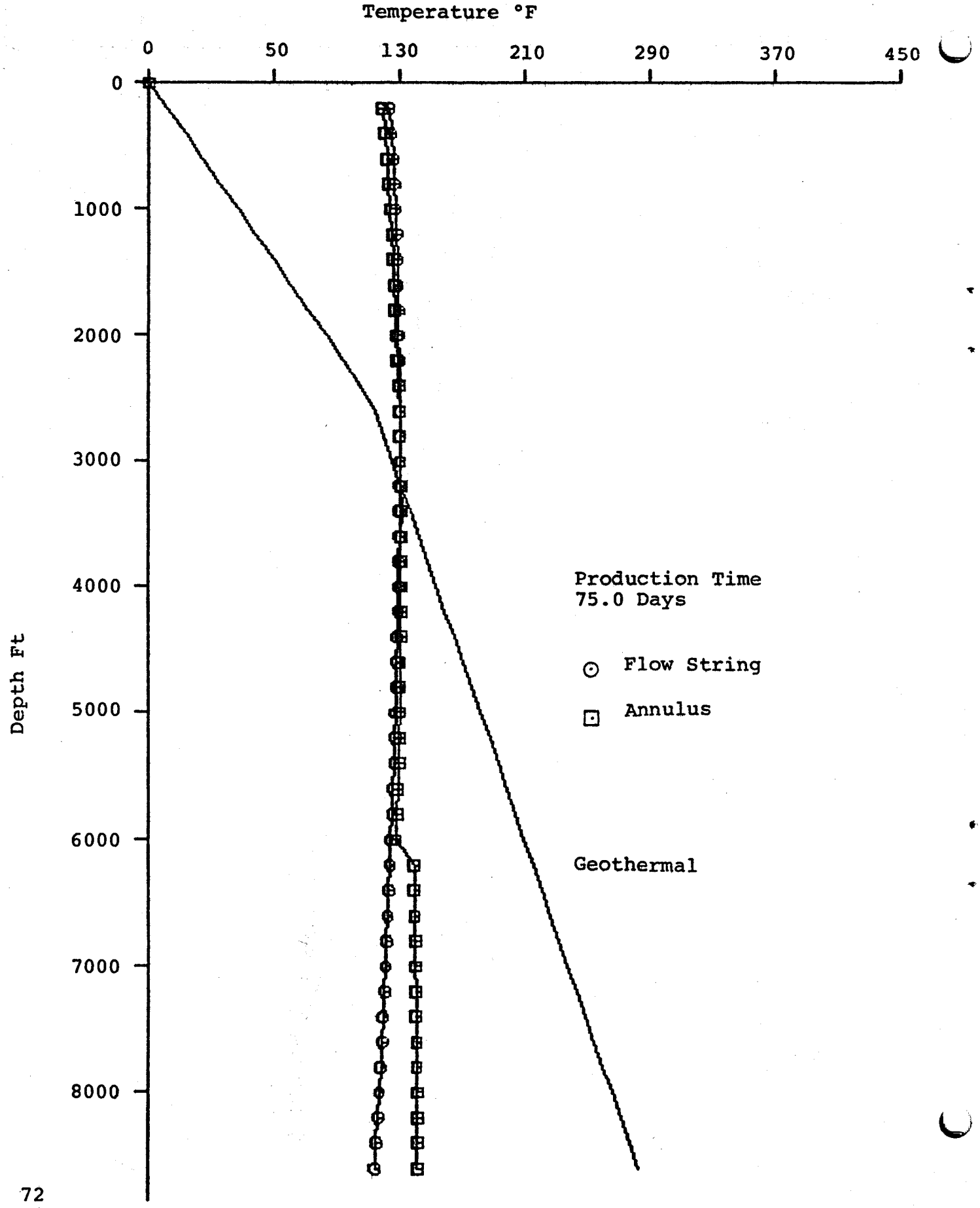

FIGURE 30: Republic Geothermal Well 56-30
Production Temperature Profiles

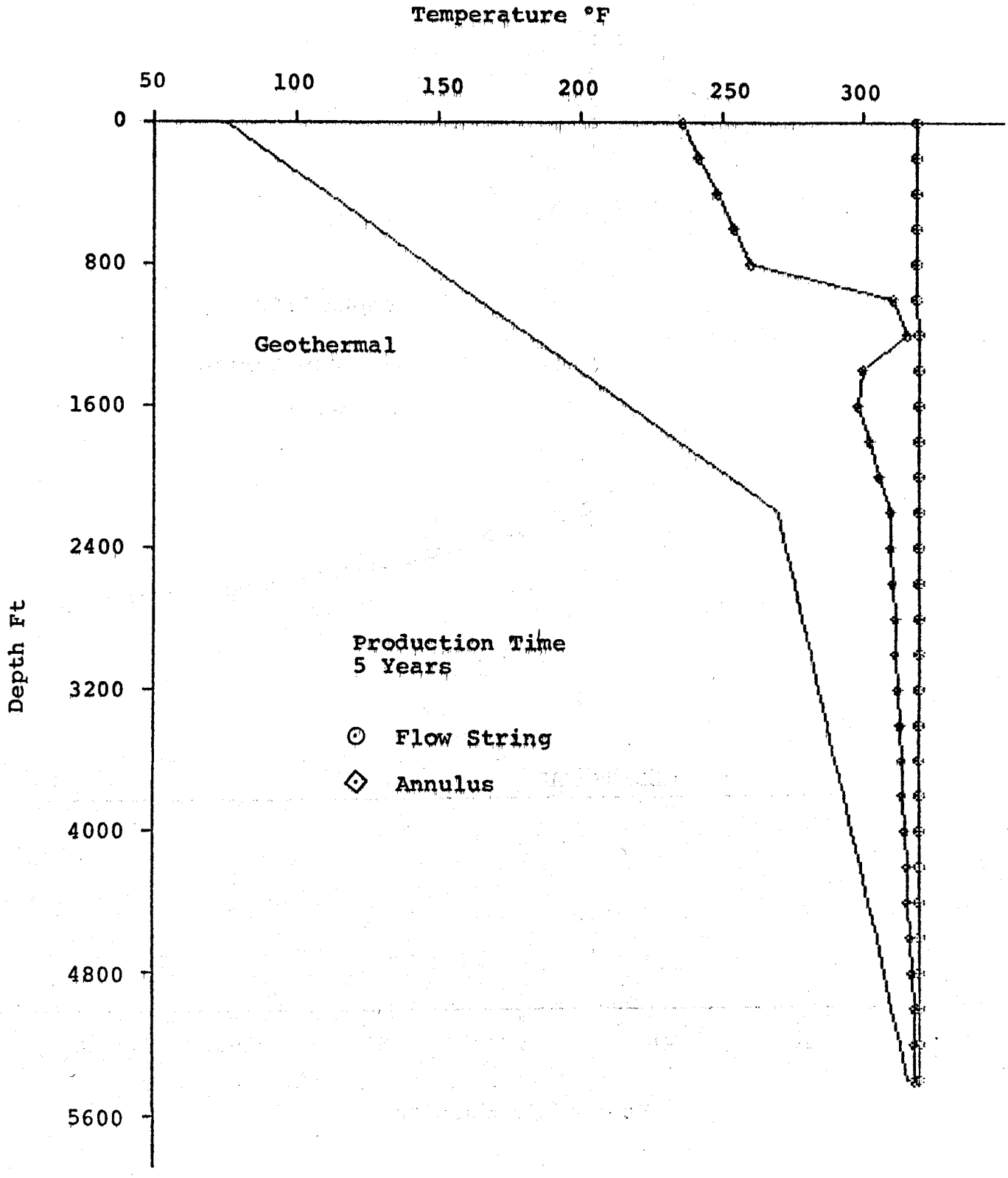

FIGURE 31: Los Alamos GT-2 Production Casing Temperature History

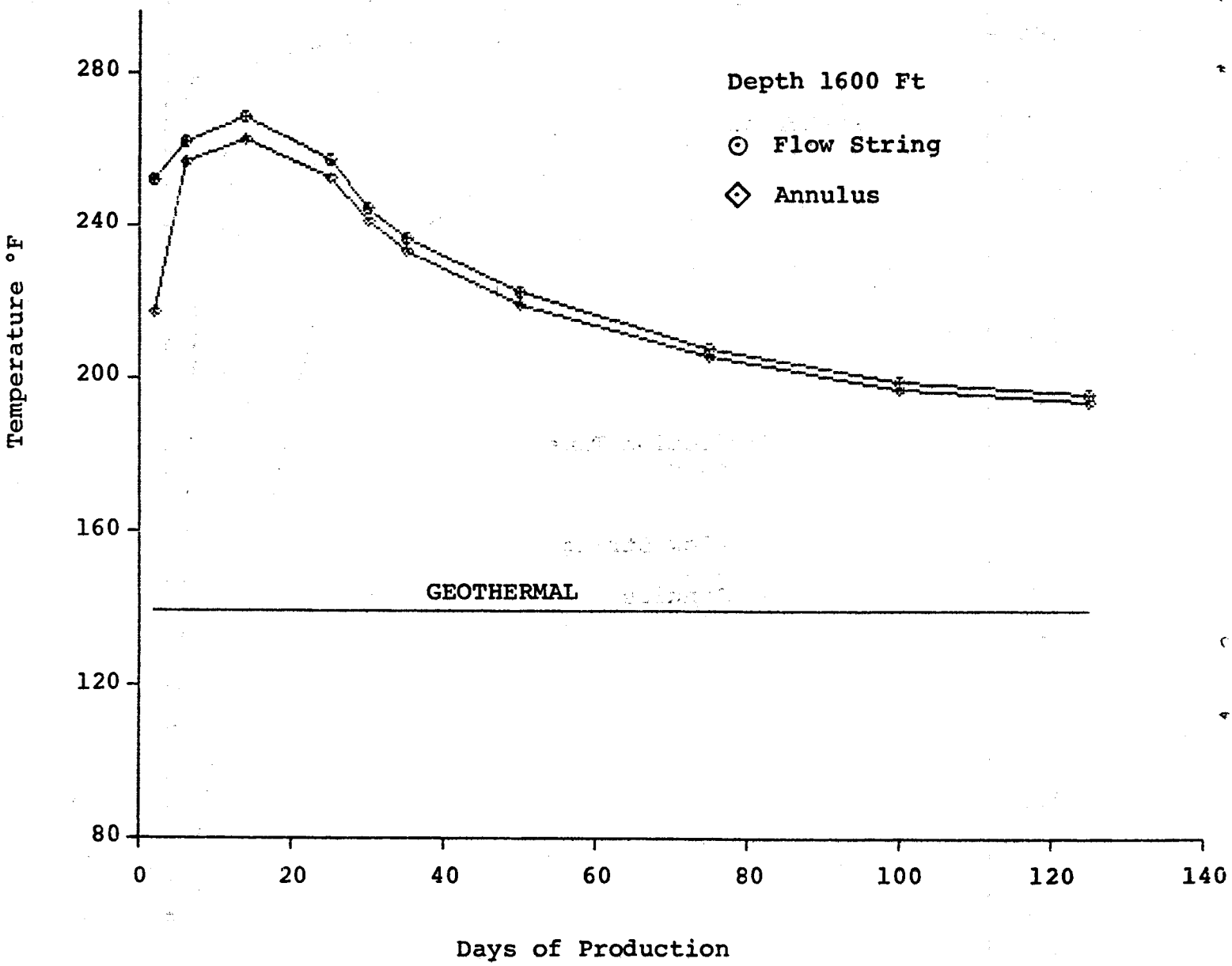

FIGURE 32: Republic Geothermal Well #56-30
Production Casing Temperature History

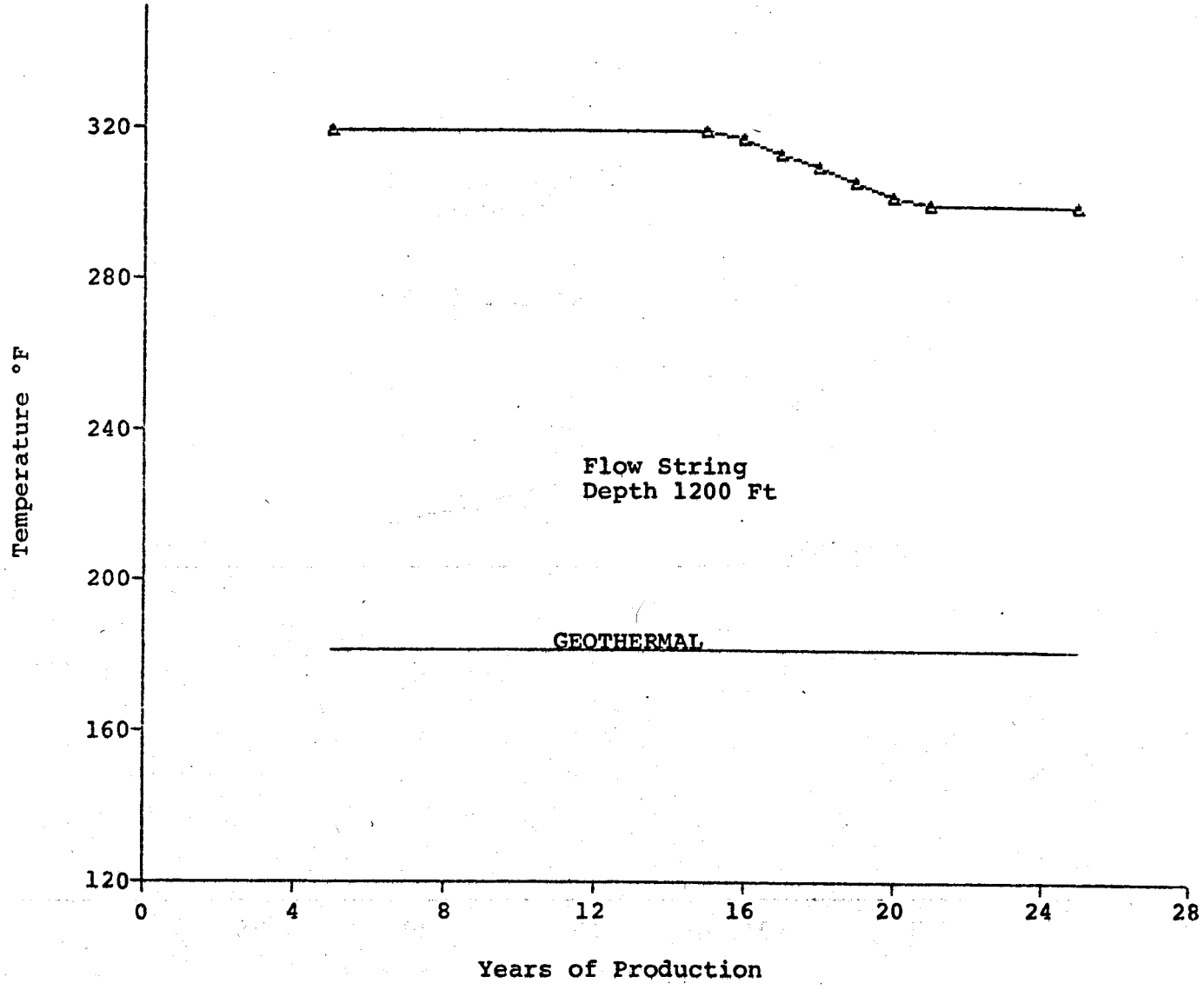

FIGURE 33: Formation Temperature Distribution
Outside Los Alamos GT-2 Production Well

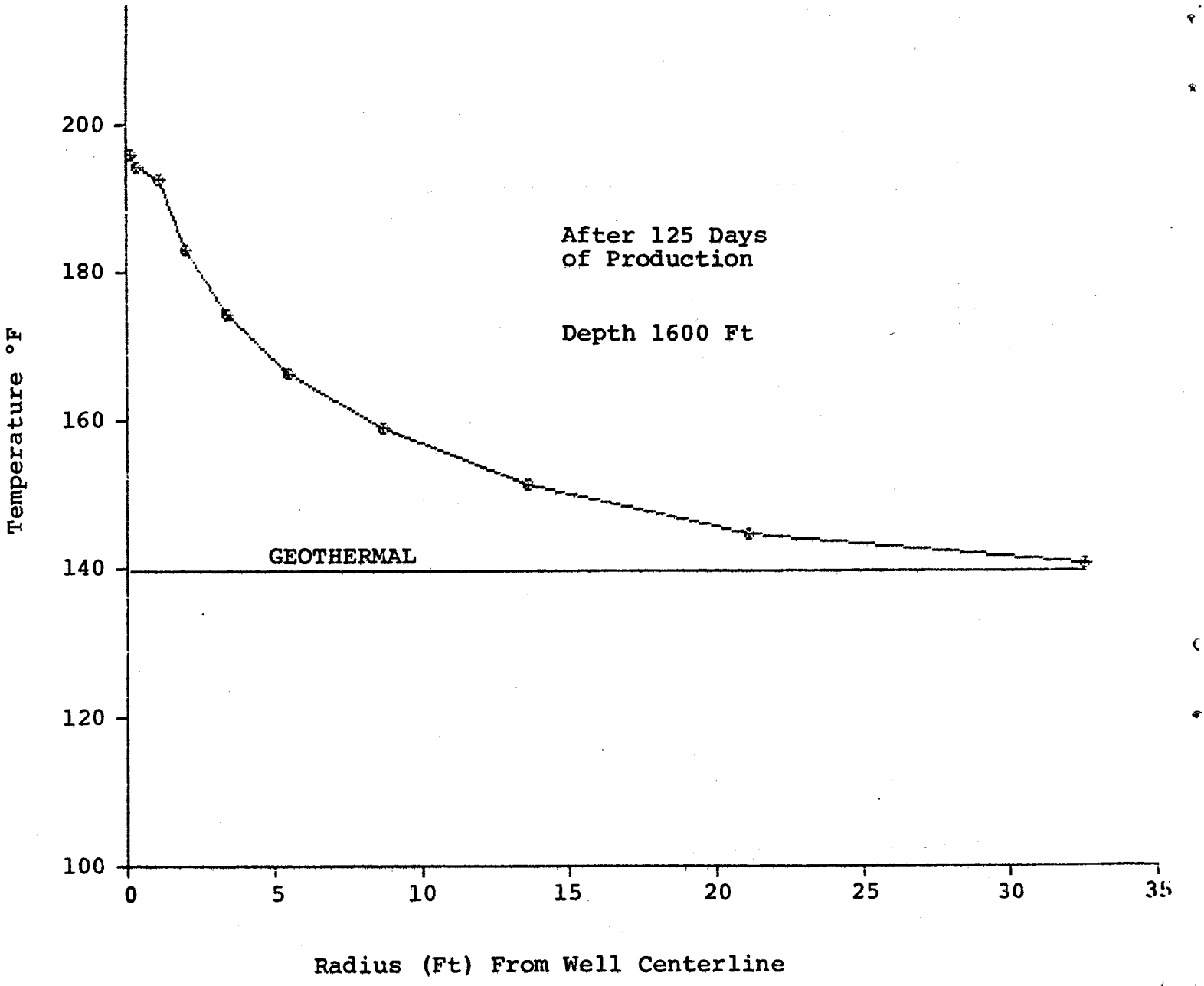

FIGURE 34: Formation Temperature Distribution Outside Republic Geothermal Production Well 56-30 (At Downhole Pump Level)

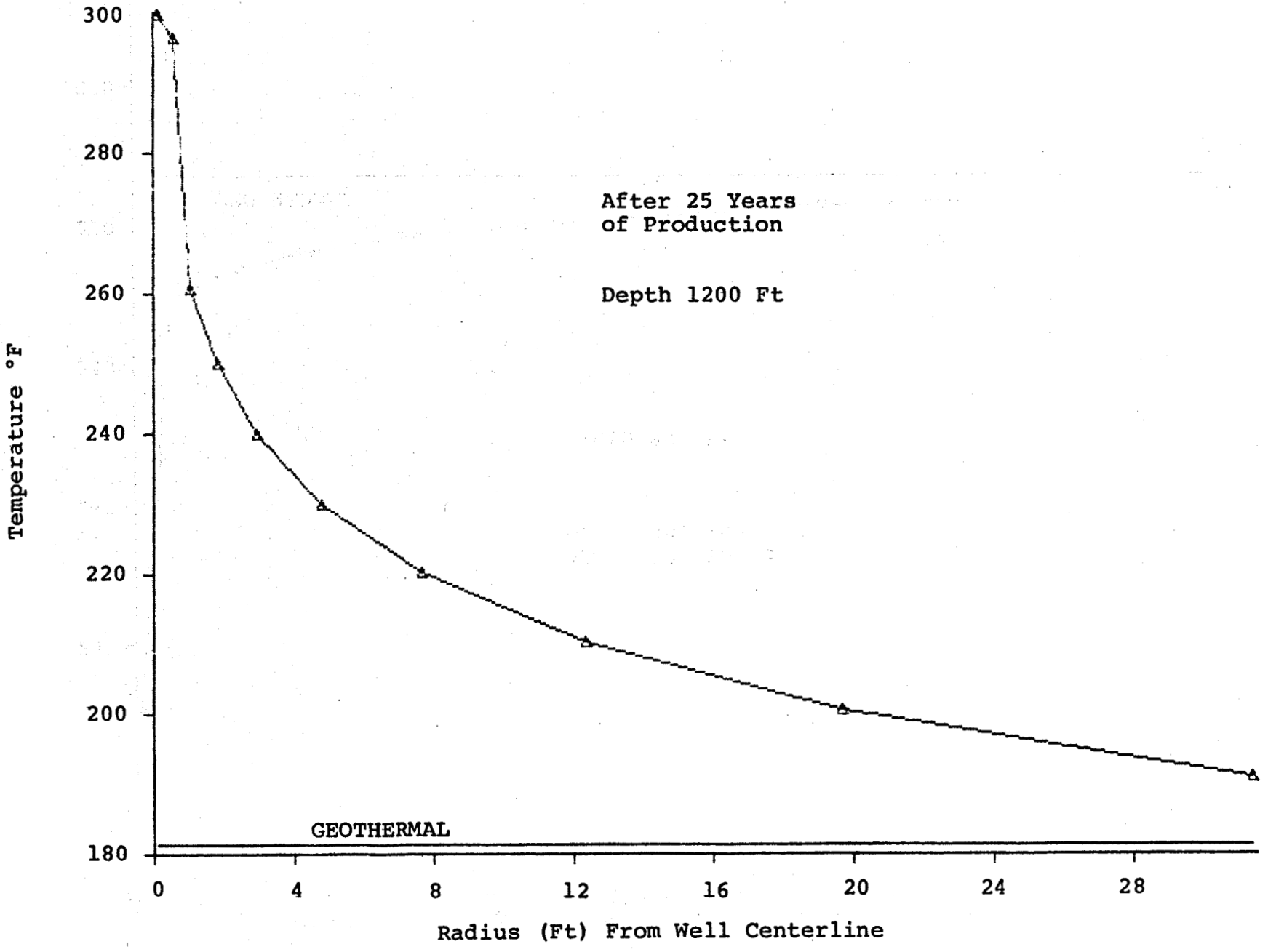

FIGURE 35: Formation Temperature Distribution Outside Republic Geothermal Production Well 56-30 (At Level of Annular Steam-Water Interface)

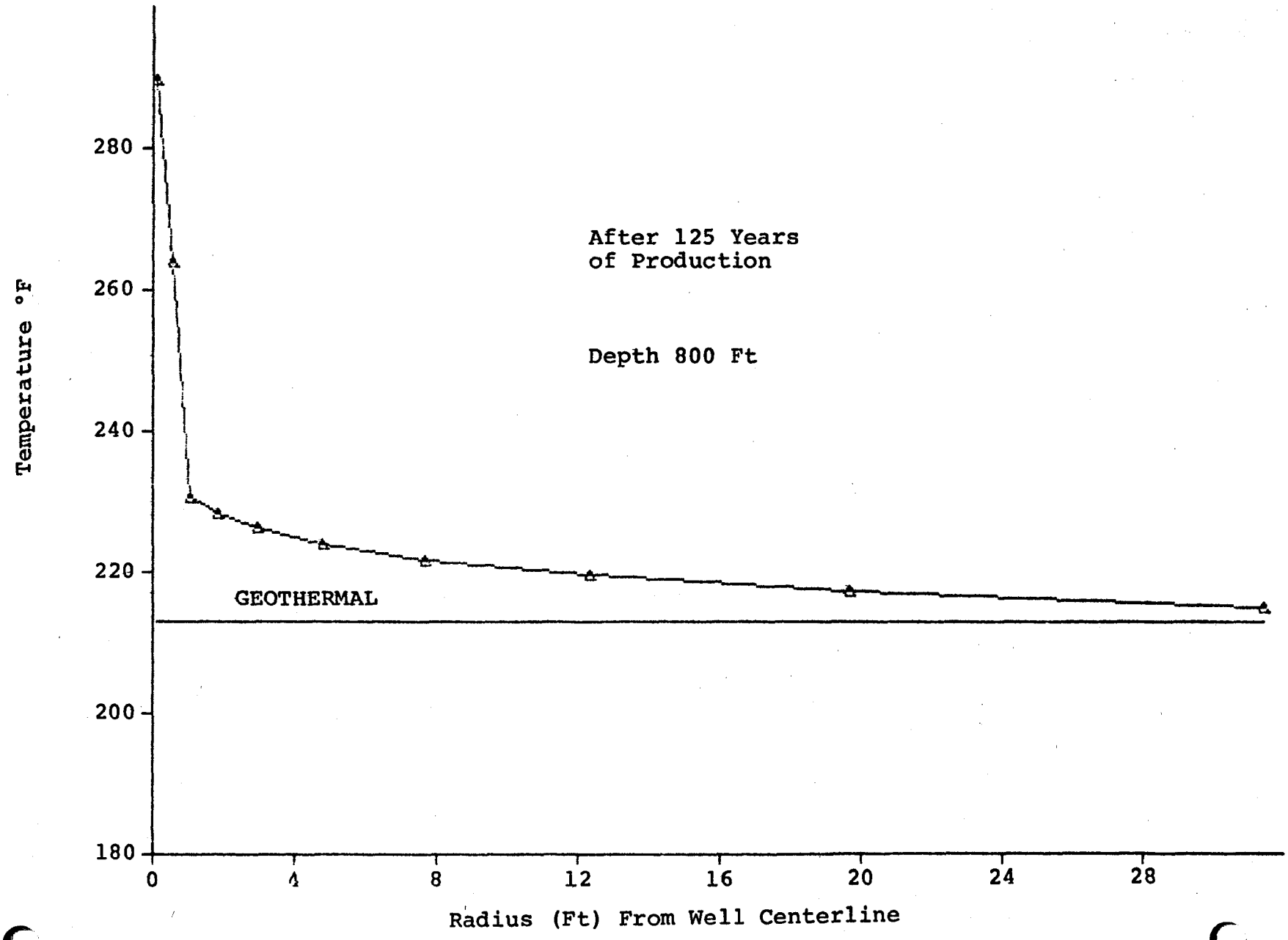

FIGURE 36: Los Alamos Injection Temperature Profiles

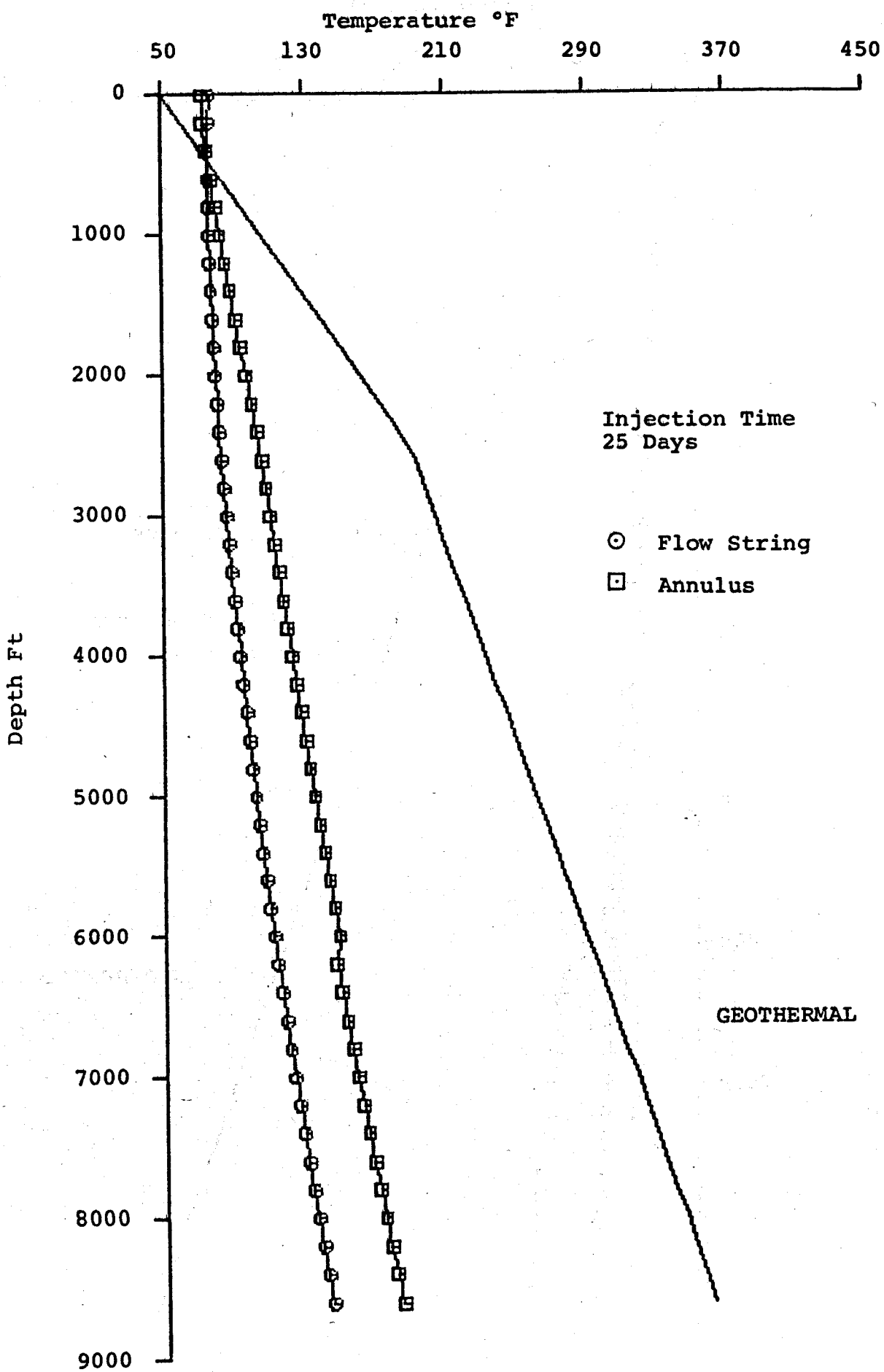

FIGURE 37: Los Alamos Injection Temperature Profiles

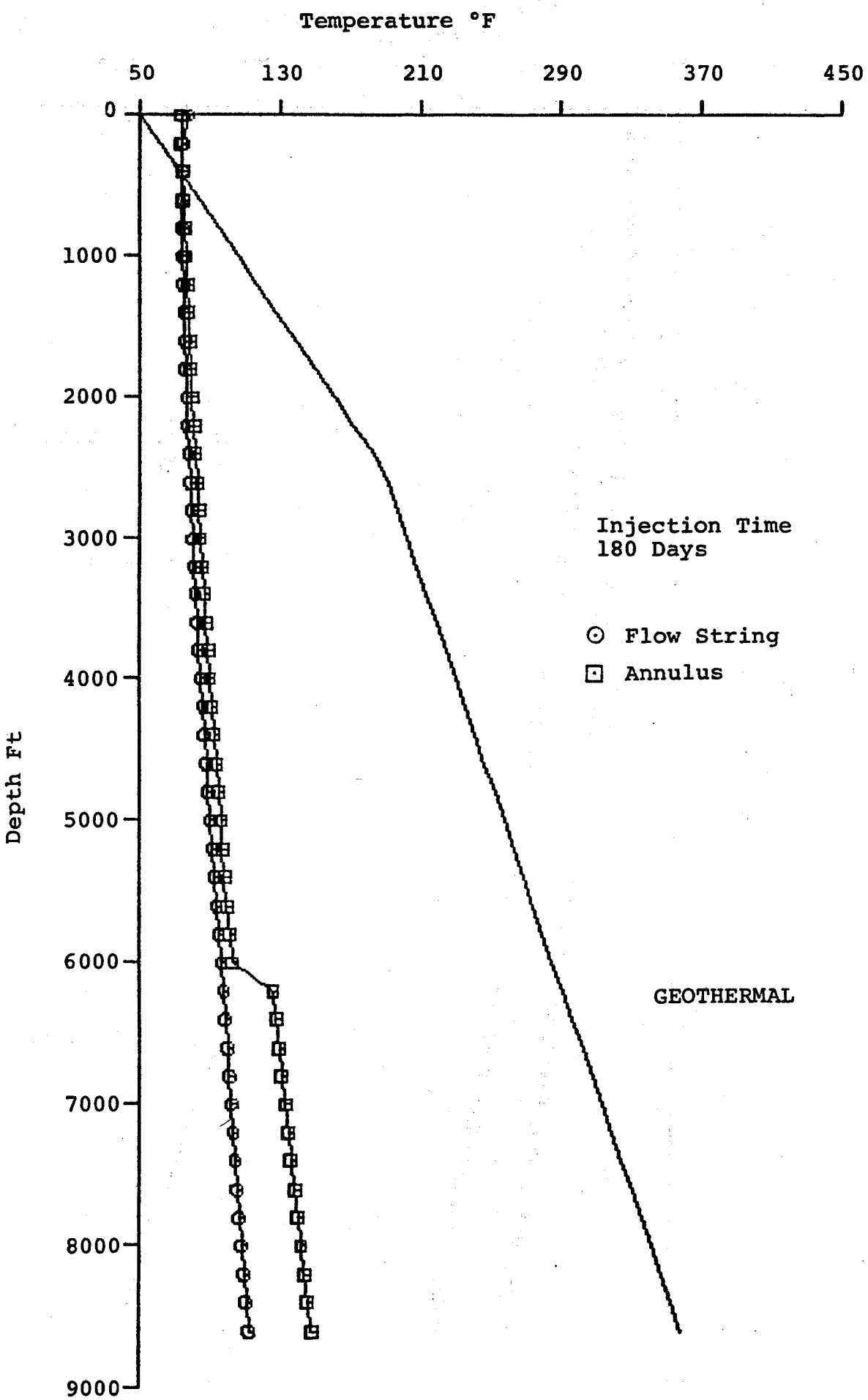

FIGURE 38: Republic Geothermal Injection
Well 52-29 Temperature Profiles

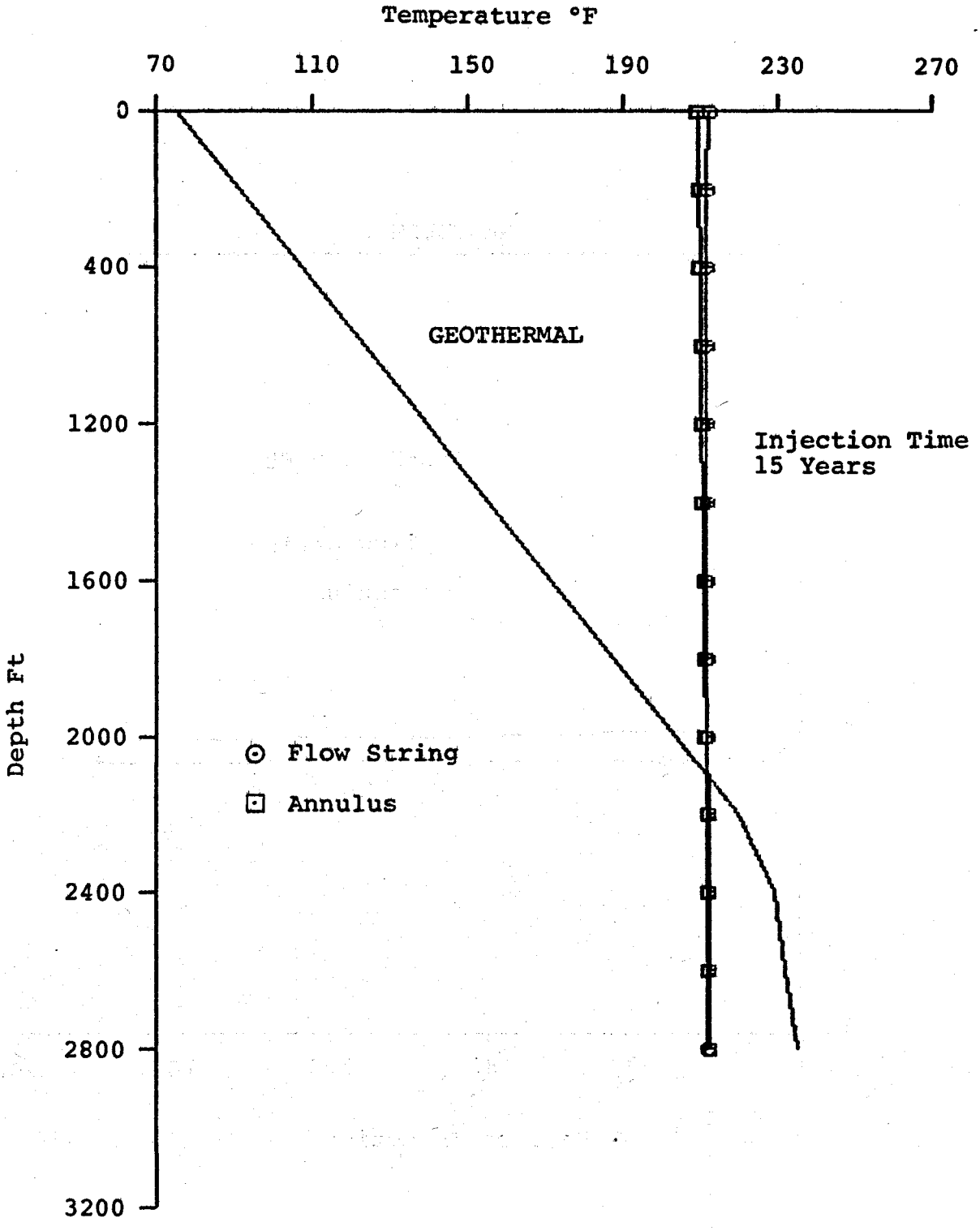

FIGURE 39: Los Alamos Injection Casing Temperature History

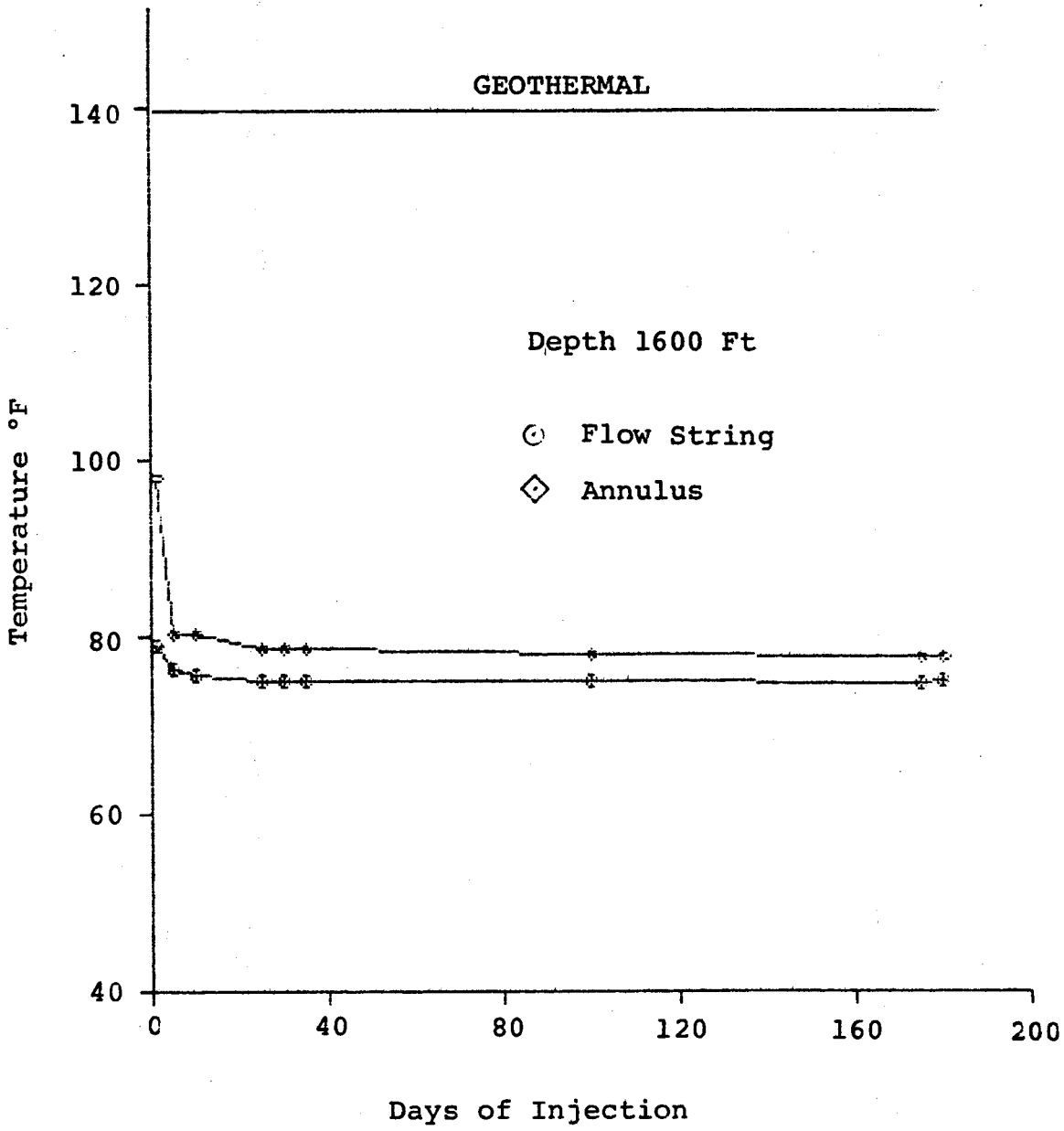

FIGURE 40: Republic Geothermal Injection Casing Temperature History

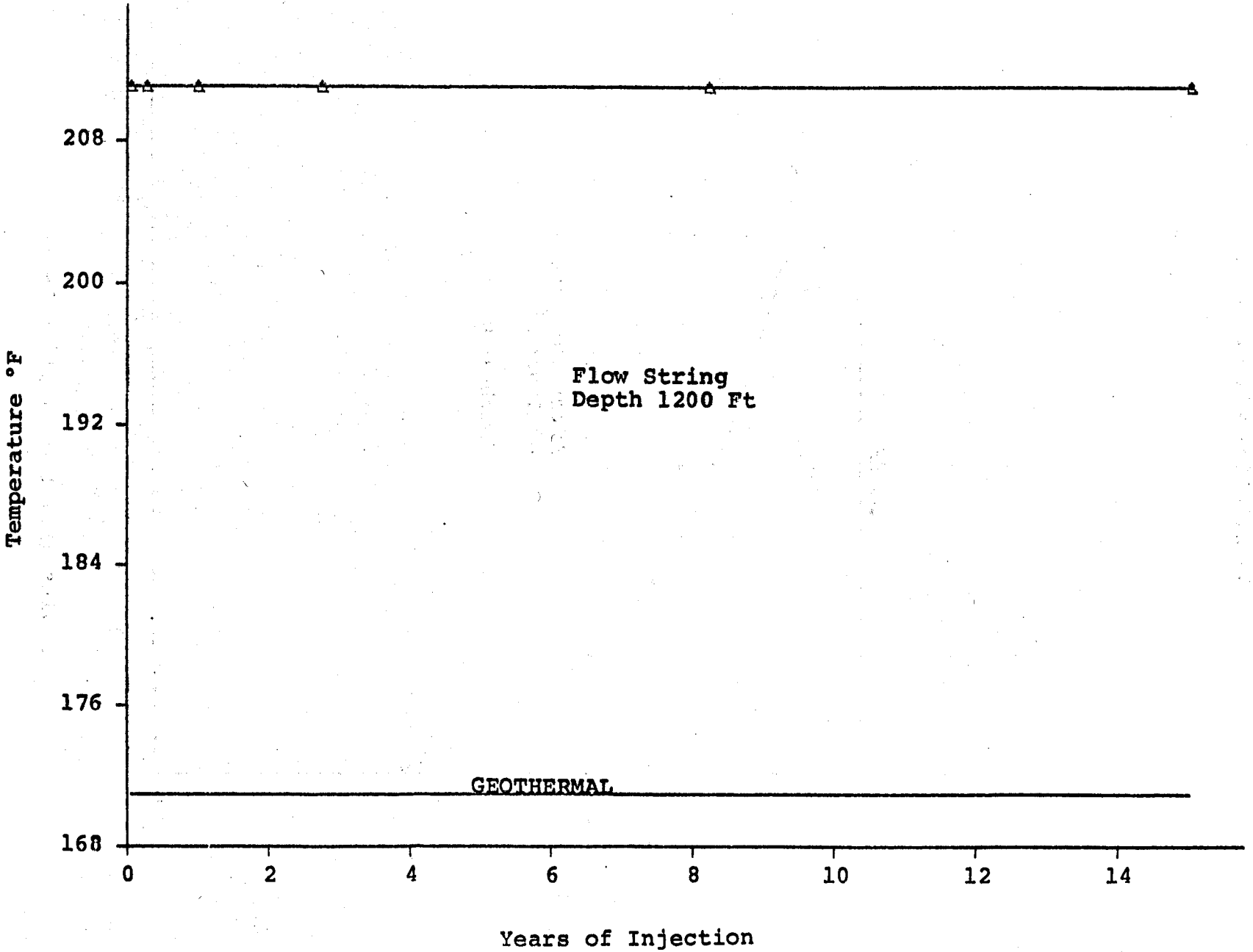

FIGURE 41: Formation Temperature Distribution
Outside Los Alamos Injection Well

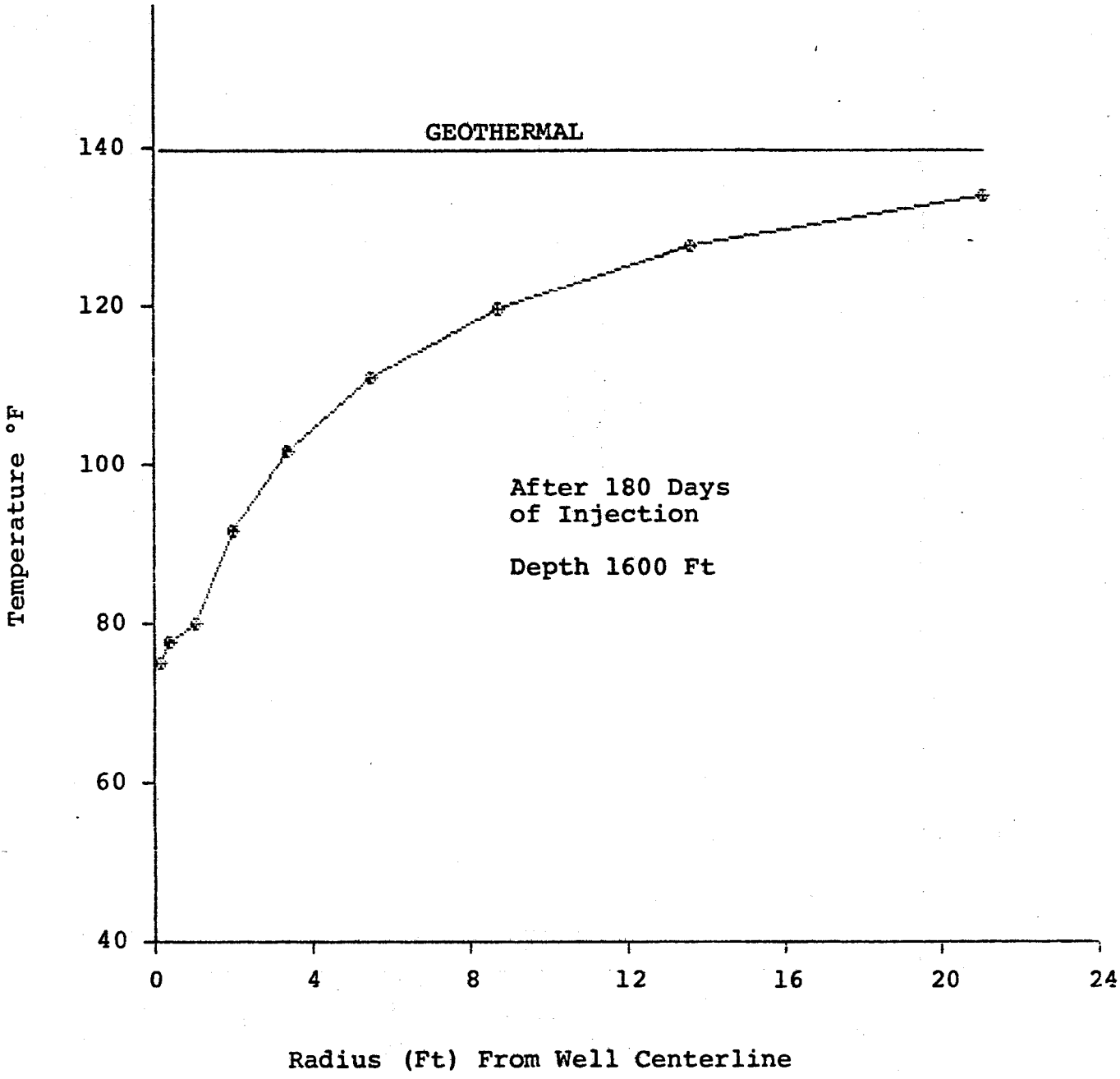

FIGURE 42: Formation Temperature Distribution
Outside Republic Geothermal Injection
Well 52-29

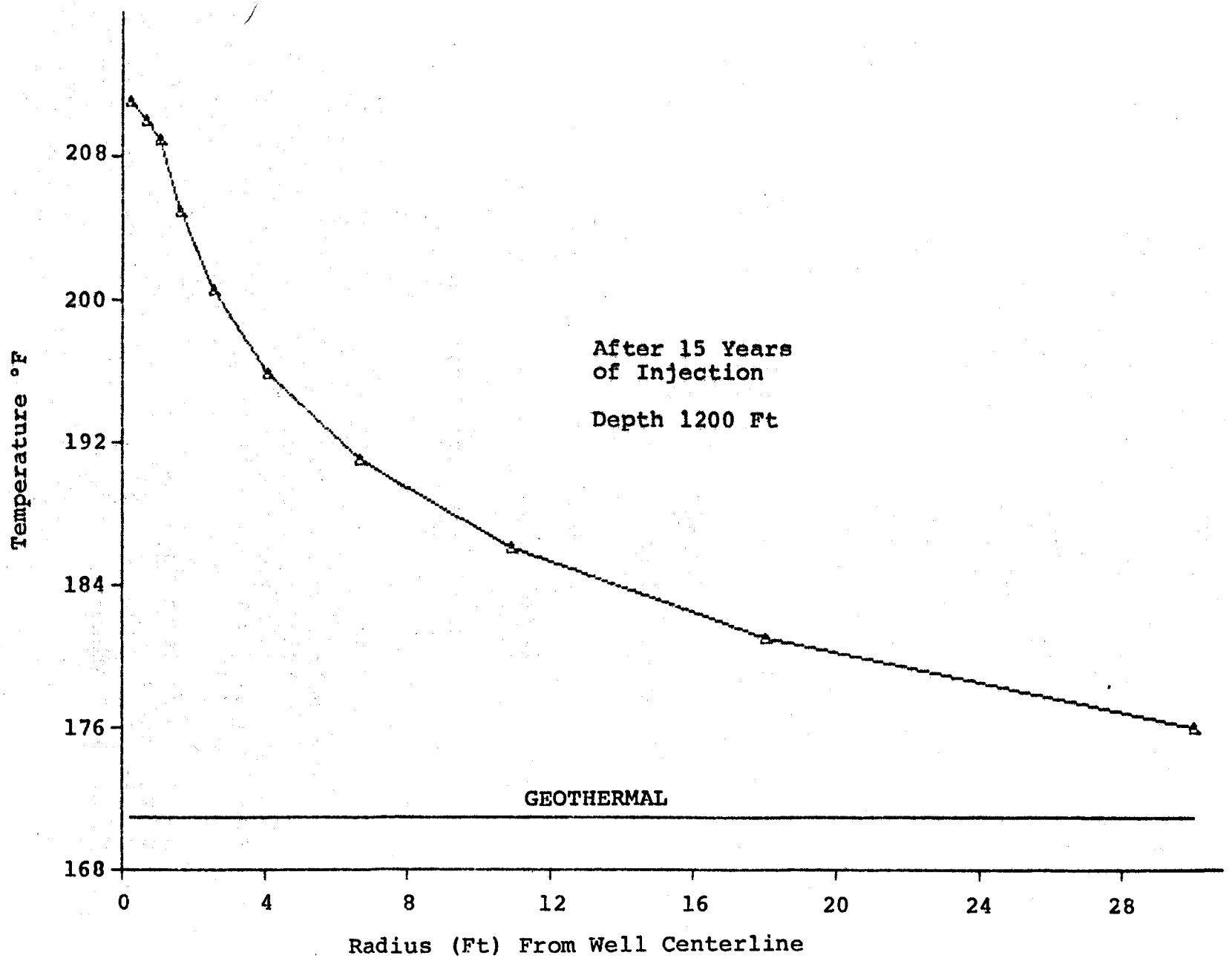

DISTRIBUTION:
TID-4500-R66-UC-66c (675)

Amoco Production Company
Research Center
P. O. Box 591
Tulsa, Oklahoma 74102
Attn: K. Millheim

Dresser Industries, Inc.
P. O. Box 24647
Dallas, Texas 75224
Attn: J. W. Langford

Dyna-Drill
P. O. Box C-10576
Irvine, California 92713
Attn: L. Diamond

Halliburton
Drawer 1413
Duncan, Oklahoma 73533
Attn: D. Smith

Loffland Brothers Company
P. O. Box 2847
Tulsa, Oklahoma 74101
Attn: H. E. Mallory

Los Alamos National Laboratory
Mail Stop 570
Los Alamos, New Mexico 87545
Attn: J. C. Rowley

Mobil Research and Development Corporation
Field Research Laboratory
P. O. Box 900
Dallas, Texas 75221
Attn: W. Gravley

NL Baroid Petroleum Services
City Centre Building, Suite 365W
6400 Uptown Boulevard
Albuquerque, New Mexico 87110
Attn: G. Polk

NL Petroleum Services
P. O. Box 1473
Houston, Texas 77001
Attn: J. Fontenot

DISTRIBUTION (Continued)

Otis
P. O. Box 34380
Dallas, Texas 75243
Attn: W. D. Rumbaugh

Phillips Petroleum Company
P. O. Box 239
Salt Lake City, Utah 84110
Attn: E. Hoff

Smith Tool Company
P. O. Box C-19511
Irvine, California 92713
Attn: J. Vincent

Texas A&M University
College Station, Texas 77843
Attn: Professor M. Friedman
Dept. of Geology

Shell Oil Company
Two Shell Plaza
P. O. Box 2099
Houston, Texas 77001
Attn: W. E. Bingman

Union Geothermal Division
Union Oil Company of California
Union Oil Center
Los Angeles, California 90017
Attn: D. E. Pyle

U. S. Department of Energy (5)
Division of Geothermal Energy
Mail Station 3344
12th & Penn, N.W.
Federal Building
Washington, D.C. 20461
Attn: C. McFarland
C. Carwile
M. Skalka
R. LaSala
R. Holliday, Jr.

DISTRIBUTION (Continued)

U.S. Department of Energy (2)
Geopressure Projects Office
Suite 8620, Federal Bldg.
515 Rusk Street
Houston, Texas 77002
Attn: F. L. Goldsberry
K. Westhusing

400	C. Winter
1000	G. A. Fowler
2000	E. D. Reed
2300	J. C. King
2500	J. C. Crawford
4000	A. Narath
4200	G. Yonas
4300	R. L. Peurifoy, Jr.
4400	A. W. Snyder
4500	E. H. Beckner
4700	J. H. Scott
4710	G. E. Brandvold
4730	D. G. Schueler
4740	R. K. Traeger
4741	J. R. Kelsey (10)
4743	H. C. Hardee
4746	B. Granoff
4747	P. J. Hommert
4748	B. E. Bader
4750	V. L. Dugan
4751	J. R. Tillerson
4754	A. F. Veneruso
4756	
5000	J. K. Galt
5600	D. B. Schuster
5800	R. S. Claassen
3141	T. L. Werner (5)
3151	W. L. Garner (3)
8266	E. A. Aas

☆U.S. GOVERNMENT PRINTING OFFICE: 1981-0-777-023/607